Vascular Network Formation via 3D Printing and Cell-Based Approaches

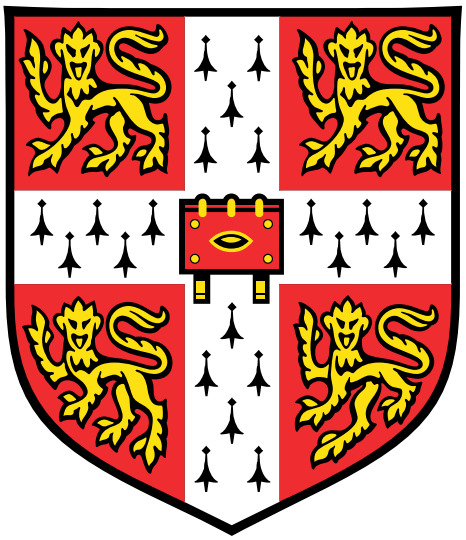

Alexander William Justin

Department of Engineering
University of Cambridge

This dissertation is submitted for the degree of
Doctor of Philosophy

Hughes Hall

May 2018

Declaration

This dissertation is submitted for the degree of Doctor of Philosophy at the University of Cambridge. The research was conducted at the Department of Engineering, University of Cambridge between October 2013 and July 2017, under the supervision of Dr. Athina Markaki.

I hereby declare that except where specific reference is made to the work of others, the contents of this dissertation are original and have not been submitted in whole or in part for consideration for any other degree or qualification in this, or any other university. This dissertation is my own work and contains nothing which is the outcome of work done in collaboration with others, except as specified in the text and Acknowledgements. This dissertation contains fewer than 65,000 words including appendices, bibliography, footnotes, tables and equations and has fewer than 150 figures.

Alexander William Justin
May 2018

Acknowledgements

I would like to thank my supervisor, **Dr Athina Markaki**, for her help and advice during the course of the project. In particular, I would like to thank her for giving me the freedom to explore a range of ideas and having confidence in my ability to carry out the work.

I also wish to acknowledge our close collaborators, **Dr Roger Brooks** and **Dr Mark Birch**, from the Division of Trauma and Orthopaedic Surgery, for their assistance and insight throughout the project. I'm very grateful for our many hours of interesting discussions which have helped me develop my thinking in this field.

This research was supported by the European Research Council (ERC, grant no. 240446), and an Engineering for Clinical Practice Grant from the Department of Engineering, University of Cambridge. I wish to acknowledge the support of the Engineering and Physical Sciences Research Council (EPSRC) through a PhD studentship (EP/L504920/1).

The research conducted on replacement bile ducts (Appendix A) was undertaken in collaboration with **Dr Fotis Sampaziotis** and **Prof Ludovic Vallier** from the Wellcome Trust-Medicial Research Council Stem Cell Institute, and **Dr Kourosh Saeb-Parsy**, from the Department of Surgery. I wish to thank them for our many interesting discussions.

Thank you to my college, **Hughes Hall**, for the support it has provided me over the years. I'm grateful for the friends I've made there and the terrific atmosphere of the college.

Finally, I wish to thank my wonderful parents, **Peter and Sheila Justin**, for their continued support and encouragement of my academic endeavours.

Abstract

Vascularization is essential for living tissue and remains a major challenge in the field of tissue engineering. A lack of a perfusable channel network within a large and densely populated tissue engineered construct leads to necrotic core formation, preventing fabrication of functional tissues and organs.

While many approaches have been reported for forming vascular networks, including materials processing techniques, such those involving lithography, bioprinting, and sacrificial templating; and cell-based approaches, in which cellular self-organization processes form vessels; all are deficient in their ability to form a vessel system of sufficient complexity for supporting a large cellular construct. What is missing from the literature is a method for forming a fully three-dimensional vascular network over the full range of length-scales found in native vessel systems, which can be used alongside cells and perfused with fluids to support their function. A large number of research groups are thus pursuing novel methods for fabricating vascular systems in order that new tissues and organs can be fabricated in the lab.

In this project, a 3D printing-based approach was used to form vascular networks which are hierarchical, three-dimensional, and perfusable. This was performed in thick, cellularized hydrogels similar in composition to native tissue; these being collagen (ECM-like) and fibrin (wound-like), both of which are highly capable of supporting cellular activities, such as cell seeding, cell spreading, and capillary morphogenesis.

In order to make use of 3D printed network templates in cellularized hydrogel environments, it was necessary to develop a new approach in which standard 3D printed materials were converted into a gelatin template, via an alginate intermediary, which can be removed quickly in physiologic conditions and which does not reduce cell viability. This multi-casting approach enables a hierarchical channel network to be formed in three-dimensions, capable of being perfused with cell medium to maintain the viability of a cell population, thereby addressing the fundamental problem.

Using standard cell staining and immuno-histochemistry techniques, we showed good endothelial cell seeding and the presence of tight junctions between the channel endothelial cells. When fibroblasts were seeded into the bulk of the hydrogel, a high degree of cell

viability and cell spreading was observed when a threshold flow rate is met. By counting the number of live and dead cells in a sample regions of the gel, we were able to show a dependency of cell viability upon the perfusion flow rate and further determine a regime in which the vast majority of cells are alive and spreading. This data informs future cellular experiments using this platform technology.

The limits of existing 3D printing technology meant that the micro-scale vasculature needed to be formed by other means. Cellular co-culture of endothelial and stromal cell types has been shown to be capable of forming capillary-like structures *in vitro*. For inclusion with the 3D printed channel system, we investigated the use of an angiogenic method for capillary formation, using multi-cellular spheroids, and a vasculogenic approach, using individual cells, in order that the full vascular system could be constructed. Endothelial and mesenchymal stromal cells were encapsulated in small fibrin and collagen gels and maintained under static culture conditions in order to form capillaries by the above approaches. The aim here was to find a particular gel composition and cell concentration which would support capillary morphogenesis while being suitably robust to handle the mechanical stresses associated with perfusion.

As future work, the next step will be to incorporate the vasculogenic co-culture technique, used to form capillary-sized vessels, into a perfusable gel containing the large templated channels, formed via the multi-casting approach. The challenge here is to anastomose the capillary-sized vessels to the large templated channels and thereby enable perfusion of the capillary vessels. This step would be a highly significant development in the field as it would mean large constructs could be fabricated with physiological densities of cells, which could lead to a range of potential therapeutic applications.

Table of contents

Chapter 1

Introduction

1.1 Tissue Engineering and Vascularization

There exists a need for replacement organs and tissues, with the demand for donor organs far exceeding the supply [148]. One of the primary aims of the interdisciplinary field of tissue engineering has been the formation of new tissues and organs, to meet this shortage. This tends to involve the growth and maintenance of large numbers of cells on three-dimensional polymer scaffolds in the presence of signalling molecules such as growth factors and cytokines, which aid in their development. Ideally, the polymer scaffold acts like the extra-cellular matrix; providing a range of physical and chemical cues for the cells, enabling interaction between cells, establishing molecular gradients, and driving such biological processes as cell seeding, cell growth, differentiation, and ultimately remodelling of the scaffold itself. Thus any successful tissue engineered scaffold must be able to provide an environment in which cells can survive and function [7].

In order to meet this requirement, cells must have access to sufficient oxygen and nutrients, as well as have a mechanism for the removal of waste products. The solution found in nature is that of the hierarchical vascular network, enabling rapid delivery of metabolites and removal of waste products efficiently for a large number of cells. Due to diffusion limits in regions dense with cells, one requires that tissues thicker than 400 μm have access to vasculature to supply sufficient metabolites for cellular function [7].

In order for tissue engineering to progress to the point where large organs and tissues can be fabricated on demand, tissue engineered scaffolds require the establishment of perfusable tubular networks within them, enabling the support of high densities of cells which are metabolically active, in a fully three-dimensional environment. Further to the provision of oxygen and nutrients, and the removal of waste products, a tissue requires a tubular system for the regulation of fluid accumulation and for the recruitment of cells of the immune system;

roles fulfilled by the lymphatic system in native tissue. Finally, functional organs often have a tubular network in order to meet biological purposes, such as collecting ducts in the kidney, bile ducts in the liver, and alveolar ducts of the lung. Therefore, there is a primary need in tissue engineering for the development of fabrication techniques for vascular systems, which enable the formation of all these tubular structures present in the physiological tissue, yielding useful, biologically-active constructs. The formation of these interpenetrating fluidic networks is seen as an open challenge in the field of tissue engineering and one which is functionally indispensable for the formation of complex engineered organs and tissues [79].

There are two ways in which one can produce vascular systems *in vitro* similar to those found *in vivo*; one can fabricate tubular networks via physical and chemical processing of biomaterials, or one can initiate the biological processes by which vessel systems would normally form in organisms. The latter takes place via two processes; these being vasculogenesis and angiogenesis. Vasculogenesis generates vascular networks *de novo* in the absence of pre-existing vessels and angiogenesis describes the process by which new vasculature is formed from pre-existing vessels [7]. The term, capillary morphogenesis, is used in the context of both processes. Further, other processes exist to form lymphatic channel networks (lymphangiogenesis) and epithelial ducts (epithelial tube morphogenesis).

Within the vascular system, the hierarchical network is predominantly defined by changes in diameter and cell population. Hierarchy is an important characteristic of these networks as it enables extensive coverage of a large tissue whilst simultaneously providing the low pressure heads required for efficient diffusion in and out of the bulk. Macroscopic vessels, such as the aorta, provide high throughput flow over long distances. These branch down to finer and finer vessels - arterioles vary in diameter from 10-300 μm, consisting of one or two layers of helically arranged smooth muscle cells, surrounding an endothelium [82]. The boundary between the arteriole and capillary is marked by the disappearance of smooth muscle cells [82] and the appearance of pericytes, which wrap around the endothelium. Capillaries have an inner diameter (lumen) of 5-20 μm, with wall thickness up to as much as half of this [82]. The transition between capillary and venule (20-50 μm) is less well defined, but the collecting venules increase to 50-300 μm [82]. Vessels at these different length-scales exhibit noticeably features; the larger ones are coated with layers of smooth muscle cells and are more permanent, whilst the capillaries are coated with pericytes and are more temporary, undergoing angiogenic remodelling as a response to growth and repair [79].

1.2 Formation of the Vascular System

As will be described in depth in later chapters, methods developed in tissue engineering are capable of inducing capillary morphogenesis, which forms capillaries spontaneously using the biological processes of vasculogenesis and angiogenesis, and which can be anastomosed *in vivo* to the native tissue blood supply. The vast majority of clinically-successful engineered tissues to date are either thin or tubular in nature, allowing for oxygen and nutrients to diffuse to the cells from the surface of the construct. Such constructs include large-scale and uniaxial blood vessels, skin, cartilage, and bladder [8]. However, for high densities of cells and for thick constructs, one requires a perfusable vascular network as diffusion from the surface alone is incapable of meeting the metabolic requirements of the cells. Currently, we are unable to direct the biological formation of larger branched vessels, owing to the high degree of biological complexity involved.

A range of fabrication techniques have therefore been developed which produce structures reminiscent of larger vessels (50 μm - 1 mm) with the aim of producing multi-scale hierarchical vascular systems. These include lithography-based approaches, in which channels are patterned in two-dimensions; bioprinting and 'direct-write' approaches, in which matrix materials and cells are deposited layer-by-layer; and planar and three-dimensional sacrificial techniques, in which the vascular templates are produced for casting and encapsulation in a matrix material.

A range of cell-based approaches have been studied which produce capillary-sized vessels via the interaction of different endothelial cell types with other cells, including fibroblasts, stromal and perivascular cells. This co-culture interaction of different cell types continues to be extensively investigated as a powerful technique for enacting capillary morphogenesis and angiogenic sprouting, though this interaction is highly complex, involving a large number of small molecules and proteins (such as growth factors and other cytokines). Aside from the myriad of *in vitro* cell-based approaches that exist, there are also a range of *in vivo* approaches which utilize capillary ingrowth and anastomoses of vessels from the native tissue in order to vascularize a scaffold. These include techniques such as the arteriovenous loop, in which a native vessel is passed through a polymeric scaffold, and which can produce a rapid vascularizing response from the surrounding tissue. Other approaches use the organism as an *in vivo* bioreactor in which to mature constructs.

1.3 Key Aims of Project

The primary aim of this project is the formation of a hierarchical vascular network system capable of supporting a large, three-dimensional, and cellularized construct, in ideal tissue engineering biomaterials, such as collagen and fibrin, capable of being freely remodelled by cellular processes. The field requires a technique by which complex vascular architectures, which are hierarchical, three-dimensional, and perfusable, can be fabricated in a reproducible manner, and which can be used in ideal biomaterials.

In this project, a novel process was developed in which standard 3D printed thermoplastic models, which are highly customizable and reproducible, are converted into a gelatin hydrogel material. This can then be used as a vascular network template in highly bioactive hydrogel materials, such as collagen and fibrin, which are pre-loaded with cells. The ability to use 3D printed materials in this way is achieved by casting an alginate intermediary around the 3D printed model. Alginate hydrogels are stable at high temperatures ($\sim$100 °C), and do not decay in acetone; both properties of which are required to remove the polyester-based model material in its entirety. By making use of the different physical and chemical properties of the 3D printed material, and of alginate and gelatin, it is possible to selectively add and remove positive and negative casts of the original network design, resulting in a channeled construct made from thermo-gelled collagen or enzymatically-crosslinked fibrin hydrogel. This approach makes use of commercially-available 3D printing technology in order to achieve a high degree of reproducibility and precision. The use of gelatin gel as a vascular template has the added advantage of enabling prompt perfusion once the final construct has formed. Key challenges however still exist in stabilizing the hydrogel materials and preventing leakages when under perfusion.

Alongside this templated structure, it was necessary to make use of cellular co-culture in order to form a capillary-like network; the key challenges here being the formation of a vessel network, the anastomosis of the capillary bed to the large-scale vessel structures, and the subsequent perfusion of the whole system. Thus the approach being proposed here is to use a 3D printing technique to form large vessels and support initial perfusion of the tissue construct, and make use of capillary morphogenesis to form the microvasculature, which improves the delivery of metabolites as the tissue develops.

Using standard co-culture and multi-cellular spheroid methods, the formation of a capillary-like network was investigated, for future connection to the large-scale network described above, enabling direct perfusion of the capillary bed in a thick construct. In this approach human umbilical vein endothelial cells (HUVECs) are used, alongside either fibroblasts or mesenchymal stromal cells (MSCs), to produce the capillaries. Multi-cellular spheroid cultures, in which cells are localized into small groups prior to casting, showed

the formation of more mature capillary structures, with larger lumen, multi-cellularity, and longer lengths, likely due to the cell-cell junctions that were formed early on in the process, and the formation of strong gradients of factors. However, there appears to be a trade-off in using spheroids in this way as coverage of the construct is not as complete as with single cell capillary morphogenesis, which was found to be more suitable for our approach and the future aims of this work.

1.4 Thesis Outline

The first half of the thesis explores the fabrication of large-scale vasculature via physical and chemical processing of polymers. Chapter 2 consists of a literature review of the fabrication techniques employed to form channels and channel networks, including bioprinting; one, two, and three-dimensional microfabrication techniques; macro-porous scaffolding methods; and establishes sacrificial 3D printing as the key approach by which complex vasculature can be formed, providing a starting point for the research. Chapter 3 describes the approach to fabricating vascular networks via conversion of standard 3D printed thermoplastics into gelatin gel, and preliminary cell experiments with this system.

The second half explores the formation of capillary-sized vessels via cellular co-culture techniques. Chapter 4 reviews the literature on angiogenic and vasculogenic capillary morphogenesis. It compares fibrin and collagen as substrates for use in co-culture experiments, compares the use of fibroblasts and mesenchymal stromal cells as the supporting cell, and establishes the use of particular growth factors in the system. Chapter 5 describes the angiogenic approach to capillary formation, via multi-cellular spheroids, and Chapter 6 describes the vasculogenic approach, using individually seeded cells. Chapter 7 reports on the conclusions and future work. Appendix A reports on a supplementary study of the formation of densified collagen tubes, which through work with collaborators, were transplanted as replacement bile ducts in mice.

Chapter 2

Literature Review: 3D Printing Techniques for Vascularization

2.1 Introduction to Fabricated Vascular Systems

Living tissue requires channel networks over multiple length-scales in order to support a high density of metabolically active cells [7]. The lack of such a vascular system has held back progress into the fabrication of new tissues and organs, as diffusion from the surface of a tissue construct becomes unfeasible for rapid delivery of oxygen and nutrients [8]. Oxygen transport is seen as the limiting factor for the survival of high densities of cells in three dimensional systems [75]. In the case of tissue containing high densities of cells, oxygen diffusion is generally limited to 150-200 μm [79], though other cells show more extreme behaviour (islets show necrosis when diffusion distance exceeds 100 μm [75]). Thus, for tissue engineered organs and tissues to be fabricated *in vitro*, with the required high densities of cells, in three dimensions and with a thickness larger than 400 μm [79], methods are required to fabricate vasculature.

In this chapter, a critical review is presented of the range of approaches suggested for producing vascular networks *in vitro*, including microfabrication methods, 3D printing, and other techniques for the processing of polymers. This will not include methods that involve the direction of cells to form new vessels via angiogenesis and vasculogenesis, which will be described in Chapter 4.

2.2 Bioprinting

3D bioprinting is a well known technique in the field of tissue engineering, in which matrix and other polymeric materials, alongside cells, are deposited layer-by-layer from a mounted nozzle, thus building up a three-dimensional structure. It promises the ability to place cells and matrix materials (i.e. bioinks) into spatially organized patterns in 3D, which would include the formation of vascular channels as the structure is built up [7, 144]. Figure 2.1a shows a typical bioprinting setup in which bioinks are printed to build up a structure. Common bioprinted structures consist of a 'woodpile' arrangement, which is shown in Figure 2.1b, in which filaments are deposited in alternating orthogonal orientations which provide a degree of mechanical strength in-plane. Spaces are frequently left between these filaments so as to yield a macro-porous structure.

There exist a number of key challenges when creating perfusable tissue engineered constructs via 3D bioprinting approaches. Firstly, fabrication of vasculature is particularly difficult with bioprinting as matrix materials are inherently hydrophilic. This means that upon deposition, a printed droplet will spread considerably if the substrate is also hydrophilic. In the case of building up a three-dimensional structure, each layer will be hydrophilic and so the feature sizes will be large. However, methods do exist which attempt to circumvent this problem.

One approach [55] is to undertake the printing process in a vat of gelatin, which prevents significant spreading of the printed drop and via viscous forces, maintains the drop in the required position prior to gelling, enabling fine vascular features to be formed, as shown in Figure 2.1c.

Another approach is to add a second, rapidly crosslinking polymer which maintains the drop in place. For example, a collagen and alginate mixture can be inkjetted onto a substrate containing upward diffusing calcium ions [131]. The calcium crosslinks the alginate and enables the collagen to gel into a small feature size. Following collagen gelation, the calcium is chelated and the alginate is then free to then diffuse away, leaving a collagen structure. This can yield a cellularized construct containing vascular features, as shown in Figure 2.1d. Other approaches include the jetting of thrombin onto a fibrinogen substrate, which undergoes rapid enzymatic crosslinking to form 3D structures [29], and to make use of photocrosslinkable polymers, enabling structures to be made from cell-laden gelatin methacrylate (Gel-MA) and polyethylene glycol diacrylate (PEG-DA) hydrogels, which are photocrosslinked upon deposition [13].

However, bioprinting suffers from another key limitation. The bioprinting process, like most 3D printing technologies, is very slow since each drop or filament is deposited one after the other, and this means the process takes an exponentially longer period of time to

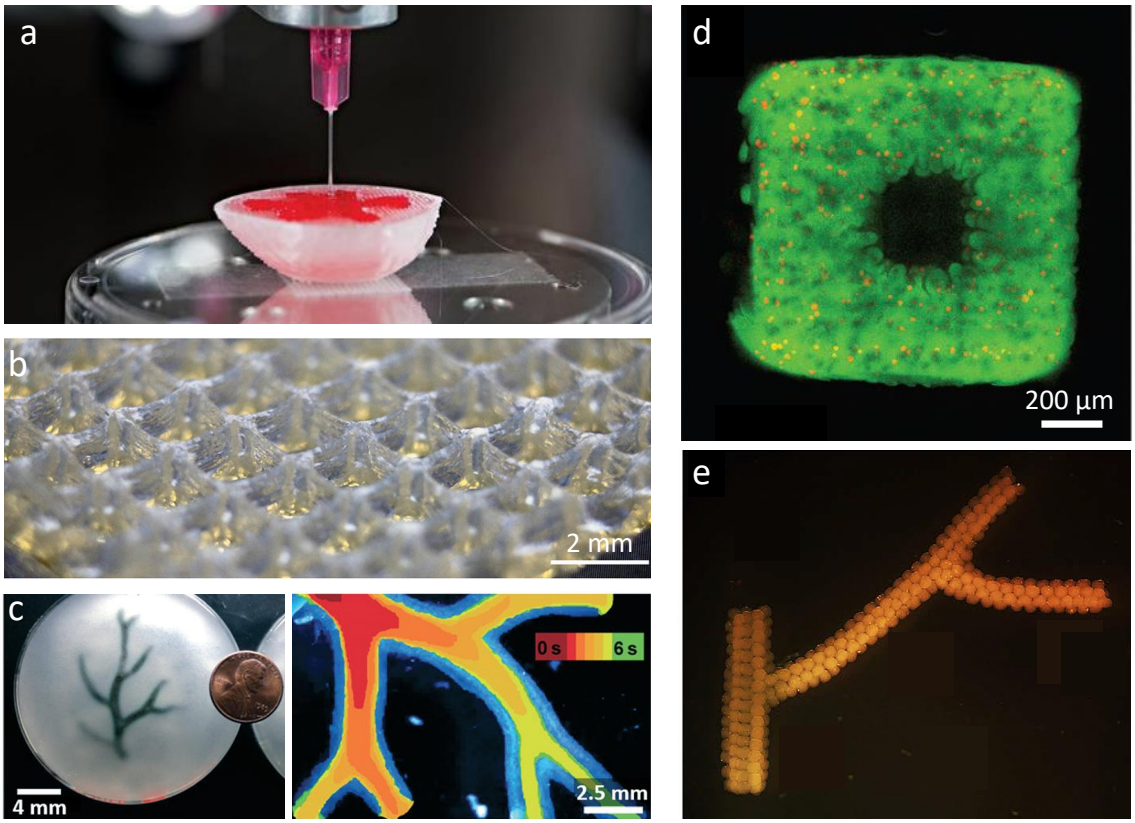

Fig. 2.1 (a) A typical bioprinting setup in which cells and matrix-like materials are deposited from a fine nozzle to build up a three-dimensional structure [144]. (b) 'Woodpile' structures are common in bioprinting, consisting of orthogonally orientated layers of polymer filaments with large pores between each feature. Shown here is a structure made of gelatin [63]. (c) Using a bath of liquid gelatin to support the structure and prevent drop spreading, alginate, collagen, and fibrin can be printed so as to produce fine vascular features [55]. (d) By printing a mixture of alginate and collagen polymers into a calcium rich environment, fine features made of collagen can be produced, capable of yielding vascular structures [131]. (e) By printing multi-cellular spheroids, one can produce vascular features via a scaffold-free approach [125].

complete as the drop size gets smaller. Importantly, this also means that there is likely a significant loss of cell viability during the duration of the printing process since perfusion of a supporting vascular network is unlikely to be able to begin until the construct is completed.

Bioprinting can impart a significant loss of viability upon printing through a fine nozzle or inkjet, required by bioprinting approaches to form the fine features of the tissue construct [7]. When cells are extruded alongside polymers through the nozzle, as is the basic idea of bioprinting, there is a great deal of shear stress imposed upon the cells, decreasing their viability [15].

Scaffold-free approaches exist within the field of bioprinting in which single cells, or multi-cellular spheroids, are deposited into 3D structures without the need for a supporting polymeric material, which could be beneficial to forming tissues [125]. By depositing groups of cells into complex structures, one is able to form three-dimensional vascular systems, as the groups of cells bond to each other, shown in Figure 2.1e. This is also a slow process and a key challenge is producing a mechanically stable structure capable of perfusion [7]. Multi-cellular spheroids have also been bioprinted alongside an agarose vascular template to form vascular network structures using this scaffold-free approach though the current method is limited in the network complexity that is achievable.

2.3 One Dimensional Vascular Systems

One can use a very simple system to fabricate a vascular-like channel using either needle-molding [21, 168] or wire extraction [121]. This involves mounting a needle, or wire, and casting around them materials such as hydrogels or polydimethylsiloxane (PDMS). Upon removal of the needle or wire, a one-dimensional channel is left which can be seeded with cells and perfused. Since needles and wires are freely available over a wide range of diameters, from the micron to millimeter scale, this simple system is very powerful for studying vascular systems and transport of oxygen and nutrients into the bulk. However, these techniques are clearly limited in the vascular structures that are producible, though one can form arrays of uniaxial channels and simple vascular junctions can also be developed by having these needles or wires cross.

2.4 Microfabrication Techniques for Two Dimensional Vascular Systems

Microfabrication techniques and soft lithography systems enable two-dimensional networks of channels to be fabricated in a highly controlled manner, over a range of length-scales. Recently, a range of lab-on-chip and organ-on-chip approaches have been reported capable of producing quite sophisticated systems, using soft lithography and photo-lithography techniques, such as lung-on-chip (shown in Figure 2.2a) [173], kidney-on-chip, liver-on-chip (shown in Figure 2.2b) [56], and whole body chips [61]. These microfabricated devices consist of multiple layers of channels, with multiple different channel systems and chambers. and can be used to set up a range of growth factor, nutrient, and oxygen gradients, vary flow rates, and form specific micro-environments for various tissue types, in a highly controlled manner amenable to imaging [61].

Standard PDMS channels can be coated with bioactive molecules, which improve cell attachment and cell spreading, and even with layers of hydrogels, such as gelatin and collagen. PDMS systems can then be perfused and studied closely, making them a valuble platform tool for studying the effects of drugs and small molecules. These approaches are excellent for modelling tissue *in vitro* and for undertaking drug discovery and drug delivery projects.

Angiogenic sprouting is limited in these PDMS channel systems since they are made of synthetic polymers that cells cannot degrade. However, it is possible to fill chambers in these devices with biopolymers such as collagen. By seeding surrounding channels with endothelial and supporting cell types, one can study angiogenic sprouting into the bulk hydrogel material, an example of which is shown in Figure 2.2c [175].

A more sophisticated version of the soft lithography approach is to use a PDMS mold as a stamp in collagen gel [175]. By removing the mold and adding a layer of collagen gel to the other side, one can fabricate a single plane of channels which are entirely encapsulated by collagen gel. Thus a three-dimensional gel system is formed with a vascular system, in which cells can be seeded into the bulk or on the channel walls, and can sprout and migrate from the channels into the bulk, as shown in Figure 2.2d. Such systems have been used to study vascular biology, thrombosis, and angiogenesis [175].

Other methods have been developed which make use of photolithography to produce very fine molds made of PDMS (with feature sizes down to 10 μm), consisting of surface grooves into which one can cast gelatin [49] or alginate [165]. Once gelled, the hydrogel materials are removed from the PDMS mold and used as very fine templates of capillary networks. Shown in Figure 2.2e is a gelatin template with template features on the scale of 10-20 μm. Upon casting in a range of other hydrogel materials and liquefication of the gelatin template,

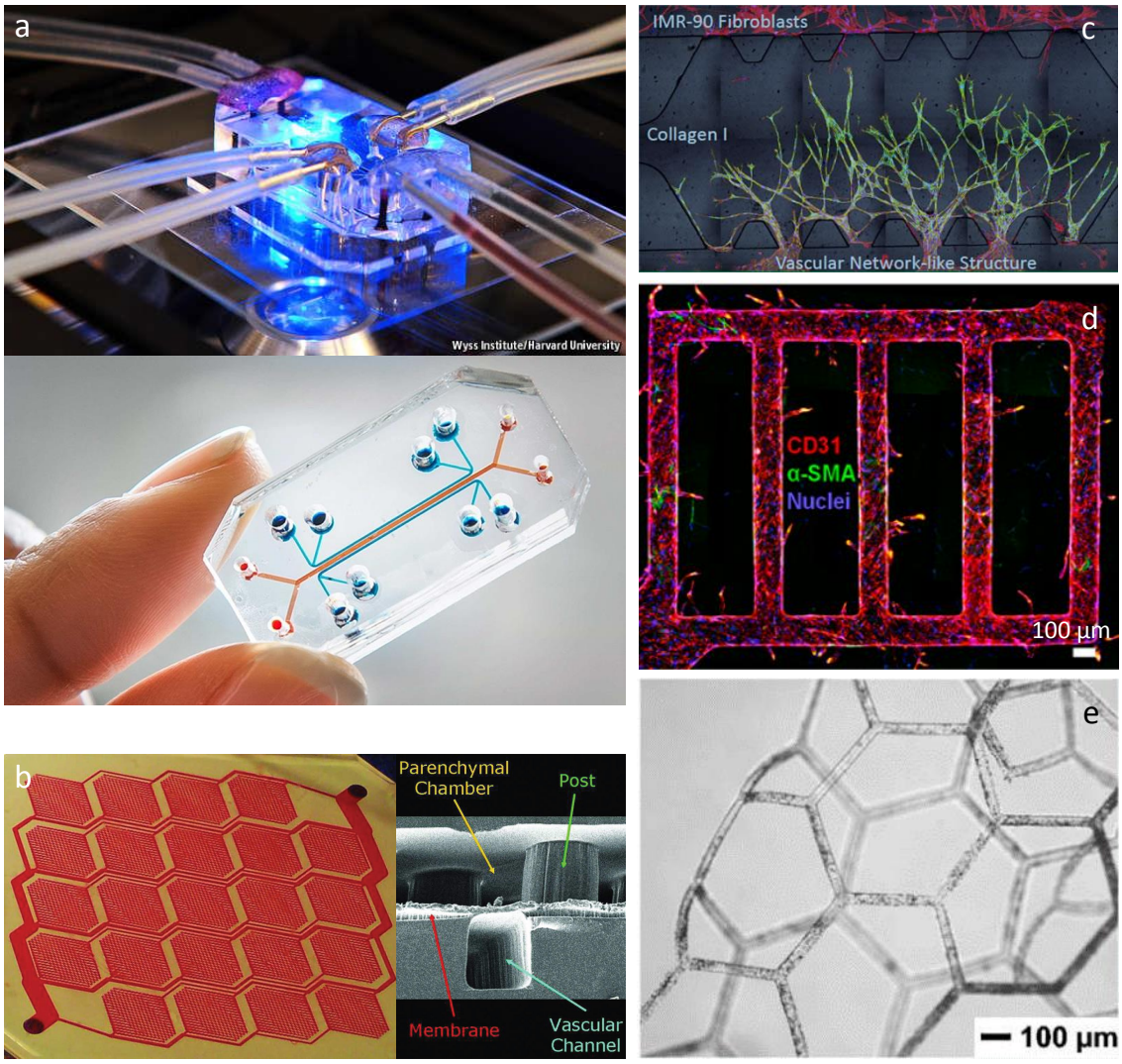

Fig. 2.2 (a) Lung-on-chip system, produced using microfabrication techniques, consisting of multiple flowing channel systems and capable of supporting a variety of different cell types [173]. (b) A lab-on-chip system with multiple compartments organized to support the formation of liver tissue structures [56]. (c) Lab-on-chip systems can incorporate chambers that can be filled with collagen gel. Here, endothelial cells are forming angiogenic sprouts towards fibroblasts on the opposite side of the chamber [94]. (d) A planar channel network can be fabricated inside a three-dimensional collagen gel, using a PDMS stamp approach. This yields structures in which cells can sprout, migrate into, and remodel the bulk collagen gel [175]. (e) Planar gelatin vascular templates can be made by casting gelatin into a PDMS mold [49].

one can produce a planar network in a fully three-dimensional gel. Whilst the ability to produce an interconnected network with features on the microscale was an important step forward, limitations still exist in that only a single plane of channels is achievable from such a system, meaning that only thin fabricated tissue constructs can be supported by perfused channels. Such channels formed in this way also have rectangular cross-sections, which produces a non-uniform shear stress from fluid flow (unlike cylindrical channels), meaning that an endothelial cell lining receives abnormal mechanical cues from that flow [79].

Also relevant here are pseudo-3D systems such as a number of systems involving a layer-by-layer construction of PDMS-molded channels. However, this technique is impractically slow for truly three-dimensional tissue constructs and has issues relating to alignment of the layers. Thus, this microfabrication method has been widely reported [20, 28, 95] but is limited by the lack of three-dimensionality which is achievable from a single plane, or a few multiple planes, of channels.

2.5 Three Dimensional Vascular Systems

A large number of approaches have been suggested for the formation of three-dimensional perfusion systems. A range of techniques exist in the literature that produce macro-porous structures capable of permeating fluid, and which can be seeded with cells [57, 169]. Approaches include freeze-drying and critical point drying, solvent casting, particulate leaching, sintering, and electrospinning, with a vast range of synthetic and biological polymeric materials [96].

Whilst improving the permeability of scaffolds, porous materials like this are limited in the capacity for exchange of nutrients and oxygen, especially at biologically relevant cell densities [101]. At high cell densities, cells near the surface of the structures tend to multiply and block transport of nutrients to the inside, thus producing the formation of necrotic cores. Further, most normal tissues have vessel systems and there is a difficulty associated with getting these vessels to spread throughout a twisting porous structure [79]. Also, porous scaffolds have no defined single inlet and outlet and so make anastomoses with native tissue difficult [79]. The lack of directionality in fluid flow also means that any mechanical cues cells may take from blood vessel flow may be lost [79]. Finally, the harsh conditions and processes for making these porous structures prevent the incorporation of cells into the construct until after the scaffold is complete.

3D printing, also known as additive manufacturing, rapid prototyping, or freeform fabrication, describes a range of different fabrication techniques that build up a structure layer-by-layer (rather than subtractive manufacturing or casting techniques). This includes

methods for extrusion-based printing, inkjet printing, and photo-crosslinking of polymers in 3D. A vast array of different materials can be printed via various approaches at relevant length-scales for tissue engineering, to form fully three-dimensional structures.

Inkjet printing produces very fine features from thermoplastics and waxes via an inket process, which is shown in Figure 2.3a. Briefly, build and support materials are passed from a heated reservoir to a heated print head, which are deposited in a fine stream of droplets onto a ceramic substrate. The material rapidly cools and hardens forming solid structures. After each layer is deposited, a plane milling head is passed across the build platform which mills the material into a very fine layer (we used a 12 μm layer thickness). The build stage is then lowered and the process repeated until the full structure is completed. Since the support wax can be removed afterwards, it is possible to fabricate large overhanging features. Inkjet printing has the advantage of high accuracy, owing to the very fine spray of material from the nozzle [22].

In fused deposition modelling (FDM), thermoplastic filament (e.g. ABS, PLA) is heated to just above its melting point and extruded through a nozzle onto the substrate; repeating this process builds up a three-dimensional structure (the setup for this approach is shown in Figure 2.3b). Support materials can also be printed by this method to produce overhanging features and large build volumes are achievable with this approach [22]. However, FDM suffers from poor accuracy and reproducibility; the diameter of the filament and distortions from rapid cooling of the filament upon deposition limit the accuracy which is achievable by this method [22].

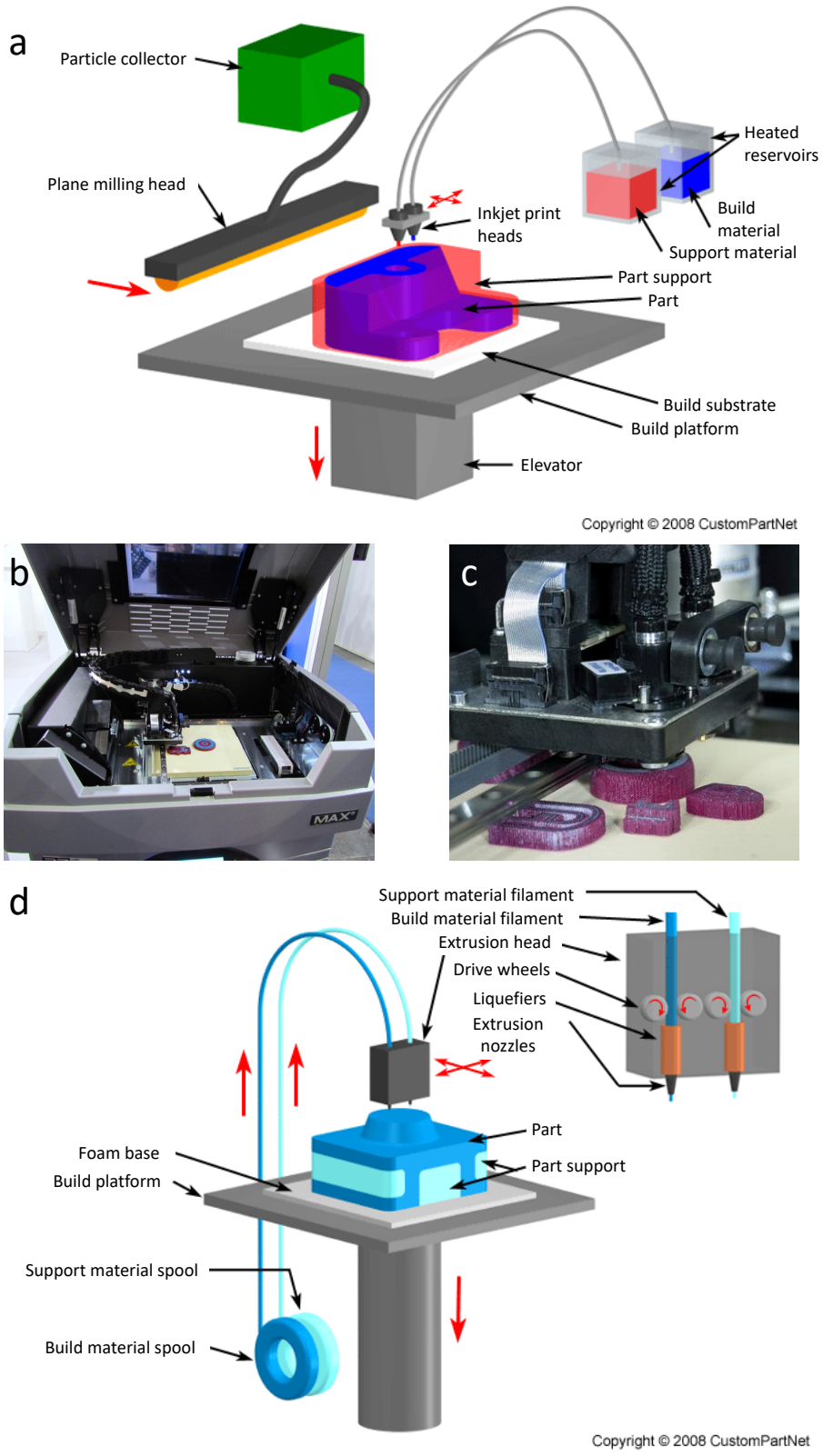

Fig. 2.3 (a) Inkjet 3D printing process [30]. (b,c) Solidscape 3D printing technology, which is used extensively in this project [43, 1]. (d) Fused deposition modelling (extrusion-based) 3D printing process [30].

Stereolithography (SLA) and two-photon polymerization (2PP) are techniques which enable photopolymers to be crosslinked when laser light is shone upon them, usually in the presence of a photo-initiator [37]. Such methods are capable of producing very fine features limited by the focal spot size of the laser and therefore can produce features at the micron length-scale. Materials used are often PEG or gelatin based, such as PEG-DA, which allow for good adhesion and functionality of the cells. However, the crosslinking mechanism is quite harsh (laser light, chemical photoinitiators) and so most constructs tend to be seeded with cells after fabrication (though not always). Since photocrosslinked materials are heavily crosslinked, they can only be used as the matrix material and not as a template for the channel system, though materials consisting of a photocrosslinked part and a second soluble part, may allow them to be fabricated into complex template structures via photocrosslinking and then removed by thermal or chemical means. Figure 2.4 shows examples of PEG-based stereolithography. It is possible to fabricate branched structures in this material with fine feature sizes.

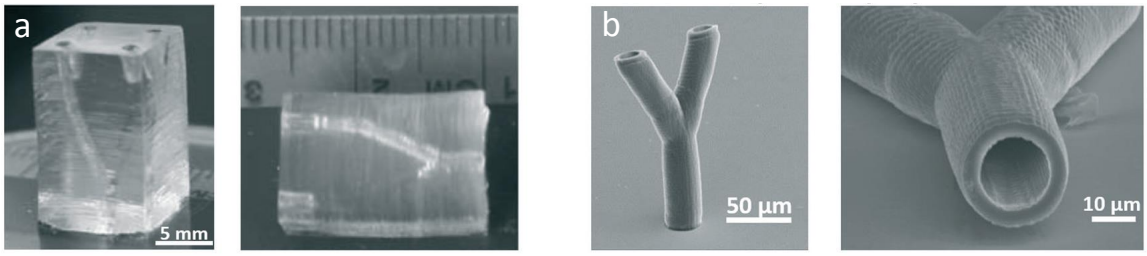

Fig. 2.4 PEG-based hydrogels can be photocrosslinked to form vascular channels. (a) PEG hydrogel stereolithography using a multi-photon variant [79]. (b) Stereolithograhy of PEG hydrogels can produce finely branched vasculature [79].

In sacrificial or indirect 3D printing, one prints a removable template structure for the vascular system and then casts the structure in various hydrogel materials, thereby producing a complex vascular system in ideal matrix materials. Since casting is used to produce the bulk matrix, and since this is done after fabrication of the template is complete, cells can be pre-loaded into the bulk gel prior to gelation. This enables a high density and uniform distribution of cells to be employed using methods which are minimally damaging to the cells.

A range of approaches have been reported in the literature in which the template structure is fabricated using a 3D printing apparatus, with the template material either Pluronic F127 [84], sugar carbohydrate glass [109], or agarose [14]. One other noticeable example uses fugitive inks which are deposited from a nozzle into a reservoir of Pluronic F127-diacrylate, which can be photocrosslinked afterwards and the template material liquefied

at low temperature [170]. This yields complex vascular designs, as shown in Figure 2.5a. Rather than create a template under fluid, others have 3D printed freely-hanging vascular templates, as shown in Figure 2.5b-d.

However, the direct use of a 3D printing rig to produce the template structure severely limits the architectures that are possible. Invariably, the technique involves drawing out a fiber from a nozzle, thereby yielding a 1D filament, which is the case in Figure 2.5b-d. In the case of the sugar-carbohydrate glass (Figure 2.5c), the speed of the nozzle determines the thickness of the template feature and junctions are created via the joining with other 1D filaments [109]. Further, the vast majority of methods for the formation of three-dimensional vascular templates yield three-dimensional arrays of channels as opposed to a hierarchical, branching network [155].

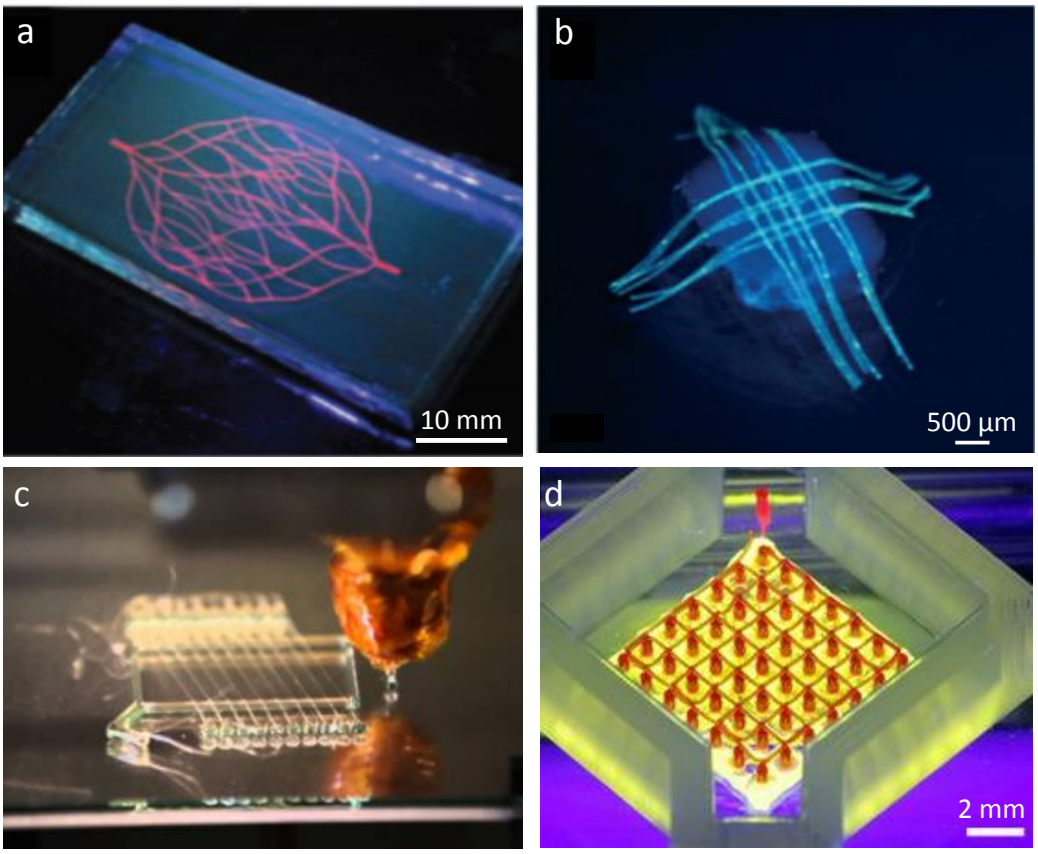

Fig. 2.5 Sacrificial 3D printing techniques for the formal of vascular networks. (a) 3D printing of sacrificial fugitive inks into a photo-crosslinkable reservoir of Pluronic F127-acrylate material [170]. (b) Agarose template material printed onto a bed of photo-crosslinkable PEG-DA [14]. (c) Sacrificial 3D printing of sugar carbohydrate glass [109]. (d) Freely hanging pluronic template consisting of pillars and overhangs [84]. Note all four approaches generate a sequence of 1D filaments which form junctions by touching at various locations.

Other work has used removable, thermoplastic 3D printed models to produce internal channels in porous scaffolds, such as with freeze-dried collagen [138, 97] and PCL (collagen coating on the channels) [74]. However, they require freezing and harsh solvents as a means of formation of the scaffold and removal of the channel template material. Thus they must remain acellular until after the process is completed and both approaches require the collagen to be chemically crosslinked for stability. Finally, 3D printed materials have recently been cast in PDMS and removed to reveal a 1D helical channel (500 μm in diameter) [139]. The use of PDMS as the bulk material limits the use of cells to the channels only.

2.6 Microfluidic Concepts

Murray's law [117, 145, 103] relates the diameter of daughter branches to that of the parent branch for a hierarchical vascular system, usually quoted as the addition of cubic terms though experimentally, the exponent has been measured to vary between 2 and 3,

$$D_0^3 = D_1^3 + D_2^3 \tag{2.1}$$

where D_0, D_1, and D_2 are the diameters of the parent and daughter channels, respectively. This equation holds for symmetrically and asymmetrically branching networks and produces a network with constant shear forces at the channel surfaces. There are also other relations that are referenced, relating the lengths of the parent and daughter branches, usually following a similar relationship.

The bifurcation angle is also something which must be considered in any flow system. High angles between parent and daughter branches allow for large volumes to be plumbed in a spatially efficient manner. However, a junction is associated with a change in the velocity of the perfusate and so generates turbulence. Such viscous flow can be detrimental to the endothelial layer.

At the bifurcation, the flow rate, Q, is conserved such that

$$Q_0 = Q_1 + Q_2 \tag{2.2}$$

where Q_0, Q_1, and Q_2 are the volumetric flow rates in the parent and daughter channels, respectively. The cross-sectional shape of the channel matters as well when considering flow. Rectangular-shaped channels produce non-uniform shear stresses at the walls, which is detrimental to an endothelium to the abnormal mechanical cues it imparts to the cells [79]. One must also consider the pulsatility of the source. Pulses of too high magnitude produce high shear forces which can rip cells from the channel walls. Air bubbles are also a big

problem for microfluidic systems. An air bubble in the system can generate a huge amount of drag upon the channel walls and shear the cells from it. Further, it will generate a large pressure drop across the channel and prevent flow, thereby increasing the flow rate around other parts of the network (for the same inlet flow rate).

Nutrients and oxygen are transferred to the bulk tissue via diffusion from the capillaries and interstitial flow (advection), caused by the difference in pressure from one end of the capillary to the other. To achieve this transfer, there is a balance of hydrostatic and oncotic pressures which drive the movement of fluids and thus nutrients and oxygen down osmotic gradients. By this process of filtration and re-adsorption, oxygen and nutrients are effectively delivered to cells, dependent on the diameter and flow rate of the channel. For a single uniaxial channel, the pressure-drop across the length follows the Hagen-Poiseuille law,

$$\Delta P = Q\left(\frac{8\mu L}{\pi r^4}\right) \tag{2.3}$$

where ΔP is the pressure drop across the channel, Q is the volumetric flow rate, μ is the dynamic viscosity, L is the channel length, and r is the channel radius [171]. For a symmetric system of bifurcating channels, the flow rate of the daughter branch is half that of the parent channel [171]. When expanded for multiple levels of bifurcations, the pressure drop across any path through the network can be calculated [171]. Our system consists of 5 channel sizes (including inlet channels) which symmetrically bifurcate and then recombine to a single outlet. Since the anastomosing channels are the same diameter and length as the bifurcating channels, the pressure drop contributions from those channels can be combined. Thus the pressure difference, ΔP, across any path of the network can be written as,

$$\Delta P = Q\frac{8\mu}{\pi}\left(\frac{2L_0}{r_0^4} + \frac{L_1}{r_1^4} + \frac{L_2}{2r_2^4} + \frac{L_3}{4r_3^4} + \frac{L_4}{8r_4^4}\right) \tag{2.4}$$

where Q is the volumetric flow rate at the inlet, and L_i and r_i denote the length and radius of a specific bifurcation level i in the network, respectively. Note that since the network is symmetric, every path through the construct will have the same pressure difference across it.

2.7 Hydrogel Materials

This project makes extensive use of the physical and chemical properties of a number of hydrogel materials. Briefly, a hydrogel (or gel) is a macromolecular polymer network that consists of a solid phase (i.e. the polymer) and a liquid phase (i.e. water) [99]. They can absorb and trap huge volumes of water; a property that arises from hydrophilic functional groups on the polymeric backbone; the solid phase of the gel does not dissolve in the solvent,

owing to crosslinks between network chains [107]. Gels can be classifed by the way the network is formed; either by chemical (i.e. ionic or covalent interactions) or physical (i.e. reversible non-covalent interactions) with the latter occurring due to pH, temperature, ionic changes or solvent exchanges [52, 36, 146].

Hydrogels can be made from either synthetic (e.g. PVA, PEG, N-isopropylacrylamide [69]), or biopolymers (e.g. collagen, gelatin, alginate, agar, hyaluronic acid [9], fibrin [3]). Biopolymers in particular are an excellent material on which cells can function, primarily due to their tunable mechanical properties and porosity, and hydrophilic nature. Some biopolymers made from proteins also have various binding sites and peptide sequences in their structure which are actively recognised by cells and bonded to by a various signalling molecules.

Gels exhibit a number of phenomena, including syneresis (spontaneous contraction of solid phase) and swelling (absorption of water), and can be sensitive to multiple factors, including pH, temperature, ionic content, light, mechanical force, electric and magnetic forces, and other chemical interactions (such as further chemical crosslinking) [163, 66]. Various polymers, most notably sodium alginate, form reversible ionically-crosslinked networks when soluble calcium is added to the solution. Also relevant are high viscosity, shear-thinning polymer solutions which gel upon the removal of the injection shearing force (such as hyaluronic acid gels) [52]. One will often see descriptions of hydrogel formation by sol-gel thermal phase transition behaviour [65, 67] or by photopolymerization [13]. Many excellent reviews exist on the formation, properties and tuning of hydrogels [146, 67, 99]. For tissue engineering, such gels are employed as a bulk casting material, or as thin sheets onto which cell culture is performed, and often display similar properties to collagen and fibrin. However advantages can be found in their inexpensive and simple means of production, and the ability to be combined with other materials.

Of particular relevance to this project are gelatin, alginate, fibrin, and collagen hydrogels. Gelatin is a biopolymer which has found a wide range of uses in the pharmaceutical industry, for soft and hard drug capsules, and also in food technology. It is made from denatured collagen, in either acidic or basic conditions, which can yield different properties (i.e. isoelectric point, gel strength, etc). It forms hydrogels via a sol-gel process in which self-assembled helices of gelatin create a macromolecular network, when the temperature is lowered below a critical threshold, determined by a range of factors (gel strength, pH, ionic content, concentration, etc). Gelatin gels can be crosslinked via a range of chemicals to produce a range of mechanically robust gels, for a wide range of applications.

Alginate is a naturally occurring anionic copolymer extracted from brown algae and is comprised of guluronate and mannuronate blocks [48, 89]. Sodium alginate can form

hydrogels via ionic bonding of calcium to these groups, which bind the polymer into a large network. As a gel, it has a number of useful physicochemical properties. A range of gels can be produced with different properties, such as viscosity, porosity, and type of crosslinking cation. Alginate gels are also thermally stable, making it particularly useful alongside other thermogelling polymers. It finds application in the encapsulation of cells and for controlled drug release, and also in food technology as a stabilizer and thickener [48]. It is also widely used in dental applications as a casting agent for taking impressions [33].

Collagen is the main constituent protein of the extracellular matrix which is organized into a heterogeneous structure by the cells, which generate, remodel, and degrade the collagen network. The collagen polymer itself consists of a triple helix which is self-organised through several steps into a hierarchically organised fiber network in a process called fibrillogenesis [70]. These fibers then interact physically and chemically with each other, and other intermediate molecules which, under the right thermal, pH and ionic conditions, form a hydrogel. Collagen, like gelatin, can be crosslinked via a number of chemical processes, most notably with glutaraldehyde [31] or EDC/NHS crosslinking [32], and also via enzymatic means using transglutaminase [126].

Fibrin is the main component of the wound-healing matrix material and finds applications in tissue engineering as an ideal substrate and in surgery as a biocompatible and resorbable surgical glue [147]. Fibrin clots form *in vivo* via a complex process known as the coagulation cascade. Fibrin gels are formed *in vitro* by the cleaving of fibrinopeptides from the fibrinogen molecule by thrombin [147]. Fibrinogen molecules then form a crosslinked hydrogel matrix. Fibrin networks can be crosslinked further via a second enzyme called transglutaminase which forms isopeptide bonds between lysine and glutamine residues. Like collagen, fibrin is freely degradable by cells [167] but also plays a key biological role in wound healing (which includes angiogenesis) making it an ideal material in which to perform capillary morphogenesis experiments.

2.8 Future Aims of the Field

The ability to fabricate a wide range of different channel architectures is a significant aim in the field. All the approaches described above are limited in one or more ways when it comes to fabrication of complex architectures in biological relevant materials and in the presence of cells. Thus new methods are required to produce channel networks that are the same time three-dimensional, hierarchical, and perfusable.

In order for a tissue construct fabricated in a lab to be useful medically, it is necessary for high densities of cells to be incorporated into these devices, in a way which enables them

to survive and modify the surrounding environment. Currently, most systems are several orders of magnitude lower in cell density than that required for a therapeutic advantage in translation [108]. No one method is presently able to produce features over the range of length-scales present in native vasculature. Thus the near future of the field is likely to involve a combination of both biomaterials-based approaches, such as those described above, and cell-based approaches, for capillary bed formation, and also the maturation of the large-scale vasculature. Thus full hierarchical networks remain a future aim of the field.

Finally, the formation of vascular structures *in vitro* similar to those found in real organs is also future aim of the field. Whilst there is likely to be a considerable amount of remodelling by the cells on the architecture of the construct, this is a slow process and it should be possible to design networks that at least imitate the gross structure of living tissue found in nature.

2.9 Chapter Summary

In this literature review chapter, a wide range of materials-based techniques for forming vascular networks have been examined. The challenges present within bioprinting were discussed, such as the hydrophilicity of ideal tissue engineering materials, issues relating to maintaining a cell population during the very slow process of printing fine features, and the loss of viability from shear stresses applied to cells upon deposition. Alternate bioprinting methods involving scaffold-free methods were also discussed, though suffer from lack of mechanical robustness. One-dimensional and two-dimensional vascular systems were described, though are limited by the degree of three-dimensionality that is achievable. 3D printing-based methods were described, including inkjet printing, fused deposition modelling, and stereolithography. The lack of suitable bioactive materials limits their use in producing large scaffolds and harsh fabrication conditions (such as chemical photocrosslinkers) can limit cell viability or inhibit their incorporation into the scaffold until after the scaffold production is complete. Sacrificial 3D printing of polymers such as agarose, sugar-carbohydrate glass, and Pluronic F127 show promise as a means of producing vascular templates in three dimensions, using a 3D printing apparatus. However, they are limited in the architectural complexity that is achievable from drawing out polymeric fibers of material. This chapter also explored relevant microfluidic concepts useful in network design and briefly described the range of hydrogel materials that are used in this project.

Chapter 3

Multi-Casting Approach for 3D Printed Networks and Cell-Based Evaluation

3.1 Summary and Overall Process

As described in the previous chapter, tissue engineering requires new fabrication methods for meso- and large-scale vasculature; one of the most promising approaches at this time is the use of sacrificial 3D printing to create a vascular template and cast a polymeric matrix around it. We require this template to be three-dimensional, customizable, reproducible, and made of a material which can be used alongside bioactive hydrogel materials, such as collagen and fibrin, and which can be removed in the presence of cells. With such a template, one can cast matrix materials which are preloaded with cells, producing constructs of a uniform cell distribution. The ability to cast and gel the construct at once allows a minimal amount of time between cell seeding and perfusion, meaning high cell viability can be maintained and high densities of cells can be used.

We have developed a new approach to sacrificial 3D printing in which we convert a standard 3D printed thermoplastic material into a gelatin template. This enables the fabrication of templates, which are highly complex in design, reproducible, and can be used alongside cell-ladened hydrogel materials. This conversion of 3D printed materials into gelatin is performed by casting with an alginate hydrogel intermediary to produce a negative of the vascular template. Alginate, which is ionically crosslinked with calcium ions, has long been used as casting medium in dental and other applications. By casting the 3D printed material in alginate and removing the 3D printed material, we are left with a negative mold into which we can cast gelatin. By removing the alginate gel, a gelatin template is produced of the original 3D printed design; this template is made from a single piece of gelatin and

as such, has no inherent weaknesses between layers (however the gelatin template is still fragile). The gelatin template is then cast in either an extracellular matrix-like, thermo-gelling collagen gel, or a wound-like, enzymatically crosslinked fibrin gel. By placing the construct in a 37°C water bath, the gelatin is quickly liquefied and the channel network made patent. Perfusion can then begin promptly. This method puts minimal strain upon the cells and thus should maintain a high viability. Thus, by making use of the different physical and chemical properties of a number of disparate polymers, we are able to bring together a process for making architecturally useful structures, in three-dimensions and with very fine features, using a template material which can be cast in ideal and cellularized biomaterials. This multi-casting process is described in Figure 3.1.

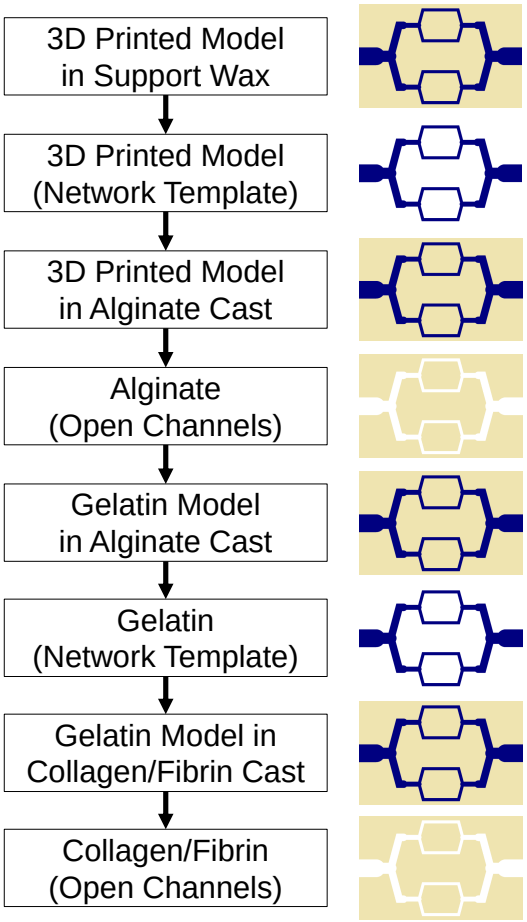

Fig. 3.1 Diagrammatic representation of the multi-casting process. 'Network template' denotes a solid cast of the channel structure and 'open channels' denotes the inverse cast in which fluid can be perfused through the channels.

As part of this work, preliminary cell experiments were undertaken in order to evaluate the ability of the network to support fibroblasts added to the bulk hydrogel. This provided information on cell viability and cell spreading, for a range of flow rates. We also seeded the channel surfaces with endothelial cells and observed tight junctions between them.

The initial development of the technique was further improved with a new chamber fabrication approach, investigating the addition of a chamber coating, a new 3D printed model design, and a number of other changes which improved the robustness of the approach. Such steps were deemed necessary in order that more advanced experiments, including capillary formation, could be performed successfully.

3.2 Materials and Methods

3.2.1 Cell Culture

Human umbilical vein endothelial cells (HUVEC, Public Health England) and human dermal adult fibroblasts (HDFs, Public Health England) were used for the experiments. The cells were trypsinized using TrypLE Express (Life Technologies), centrifuged at 250 g for 5 min, and counted using a Scepter Cell Counter (Millipore). HUVECs were cultured in a T75 flask to 80% confluence, using endothelial growth medium (no vascular endothelial growth factor or platelet-derived growth factor) (EGM Plus, Lonza), and HDFs were cultured in a T75 flask to 80% confluence using high-glucose Dulbecco's modified eagle medium (Life Technologies) containing 10% fetal bovine serum (FBS, Life Technologies).

HUVECs were imaged using Green Cell Tracker dye (Life Technologies), allowing for immediate imaging and tracking of cell seeding and distribution in the channels. Lyophilized fluorescent dye was resuspended in dimethyl sulfoxide (DMSO, Sigma) at 10 mM and stored at -20 °C until use. A working solution was prepared in DMEM at 10 μM. Plated cells were washed with phosphate buffered saline (PBS, Life Technologies) and the working solution added. Flasks were incubated at 37 °C for 45 min prior to trypsinization.

3.2.2 3D Printed Design and Printing

The CAD model vasculature was designed using Autodesk Inventor 2014 (Figure 3.2a); the structure consists of a 1 mm inlet which symmetrically bifurcates into a series of 200-250 μm channels, which then converge into a single outlet of 1 mm. Thermoplastic models in support wax were a gift from Solidscape UK. Models were fabricated using 12 μm layer thickness and 10 base support layers, on a 3Z Studio printer. Following printing, models in support wax were removed from the ceramic base (8 mm) by placement on a hot plate at 120 °C for 7 min.

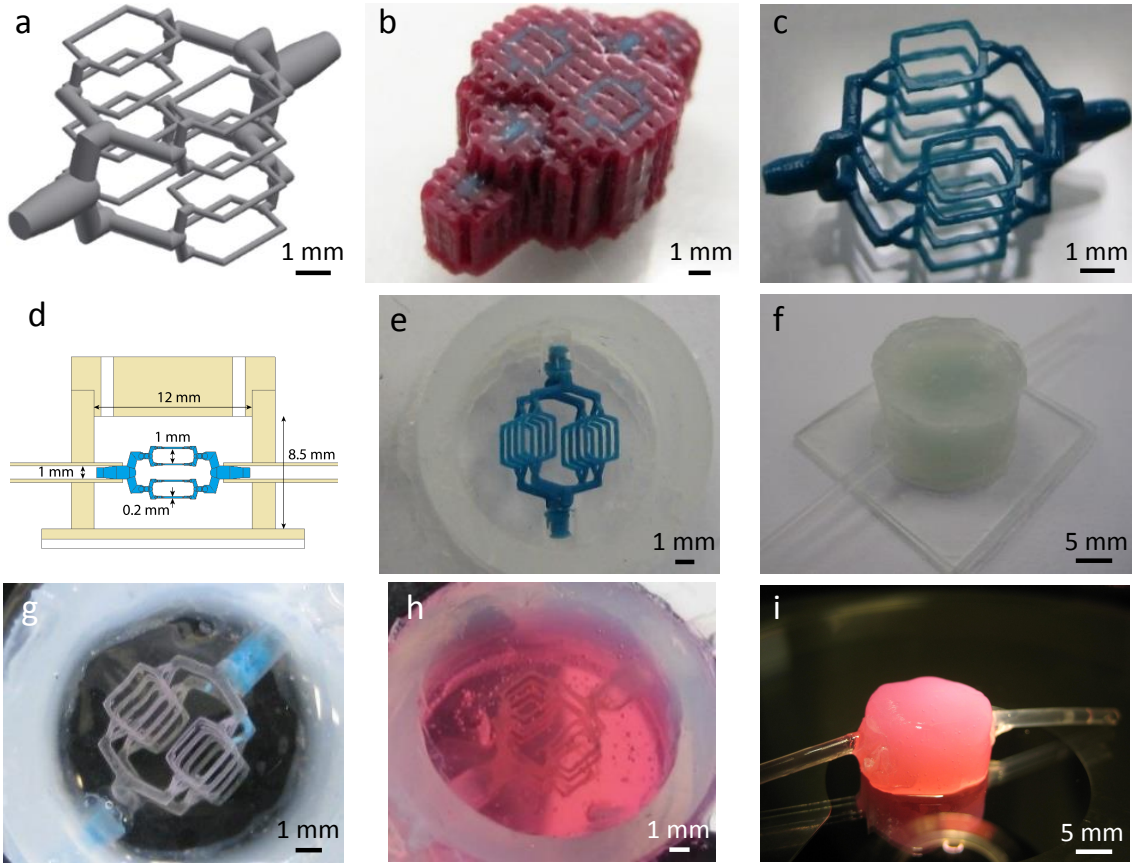

Fig. 3.2 Process steps for converting CAD model into hydrogel channels. (a) CAD design, consisting of 1 mm inlet symmetrically bifurcating to sixteen 200-250 µm channel features. Each of the finest channels is 2 mm in length. (b) Using a Solidscape 3D printer, models are produced in support wax. (c) Support wax is removed using a selective solvent to reveal a high precision thermoplastic model. (d) Schematic of custom-made silicone chamber; consisting of a silicone sheet mounted on a glass imaging slide, thick-walled silicone tubing for chamber walls, flexible silicone tubing for inlets, and a CNC-milled silicone lid, which has two holes for casting. Also shown is the 3D printed model from (a) for size comparison. (e) Model is mounted into silicone chamber. (f) Chamber is filled with alginate hydrogel and a lid is fitted to the chamber. (g) Following model removal with heat and acetone, gelatin is infiltrated into the channels, and the alginate is removed by chelation. (h) Gelatin template is cast in collagen (shown here) or fibrin hydrogel, which can be loaded with cells prior to gelation. (i) Collagen gel, containing vascular channels, can be removed from chamber and perfused.

Models in support wax could then be gently removed using stiff card. To remove the support wax from the models (Figure 3.2b), they were put in a bath of selective solvent (BioAct VSO, Solidscape) and placed in an oven at 55 °C for 4 h. The model was subsequently stored in fresh solvent at room temperature, until use (Figure 3.2c).

3.2.3 Silicone Chamber Design and Model Mounting

The vascularized hydrogel was produced in a custom-made silicone chamber. For the base, a 1 mm silicone sheet (Silex) was adhered to a glass imaging slide (Fisher Scientific) and a section of 12 mm internal diameter silicone tubing (VWR) attached to this sheet, both using silicone sealant (Dow Corning). Two holes were drilled on opposite sides of the chamber and flexible silicone tubing with 1 mm internal diameter (VWR) fitted. A silicone lid was made using a CNC milling machine from a 3 mm silicone sheet (Silex), into which two 2 mm filling holes were drilled (chamber design shown in Figure 3.2d). The models were briefly dried on tissue paper and then very carefully placed between the filled silicone inlets using tweezers. The inlets were rotated so as to angle the model such that all channel features are visible under an optical microscope at the same time (Figure 3.2e). The silicone inlets were then super-glued in place.

3.2.4 Alginate Preparation

Calcium alginate gels were prepared using an 'internal setting' method. This involved adding 300 mM $CaHPO_4$ (Sigma) and 600 mM gluconolactone (Sigma) to 7.5% (w/v) sodium alginate (Sigma). In order to prevent the trapping of bubbles between the fine features of the 3D printed template, the chamber was first filled with DI water. The viscous alginate precursor solution was then slowly injected into the silicone chamber, displacing the water and fully encapsulating the thermoplastic model. The gluconolactone functions as an acidifier and causes the slow release of calcium, enabling a controlled gelling mechanism and a uniformly crosslinked hydrogel. The alginate gel was left overnight at 4 °C for maturation (Figure 3.2f).

3.2.5 Model Removal and Gelatin Template Preparation

The model material was removed by placing the chamber in a bath of near-boiling DI water. After 5 min, the liquid model material was removed from the channels by gentle suction with a 1 mL syringe. Following 10 min on ice, the channel structure was cleaned by injecting 2 mL of acetone into the channels to purge any remaining model material. Subsequently,

6 mL of 250 mM $CaCl_2$ (Sigma) was injected around the network which crosslinks the surface of the alginate channels more thoroughly, without causing syneresis of the gel.

Liquid gelatin (Sigma, porcine skin, low bloom, 15% (w/v), pH 7.4) was infiltrated into the channel structure via suction. The chamber lid was removed and the chamber placed in a bath containing 200 mM sodium citrate (Sigma) and 200 mM glycine (Sigma) to chelate the calcium crosslinking ions, and was then left for 24 h at 4 °C, at which point the alginate was fully dissolved into solution. Once the alginate gel had dissolved, the chamber was placed in a bath of sterile, calcium free PBS to remove any residual alginate in the chamber, and a lid attached under liquid, which was then sealed using super-glue. The chambers were finally purged of any remaining citrate or alginate by flowing 5 mL of PBS through the lid holes (Figure 3.2g).

3.2.6 ECM Hydrogel Preparation

Collagen hydrogels were used at 7.5 mg mL^{-1} final concentration. Soluble collagen solution was prepared using rat tail tendon. We solubilized the tendon using 0.1% (v/v) acetic acid on a magnetic stirrer (250 mL/g tendon) for 60 h at 4 °C, and centrifuged the solution at 9000 g for 90 min. The collagen was subsequently lyophilized, weighed, and resuspended at the required stock concentration in 0.1% (v/v) acetic acid. Collagen was gelled using a standard approach [113], employing the addition of 10×M199 (Sigma), 1 M NaOH, and 0.2% (w/v) $NaHCO_3$ (Sigma), in order to raise the ionic content and pH of the collagen solution, thereby inducing a gelling response. HDFs were carefully mixed into the neutral precursor solution at 1×10^6 cells mL^{-1}, just prior to casting. Owing to the high viscosity of the collagen solution, it was injected slowly on ice into the chamber using a syringe pump at 15 mL hr^{-1}, displacing the PBS supporting the gelatin template (Figure 3.2h). Following 20 min at room temperature, the chamber was placed for an additional 20 min in a sterile 37 °C bath which rapidly gelled the collagen and melted the gelatin. Collagen hydrogels could be removed from the silicone chambers at this point and connected directly to silicone tubing (Figure 3.2i). However, it is preferable to continue to keep the gels in the silicone chamber to maintain their shape and keep them under positive pressure.

Fibrin hydrogels were produced using a final concentration of 10-20 mg mL^{-1} bovine fibrinogen (Millipore) and 2 U mL^{-1} human plasma thrombin (Sigma). Lyophilised fibrinogen was resuspended in pre-warmed 0.9% (w/v) NaCl at 60 mg mL^{-1} and thrombin was resuspended in 0.9% (w/v) NaCl at 50 U mL^{-1}. Both were stored at -20 °C until use. 0.1 M NaOH was added to the fibrinogen solution to raise the pH to 7.4. HDFs, in cell medium, were carefully mixed into the precursor solution at 1×10^6 cells mL^{-1} and thrombin was added just prior to casting. The solution was subsequently loaded into a 1 mL syringe

and injected into the chamber via the lid holes, displacing the PBS supporting the gelatin template. Following 5 min at room temperature, the chamber was placed in a sterile 37 °C bath for an additional 15 min, which melted the gelatin.

3.2.7 Gelatin Removal, Channel Seeding, and Perfusion

Channels were checked for patency using fluorescent 1 μm red tracer beads (Life Technologies). HUVECs were subsequently suspended in 100 μL of endothelial growth medium and injected into the channels at 2×10^7 cells mL^{-1}. The chamber was left for 5h-overnight prior to commencing perfusion. Non-adherent HUVECs were flushed from the channels and perfusion continued with endothelial growth medium at 0.1 mL hr^{-1} for 7 days, using a syringe pump. For HDF experiments, high-glucose DMEM containing 10% FBS was perfused at a range of flow rates (1-30 mL hr^{-1} at the 1 mm inlet) for 7 days using a peristaltic pump, and the medium reservoir was replaced every 2 days. The perfusion circuit (Figure 3.3d,e) for bulk cell experiments consisted of a peristaltic pump, media reservoir, with membrane for pressure equalization; pulsatililty dampening chamber, to reduce the high pulsatility generated by the peristaltic pump; a bubble trap, which prevents destructive air bubbles from entering the device; and humidified experimental chamber, preventing evaporation from the construct through the PDMS chamber walls.

3.2.8 Characterization of Microchannel Formation

After 7 days of perfusion, the development of tight cell-cell junctions between the channel HUVECs was determined using CD31 immunocytochemistry. Cells were fixed by injecting 4% (w/v) paraformaldehyde (PFA) into the channels and leaving the chamber at 4 °C for 1 h. Following three 5 min washes with PBS, a permeabilizing solution containing 0.25% (v/v) Triton X-100 (Sigma) was injected into the channels for 10 min at room temperature, followed by a blocking solution of 1% bovine serum albumin (BSA, Sigma) for 30 min at room temperature. The primary antibody, mouse monoclonal anti-CD31 (HEC7, Abcam), was added at 1:100 in 1% BSA, injected through the inlet and incubated overnight at 4 °C. Unbound antibody was flushed out using three 5 min washes of PBS, and a secondary antibody, goat anti-mouse IgG H&L conjugated to AlexaFluor 568 (Abcam), was added at 1:200 in 1% BSA, injected into the channels, and incubated for 2 h in the dark at room temperature. The unbound antibody was subsequently flushed out using three 5 min washes of PBS. Fluoroshield with 4',6-diamidino-2-phenylindole (DAPI, Life Technologies) was subsequently injected as a nuclear counterstain. Cell viability was performed using a Live-Dead kit (Life Technologies). Fibrin gels containing 1×10^6 cells mL^{-1} were cross-sectioned

through the center of the construct, and the surface stained with 1 μL mL^{-1} calcein AM and 4 μL mL^{-1} ethidium homodimer-1. After 20 min, slices were washed in PBS and imaged.

3.2.9 Imaging

Imaging was performed using phase contrast and epi-fluorescent microscopy (Zeiss Observer.Z1 with ORCA-Flash4.0). Images were processed using Zen software (Zeiss) and ImageJ. Other images were taken using an overhead microscope (Olympus SZX16 with PixeLINK camera and software), and also with an optical camera (Canon Digital IXUS70).

3.2.10 Statistical Analysis

Statistical analysis of live-dead data was performed using IBM SPSS Statistics 23. Cells were manually counted using ImageJ by taking representative sample areas of 1 mm^2 (at least 4 were analyzed per flow rate). A Levene's test showed variances were not homogeneous and so a comparison of values was carried out using a Kruskal-Wallis and a Games-Howell post hoc test. Differences were considered statistically significant for $p < 0.05$. Data is presented as the mean $\pm$ standard deviation.

3.3 Discussion

The channel network produced for this study has a hierarchical structure, with channels bifurcating symmetrically from 1 mm to 200-250 μm, producing a single inlet and outlet, and sixteen channels to support a large three-dimensional volume. 3D printed models are prepared using a commercially available printer, mounted into a custom-made silicone chamber which is filled with alginate gel. Following evacuation of the 3D printed model material from the alginate cast, gelatin is subsequently infiltrated into the channels and the alginate is removed by chelation of the crosslinking calcium ions. This template is then cast in a collagen or fibrin gel, which can be pre-loaded with cells, and the gelatin liquefied at 37 °C.

The use of standard CAD and commercial 3D printing to generate the first stages of the process conveys a high degree of precision and reproducibility to the gelatin, and thus the vascular channel structure. Some 3D printing technologies have a noticeable weakness in terms of accuracy and reproducibility (e.g. fused deposition modelling technology [22]. However, Solidscape inkjet technology has a notably high accuracy [22] and displays the necessary degree of reproducibility required for this project, though there still exists some spread in the diameters of the finest features that were printed (see Figure 3.4b). This is likely since the finest features of the models are at the lower limit of what is printable on these machines. Despite this, the Solidscape machines enable very precise features to be fabricated at significant volumes, and the use of support wax enables a wide range of designs, including overhanging features. Additionally, there is some choice in the shape of the channel cross-section and the morphology of the channel junctions. Thus, our approach enables gelatin templates to be fabricated with a highly complex and fine network architecture, which is fully scalable.

The CAD design in this study was influenced by a number of considerations, including a correspondence to physiological channel structures and fluidic conditions, but also to an ease of handling and imaging. Vascular systems are constrained physiologically by a number of relationships, most notably Murray's law relating parent and daughter branch diameters, usually quoted as the sum of cubic terms which, amongst other results, yields a constant shear force around the whole network [145, 11]. In this study we have designed a network that uses the sum of squared terms. If we were to follow the sum of cubic terms, a higher number of bifurcations would be needed and the same volume would have a much higher density of channels. Mounting of the 3D printed models requires an inlet size that is not difficult to handle; hence we used inlets with a diameter of 1 mm. For ease of imaging, a template was desired with fewer channels such that there is minimal overlap between them. The chamber is constrained in this study to a volume of 1 mL in order to maximize cell

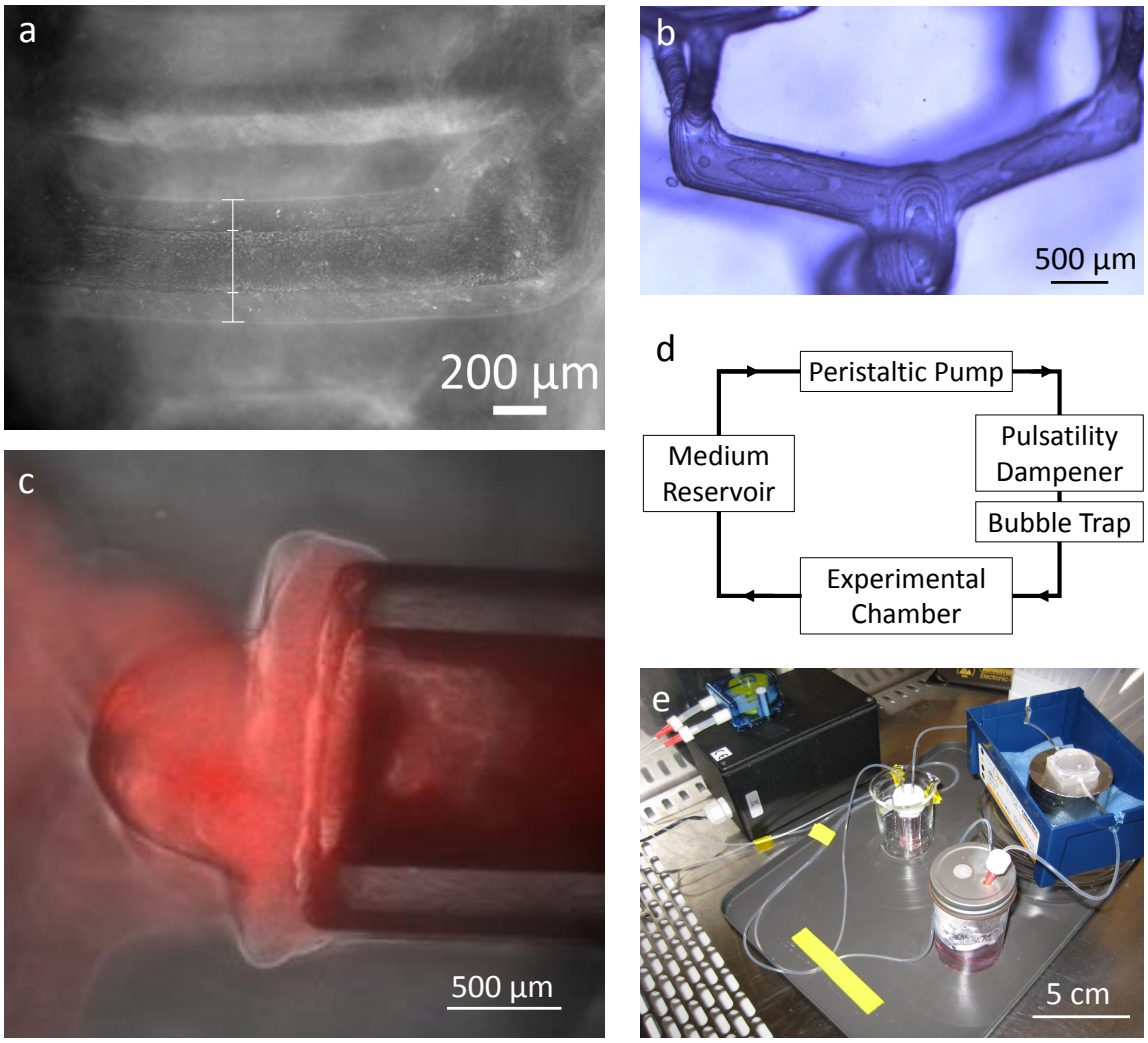

Fig. 3.3 (a) Gelatin halo is formed around the desired template features when the alginate hydrogel is insufficiently crosslinked or gelatin infiltration is undertaken at too high a temperature. Line denotes outer boundaries of gelatin halo and templated feature. (b) Surface contours of gelatin template display 12 μm thick terraces from layer-by-layer 3D printing process. (c) Tight interface between fibrin hydrogel and silicone inlet. Shown in red are 1 μm fluorescent beads, which do not leak around the side of the inlets for a 20 mg mL^{-1} fibrin gel. (d) Perfusion circuit schematic. (e) Photo of perfusion system.

concentration, though we postulate that much larger volumes are possible since this is a casting-based technique, and thus a closer proximity to Murray's law is possible in the future.

The angles between parent and daughter branches are chosen as 70°, to minimize flow stagnation at junctions [79] whilst also maximizing the volume supported by the finest channels of the network. The finest channels are 2 mm in length and are separated by 1.5 mm in plane and 1 mm between planes. Thus, these thoroughfare channels enable diffusion of nutrients and oxygen into a significant proportion of the bulk hydrogel.

The choice of the gelatin and alginate used is essential for this process to be successful. A low bloom (80 g) gelatin is used that can withstand alginate removal and subsequent casting with collagen or fibrin, but has a viscosity which is low enough to be easily removed from the final hydrogel. It is type A gelatin, which has a better gel strength to viscosity ratio than type B [26]. A concentration of 15% (w/v) is sufficient for the chelation and casting process, and has a melting point such that a low viscosity liquid is produced upon melting at 37 °C. However, the gelatin template still requires mechanical support from the surrounding liquid in order to preserve its structure, prior to casting.

To enable the alginate to be cast and removed effectively, a low viscosity sodium alginate is used at a concentration of 7.5% (w/v), which provides sufficient rigidity for the fabrication process; in particular resisting syneresis from high temperatures, solvent exchange, and $CaCl_2$ addition. The alginate gels are fabricated using an internal setting process using $CaHPO_4$ and gluconolactone as an acidifier, which slowly releases the calcium producing a uniform alginate hydrogel. Overloading the alginate gel with calcium at gelation causes significant syneresis and thus poor reproduction of the original CAD design. However, if extra calcium is not added, the pore size of the alginate gel is sufficiently large to allow the liquid gelatin to penetrate the surface of the alginate gel. Following chelation, this generates a 'halo' of gelatin around the templated gelatin channels, greatly increasing the diameter of the finest channels, as illustrated in Figure 3.3a. Additionally, the molecular weight of gelatin reduces with increasing temperature [84] and thus using gelatin at higher temperatures produces a thicker halo.

To overcome these issues, one must further crosslink the channel surfaces of the alginate hydrogel by injecting $CaCl_2$ via the inlets, and use gelatin at 37 °C. Sufficient crosslinking of the alginate at the channel surface prevents the halo effect and produces channels close to the 3D printed model design. In order that the injected calcium penetrates to the alginate surface, the 3D printed model material must be completely removed; a layer of model material prevents the calcium from crosslinking the alginate sufficiently. To this end, the remaining (polyester-based) model material is dissolved using acetone once the channels have become patent. If acetone is not used, the gelatin template is turbid and some model material can be

left on the surface. 250 mM $CaCl_2$ is then injected around the channel network, crosslinking the alginate channel surface but without causing significant syneresis of the whole gel.

The thermoplastic model has in its surface 12 μm thick terraces due to the layer-by-layer nature of the 3D printing process. This fine stepping is visible in the gelatin template, as shown in Figure 3.3b, which demonstrates a high casting fidelity of surface features.

The choice of bulk material was influenced by a need for perfusion and thus a requirement for a tight interface to an external pumping system; thus silicone inlets were used. It is well known that hydrophobic materials, such as silicone and Teflon, have some protein-binding capacity [136]. In this study, we rely on this adsorption of protein to the surface of silicone rather than the use of other agents to directly bond the gel at the interface. This interface, as shown in Figure 3.3c, was tested using fluorescent red 1 μm beads, which showed minimal leaking around the silicone inlet surface when used with fibrin gels. Further, perfusion was tested up to 30 mL hr^{-1} (at the inlet) with 10 mg mL^{-1} fibrin gels, which showed no signs of leaking from the chamber.

Using negative pressure, liquid gelatin was infiltrated into the channel network. If positive pressure is used instead, gelatin infiltrates the interface between alginate gel and silicone chamber, and also coats the inlets, which prevents the fibrin hydrogel from adhering to the (hydrophobic) silicone chamber. When the gelatin is liquefied, this opens leak paths around the fibrin hydrogel. The alginate gel was chosen to withstand the applied negative pressure without collapsing.

The perfusion system made use of a peristaltic pump in order to recycle medium around the system, at relatively high flow rates (Figure 3.3d,e). 20 mL of cell medium was deposited in a media reservoir. The fluid is drawn through the peristaltic pump mechanism and into another chamber which acts predominantly as a pulsatility dampener. This sealed chamber is under pressure such that the air at the top of chamber acts to oppose any changes in flow rate. Fluid is forced up into the outlet to this chamber and into a bubble trap which consists of a housed hydrophobic membrane. Fluid flows across one side of the membrane and any air bubbles are cross the membrane to another outlet open to atmospheric pressure. This provides an effective means of removing even small air bubbles from the line leading to the humidified experimental chamber. This sits at the highest point of the perfusion circuit such that pressure at the inlet comes only from the remaining network and not from any gravitationally-driven pressure, in order to prevent leaking. Finally, the outlet of the device is connected to the media reservoir, which is open to atmospheric pressure.

The multi-casting process produces a fully three-dimensional gelatin template with features very similar to the 3D printed model (Figure 3.4a). However, due to the weak mechanical properties of gelatin and the suction employed for its infiltration into the alginate

channels, there is a slight, but measurable, change in the diameter of the channel features in the various polymeric materials. The choice of alginate as an intermediary casting medium enables fine features of the network to be translated into the gelatin network, though some variation was observed between the CAD design and the 3D printed model, between the model and the gelatin template, and between the gelatin template and hydrogel channels, as shown in Figure 3.4b. The variation between CAD and 3D printed model is due to printing feature sizes at the lower limit of the Solidscape machines; a CAD feature with a diameter of 170 μm yielded a 3D printed model with features in the range of 210-250 μm. However, as shown in Figures 3.4c-j, there is still a good correspondence between 3D printed model and gelatin template and any differences are marginal.

In this study, both fibrin and collagen hydrogels were used to test the use of the gelatin template with ideal tissue construct materials. Fibrin was easier to handle since at 20 mg mL^{-1}, the precursor solution has a low viscosity and once thrombin has been added, can be cast quickly using a 1 mL syringe. Conversely, at concentrations of 7.5 mg mL^{-1}, collagen gel is much more viscous and requires slow casting using a syringe pump. Collagen precursor solutions gel rapidly at room temperature and so must be kept on ice during this process.

The use of gelatin as the sacrificial template material has the advantage that it is thermally removed at physiological temperatures. This allows the cell-loaded constructs to be immediately placed in incubator conditions and puts minimal stress on the cells themselves. The use of gelatin enables a wide range of materials to be employed as the final cast, beyond those of thermally-crosslinked collagen and enzymatically-crosslinked fibrin hydrogels. The template is capable of withstanding a viscous casting material, as shown by 7.5% (w/v) collagen (Figure 3.2h), which can be infiltrated without significant displacement of the gelatin template, by way of slow casting with a syringe pump. The release of the template constituents upon thermal dissolution impacts minimally upon the surrounding cellular environment due to the relatively benign nature of gelatin. We postulate that the gelatin template could be used with other hydrogels of relevance to the tissue engineering field, such as alginate, hyaluronic acid, Matrigel, and synthetic materials such as PDMS.

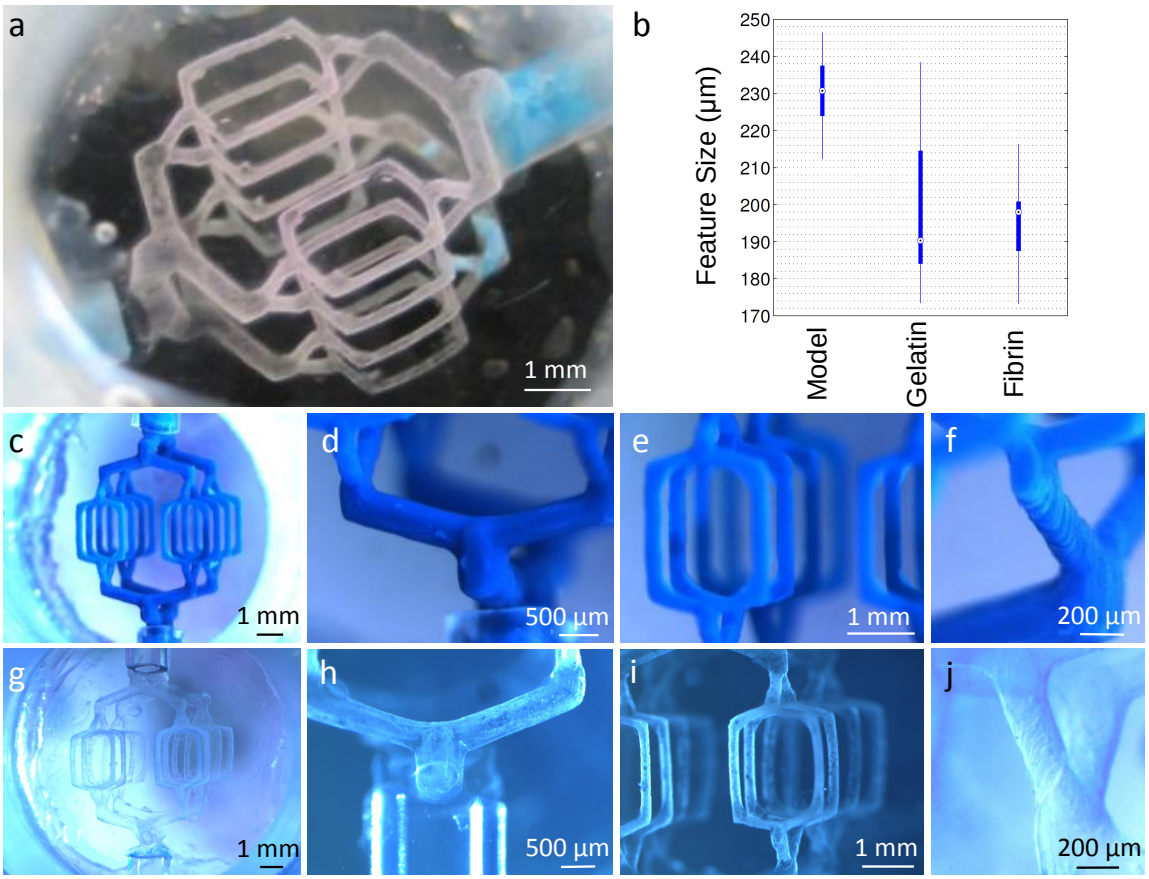

Fig. 3.4 Fidelity of hydrogel channels and gelatin template to 3D printed model design. (a) Gelatin template without acetone wash, displaying three-dimensionality of the network. Note that without acetone wash, model material remains on the walls of the template. (b) Comparison of the diameters of the templates finest features, at different stages of the fabrication process. The CAD model had finest features of size of 170 µm. Box plot displays minimum and maximum diameters, and 1st and 3rd quartiles. Circles represent median diameters. Correspondence of 3D printed model (c-f) to gelatin template (g-j) for specific large-scale features.

3.4 Cell-Based Evaluation

3.4.1 Bulk Cell Experiments

As a preliminary evaluation of the vascular system, a series of pilot cell experiments was performed. To evaluate the ability of the channel network to support cells in the bulk of the hydrogel, HDFs were mixed into the fibrin precursor solution prior to gelation and cell-loaded fibrin gels (10 mg ml^{-1}) were perfused at a range of flow rates (0.5–30 ml h^{-1}). After 7 days, a live–dead viability assay was performed by cross-sectioning the gel and staining the central surface with calcein AM and ethidium homodimer-1 (Figure 3.5a). To quantify any improvement in viability with increasing flow rate, live and dead cells were counted in representative sample regions and plotted against flow rate, as shown in figure 3.5b. Static conditions (non-perfused) or low flow rates were incapable of supporting the metabolic requirements of the cells. Flow rates of 10–30 mL h^{-1} were shown to be suitable for maintaining cell viability. There was also a variation in the degree of cell spreading in the constructs at different flow rates; for flow rates above 10 ml h^{-1} in which a good viability of HDFs was observed in the bulk , there was increasing cell elongation with increasing flow rate, as shown in figure 3.5c.

3.4.2 Channel Cell Experiments

HUVECs were seeded into the channels via the inlets, as shown in Figure 3.6a. HUVECs spread evenly around the symmetrically bifurcating channels and, after several hours, had adhered to the hydrogel channel walls. After 8 days of perfusion, a higher number of HUVECs was observed in all four channel levels of the template (Figure 3.6b–e). These cells were perfused at relatively low flow rates (0.1 ml h^{-1}) so as to not dislodge the cell layer in the initial stages of the endothelium formation. Further, the observation of high numbers of cells over all layers shows that flow is not confined to a single layer and that nutrients and oxygen would reach a fully 3D volume when cells are added to the bulk. Immunocytochemistry for the cell adhesion marker CD31 showed the formation of tight junctions between HUVECs in the channels (Figure 3.6f).

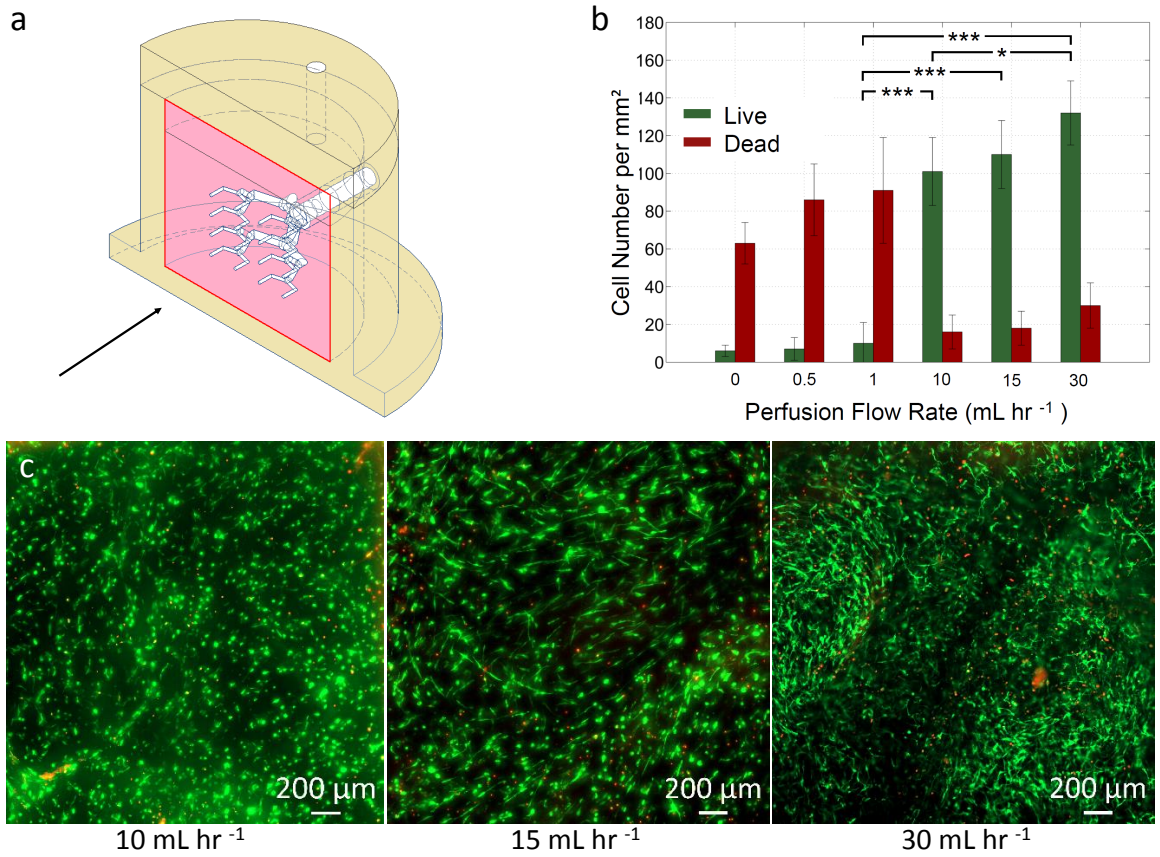

Fig. 3.5 To determine the ability to support cells in thick constructs, HDFs were encapsulated in 10 mg mL^{-1} fibrin gels at 1×10^6 cells mL^{-1} and perfused at a range of flow rates. (a) After 7 days, the gels were cross-sectioned and stained with calcein AM (green) and ethidium homodimer-1 (red). Shown is a cross-section through the middle of the gel normal to the long axis of the channels. Arrow denotes imaging direction. (b) Live-dead staining for flow rates at which the majority of cells are viable. At 10 mL hr^{-1}, most cells are round whilst at 30 mL hr^{-1}, most cells are spread out. (c) In order to quantify cell viability at different flow rates, the number of live and dead cells were counted in sample regions. Static conditions (no perfusion) and low flow rates produced constructs with high numbers of dead cells and flow rates above 10 mL hr^{-1} produced constructs with high numbers of live cells ($*p < 0.05$, $***p < 0.001$). Comparisons show a statistically significant difference between live cell numbers for flow rates of 1 mL hr^{-1} and 10-30 mL hr^{-1}, and for those between 10 mL hr^{-1} and 30 mL hr^{-1}.

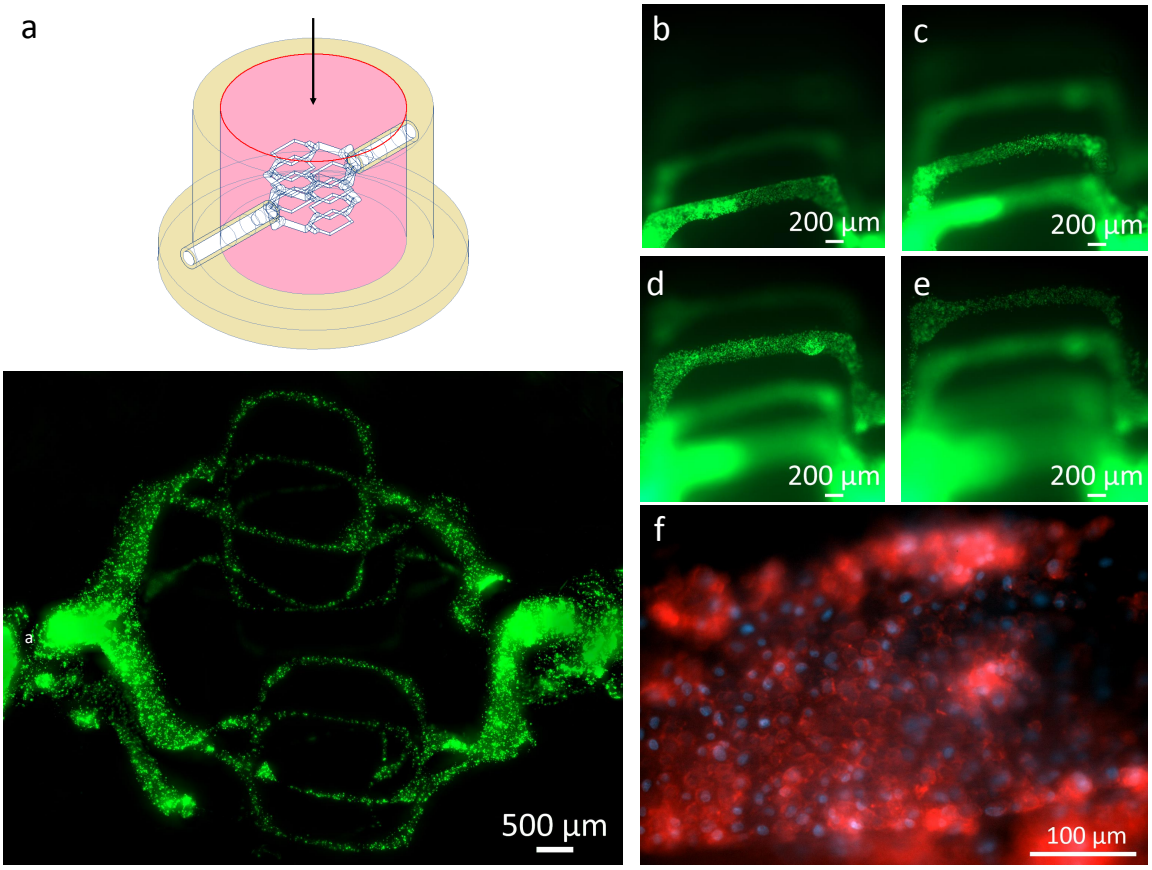

Fig. 3.6 (a) HUVECs, labelled with green Cell Tracker dye, were injected into the channels of 20 mg mL^{-1} fibrin hydrogels at 2×10^7 cells mL^{-1} and left overnight, prior to perfusion at 0.1 mL hr^{-1}. Arrow denotes imaging direction. (b-e) After 8 days, all 4 channel layers of the vascular network have high levels of seeded HUVECs. (f) CD31 immunostaining was performed on hydrogels containing HUVECs in the channels in order to determine the early formation of tight junctions between endothelial cells. Shown here is a single channel lined with HUVECs, after 8 days of perfusion at 0.1 mL hr^{-1}. Red and blue colours display cell-cell adhesion marker and nuclear stain respectively.

3.5 Further Development of the Process

3.5.1 New Method for Chamber Fabrication

A more advanced method was developed, using 3D printed molds for casting of PDMS, in order to better meet our requirements for a more robust and sealed chamber, whilst also allowing for a greater degree of precision in the design; most notably, a precise placement of inlet tubing and an interlocking lid structure. Furthermore, PDMS provides a suitable substrate for the application of a chamber coating onto which alginate can be actively bound. Finally, a 3D printed chamber mold allows one to customize the external shape of the gel construct.

An inverse 3D printed mold was fabricated out of PLA into which PDMS could be cast (Figure 3.7a). In order to be able to remove the PDMS casts from the chamber, it was necessary to fabricate the mold in two parts; a base piece and wall piece, which could be separated after the PDMS had cured. Conventional 3D printers produce models with a high surface roughness and casting PDMS directly onto its surface produces a optically turbid material. Since this was not acceptable for clear imaging through the base, a solution was found by which a circular glass coverslip was mounted onto the central surface which, when cast in PDMS, would enable a transparent base for imaging. A small inset was designed into the 3D printed mold and the glass coverslip was adhered to the mold via Araldite. In order to construct the inlet tubes through the PDMS into which silicone tubing would later be placed, stainless steel hypodermic tubing was mounted through holes in the 3D printed mold. Whilst the two halves of the 3D printed mold fitted together well, there was some leaking of PDMS during the degassing stage. Thus it became necessary to fill the space between them with silicone sealant. Silicone sealant is sufficiently soft enough to be cut through which allowed the two halves of the mold to be separated after PDMS curing. In order to fashion PDMS chamber lids, 3D printed molds were made and attached to glass petri dishes using silicone sealant. This provided a surfaces with sufficient optical clarity for imaging.

PDMS was prepared at a ratio of elastomer to catalyst of 10:1. Following 5 min of vigorous mixing with a spatula, the solution was centrifuged at 4000 g for 10 min and then cast into the 3D printed mold. Whilst the centrifuge removed much of the large bubbles, it was important to remove the small bubbles that formed during pouring of the PDMS, and those trapped between the 3D printed mold and the viscous PDMS solution. Thus the chamber, containing the viscous PDMS solution, was placed in a vacuum chamber. By gradually ramping up to 30 mm Hg, bubbles were eliminated from the PDMS, and the PDMS solution was then cured at 70 °C overnight. To remove the PDMS from the chamber, a sharp blade was used to cut through the silicone sealant between the base and wall pieces of the 3D

printed mold. Then the two halves were prised apart and the base piece removed. To remove the PDMS chamber from the wall piece, a metal spatula was used to go between the interface between the two materials. The PDMS chamber could be then pushed out of the 3D printed mold (Figure 3.7b).

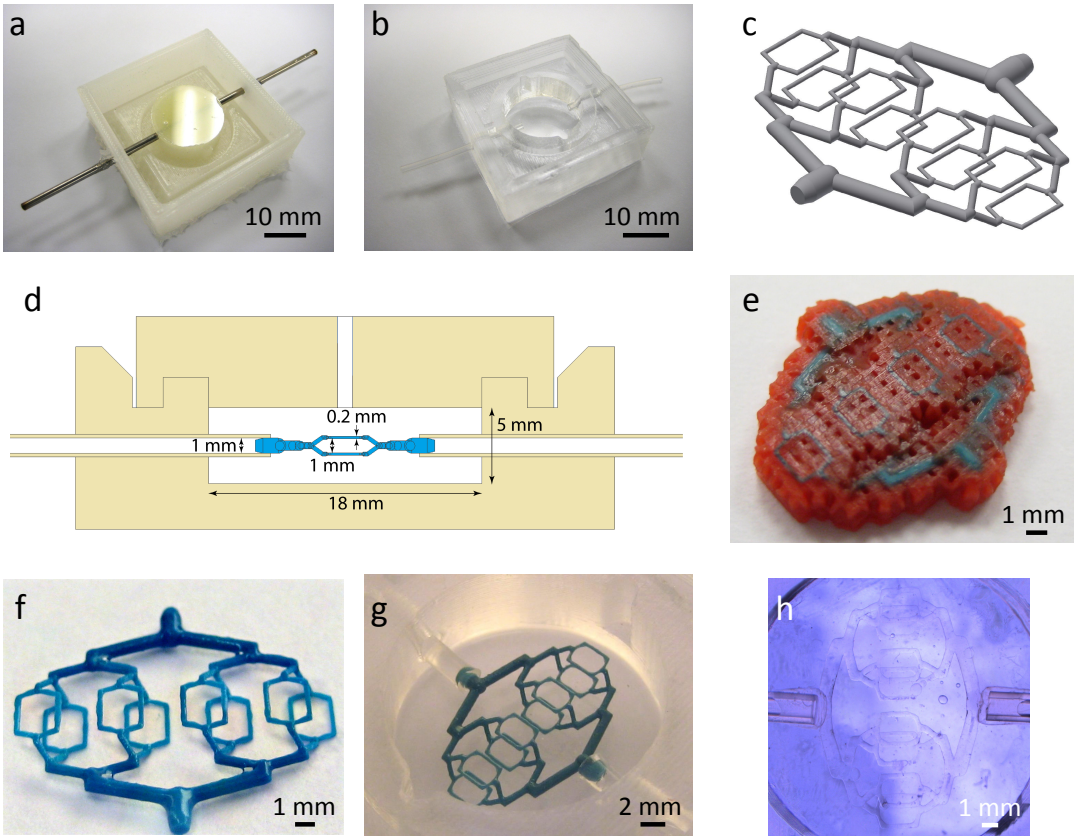

Fig. 3.7 (a) 3D printed molds were fabricated in order to cast PDMS and produce more robust PDMS chambers. Alongside printed PLA, molds consisted of a mounted glass coverslip, to improve imaging clarity, and hypodermic tubing, for molding of the inlets. (b) PDMS chamber with silicone tubing for inlets. Grooves in top enable the tight fitting of a PDMS lid, also fabricated via this 3D printing approach (not shown). (c) CAD design for new 'flat' model. Design still incorporates symmetrically bifurcating channels and has sixteen finest features of length 2 mm. (d) Schematic of PDMS chamber with mounted flat model. (e) Flat model in support wax. (f) Flat model without support wax. (g) Flat model mounted in PDMS chamber. (h) Improved 3D printed model to gelatin process yields better gelatin templates.

3.5.2 Improvements to 3D Printed Model Design

The original model design (Figure 3.2a) is excellent at supporting cells in a compact and three-dimensional structure. However, we also require a vascular network design which enables the clearest imaging, especially in future when investigating capillary morphogenesis in these systems. We found compact designs like this were particularly difficult to image due to overlap of vascular channels when imaged from below, the short working distance of even long-range objectives, and a high fluorescent background level from defocused light. Thus, a second model was designed which consisted of the same number of channels orientated into only two planar levels, as shown in Figure 3.7c. It follows the same design characteristics as the compact model but with junctions rotated to make the structure thin enough for ease of imaging when high numbers of fluorescent cells are used, whilst still maintaining a degree of three-dimensionality. Finally, to avoid each level overlapping when imaging from above, the final bifurcation was rotated to 45° about the channel axis. Every path through the vascular network is identical; this symmetry should provide the same flow rate and pressure differences for each path. This model, when combined with the new chamber protocol, forms a more robust system for advanced cell experiments (Figure 3.7d). The dewaxing process proceeds in the same way (Figure 3.7e) and still yields models with sufficient mechanical strength for handling and mounting in the PDMS chamber (Figures 3.7e,f).

3.5.3 Chamber Coating

Previously, we relied upon a hydrophobic bonding between silicone or PDMS chambers, and the alginate, fibrin, and collagen hydrogels. Proteins bond to hydrophobic surfaces by denaturing onto the surfaces, thereby revealing hydrophobic groups. This however is not a particularly strong bond, as was discovered over the course of the project. Both collagen and fibrin syneresis, and the contractile forces applied on the matrix by the cells, contribute to the shrinking of the gel construct, revealing a flow path which redirects nutrients and oxygen away from the channeled network and bulk of the gel construct. Many groups rely on hydrophobic bonding such as this, but others have added a layer of poly-L-lysine coating to prevent fibrin gel shrinking [68].

Polyethyleneimine (PEI) should have a similar effect as they're both cationic polymers which are highly charged at a neutral pH. It was found that a coating on the PDMS surface on PEI prevents the alginate gel from shrinking during the model to gelatin phase of the procedure, and may also help prevent the fibrin and collagen gels from undergoing cell-mediated shrinkage and syneresis, by interaction with the alginate layer. While the PEI-alginate bond is robust, the bond formed between the alginate and fibrin is weak, since the

gelatin template is supported by fluid and therefore any bond is necessarily done under wet conditions.

Following ethanol cleaning and drying of the PDMS chambers, they were plasma cleaned for 2 min. This exposes silanol groups (-SiOH) on the surface of PDMS, which are negatively charged. PEI is a branched cationic polymer, consisting of a high density of amine groups, and has an isoelectric point of 10.6; thus at neutral pHs, it has a high degree of protonated amine groups and is positively charged. By filling the chamber with 1% PEI solution in DI water for 2 h (pH 7.4), followed by 3x DI water washes, PEI was adsorbed onto the PDMS surface. The pKas of the mannuronate and guluronate residues, which make up the alginate polymer, are 3.38 and 3.65 respectively. Thus at neutral pHs, these are highly deprotonated and therefore negatively charged. This leads to electrostatic interaction between the protonated amine groups of the PEI and the alginate polymer, producing a strong bond between chamber and alginate cast.

3.5.4 Improvements to Alginate and Gelatin Steps

With the advent of the new coating which provided a strong bond between alginate and chamber, a number of process steps could be modified. With the coating, it was possible to inject a larger amount of $CaCl_2$ into the alginate channel network without the risk of the alginate gel shrinking. It was also possible to inject the gelatin solution under positive pressure, rather than by suction, though with sufficient pressure, gelatin was still able to penetrate the edge of the gel and reach the surface, providing a leak path when cast in fibrin. Further, injecting gelatin at high pressure causes the alginate channels to expand radially which produces gelatin template features of a larger diameter than by the suction method.

The pressure required at the inlet in order to flow gelatin around the network can be lowered by reducing the rate of gelatin flow (Q) and by reducing the viscosity of the gelatin (μ), as described by the Hagen-Poiseuille network pressure drop equation (Equation (2.4)). The viscosity of gelatin can be lowered by increasing the temperature of the system [141]. However, to maintain simplicity and reproducibility, suction was still used as the means of loading the gelatin. Since a larger amount of $CaCl_2$ can be applied without shrinking the alginate cast, there is no longer an issue of gelatin halo formation, described in Section 3.3.

It was found that the injection of alginate into the model-mounted chamber could cause a blockage in the inlets. Upon melting of the 3D printed model, it thus became impossible to remove the model material due to this calcium alginate filling these inlets. Further, the addition of negative pressure to the inlet could cause a catastrophic ripping of the alginate gel near the inlet. This meant that upon gelatin casting, a large mass of gelatin would have formed as a feature in the final template structure. The solution was to add the viscous

Table 3.1 Swelling data for various chelation buffer configurations.

Chelation Buffer Type	% Mass Difference (24 h)	
	10 % High Gelatin in 50 mM HEPES pH 7.4	20 % Low Gelatin in 50 mM HEPES pH 7.4
Sodium Citrate 100 mM pH 7	34.2	91.4
Sodium Citrate 100 mM pH 7 + 1 % Dextran	32.5	84.3
Sodium Citrate 200 mM pH 7	25.8	79.5
Sodium Citrate 300 mM pH 7	12.4	59.4
Sodium Citrate 100 mM pH 7 + 5 % Dextran	10.3	57.9
Sodium Citrate 400 mM pH 7	0.6	39.4
Sodium Citrate 500 mM pH 7	-14.4	12.0
Sodium Citrate 100 mM pH 7 + 10 % Dextran	-15.6	17.7
Sodium Citrate 500 mM pH 7 + Dissolved Alginate	-20.2	9.1

alginate solution slowly to the chamber and not use a chamber lid. The DI water in the chamber, which is replaced in the step, is less dense the alginate solution and tends to collect on top of the alginate gel during filling, which can be subsequently aspirated off. Since the alginate crosslinks slowly, there is sufficient time for the viscous alginate to diffuse into any remaining pockets of DI water, thereby casting effectively without risking infiltration of alginate into the inlets. The PEI coating provides a good bond between chamber and alginate, though superglue was also applied to bond the outer edge of the alginate gel to the PDMS chamber, once the alginate gel had formed.

Swelling of the gelatin template weakens the structure and provides a degree of variation between model and final channels in collagen and fibrin. Thus a short experiment was undertaken in which blocks of gelatin were gelled and then placed in citrate buffer of various concentrations. Further addition of dextran was also tested as a way of using a lower citrate buffer concentration while still preventing gelatin swelling, and dissolved alginate was included to simulate the process of the alginate gel dissolving in the multi-casting process. Gelatin was allowed to gel in a 48 well plate for 24 h. The gels were then removed from the wells, weighed, and placed in 6 well plates, into which 10 mL of chelation buffer solution was added. After a further 24 h at 4°C, the gelatin gels were reweighed and the percentage mass difference calculated; the data for which is shown in Table 3.1. It was found that 400 mM sodium citrate buffer was ideal as it prevented swelling of the gelatin blocks (compare to 200 mM citrate used in the main protocol). Dextran was shown to be helpful in lowering the buffer concentration if desired, though concentrations of citrate less than 200 mM increased the time taken for alginate removal.

The concentration and buffer of the gelatin template material was investigated; most notably whether a low or high bloom gelatin was better as the template material. Low bloom, while producing weaker gels, has a low viscosity and can be used up to 20%(w/v).

High bloom, while producing strong gels, has a high viscosity which greatly increases with concentration, limiting its use up to 15%. The choice of buffer for the gelatin was considered. Gelatin is most stable at its isoelectric point (pI of type A is 7-9) and so the use of a buffer, such as HEPES, is useful. The solution that was decided the best balance of strength and viscosity was 10%(w/v) high bloom gelatin, in 50 mM HEPES buffer, with the pH adjusted to 7.4. By incorporating these considerations, and those above, into the multi-casting method, one is able to produce a gelatin template with improved properties to the original (3.7h).

An alternative method was briefly tested of using methylcellulose instead of alginate, as the primary casting agent. Methylcellulose is a sol-gel which forms a hydrogel by hydrophobic interactions, and can be prepared such that it forms a gel when put in hot water and melts when the water is cooled. It was possible to maintain the methyllcellulose in a solid hydrogel phase, remove the model material, wash, and inject gelatin. Upon cooling, the methylcellulose return to liquid form. However, due to its viscosity, one has to allow the methylcellulose to diffuse away overnight in a way similar to the sodium alginate. While this approach was seen as novel, alginate continued to be used since it allows for a more controlled process, and allows more time for the gelatin template to gel inside the alginate, if so desired.

3.5.5 Improvements to Collagen and Fibrin Casting Step

A difficulty was found when casting the gelatin template in that there was insufficient mixing between the template-supporting liquid already in the chamber (i.e. PBS) and the precursor solution of the fibrin gels, due to the rapid rate of gelling once thrombin was added to the precursor. As such, there occasionally remained pockets of ungelled liquid within the chamber volume. This was found to be a catastrophic issue if this pocket of liquid formed around one of the inlets, as the gel would then not perfuse effectively and instead disrupt the gel structure. The solution was to pre-fill the chamber with a fibrinogen solution, without the thrombin and other components of the final gel. Since there was no thrombin, the fibrinogen could be added very slowly and allowed sufficient time to mix thoroughly with the existing fluid. Subsequently, upon addition of the cell-ladened fibrinogen solution containing thrombin, fibrinogen in the pre-fill would also become crosslinked with the fibrinogen from the cell-ladened solution, whilst maintaining the overall concentration of the fibrin in the chamber. A similar problem was encountered with the collagen, which would gel before the viscous precursor solution had time to diffuse thoroughly around the whole chamber. However, while not ideal for the cells, maintaining the collagen-filled chamber on ice allowed time for sufficient mixing prior to the thermally-activated gelling of collagen.

3.6 Future of the Approach

It is conceivable that with improvements in commercial 3D printing technologies, models could be produced with higher precision, smaller feature sizes, and in new materials with improved mechanical, physical, and chemical properties. The process described here, of converting these 3D printed models into gelatin vascular templates, and subsequently cellularized hydrogel materials, would utilize these advances. Further, since we make use of standard 3D printing technology, the fabrication method is relatively inexpensive in comparison with other approaches, such as those requiring custom-made printers, and so could be widely used for three-dimensional network formation in cellularized constructs.

3.7 Chapter Summary

In this chapter, a novel 3D printing-based method has been described for fabricating three-dimensional, hierarchical, and perfusable vascular networks. By converting standard 3D printed materials into gelatin through a multi-casting process, it was possible to use complex vascular templates alongside ideal tissue engineering materials, such as collagen and fibrin, and in the presence of cells. The vascular system was subsequently evaluated as a means of maintaining a cell population in the bulk of a collagen gel. It was found that for flow rates above 10 mL/hr, the vast majority of cells were viable and subsequent increases in the flow rate (up to 30 mL/hr) notably increased the amount of cell elongation. Endothelial cells were also seeded into the channel network itself and a nascent endothelial layer was formed. Further improvements were subsequently undertaken, including the development of a new PDMS chamber fabrication method, a chamber coating to improve the alginate casting step, and other minor improvements to the multi-casting process.

Chapter 4

Literature Review: Cell-Based Approaches to Vascularization

4.1 Introduction

Endothelial tube networks are fundamental components of living tissue. With a few exceptions, all tissues in the human body are vascularized which enables rapid transport of oxygen and nutrients to cells, and removal of waste products. The previous chapters showed that it was possible to fabricate complex three-dimensional networks of tubes at the millimeter and meso-scale, and support cells via network perfusion; here we describe the cellular processes by which micro-scale vessels are formed and the wide range of approaches undertaken by researchers in fabricating these capillary networks for *in vitro* systems and we also describe a limited number of *in vivo* systems. Finally, we attempt to determine the best conditions for capillary formation for our system, based on the literature.

4.2 Capillary Morphogenesis via Vasculogenesis and Angiogenesis

Capillaries have a diameter of 5-20 μm and are the smallest endothelialized channels of the vascular system. They facilitate efficient transfer of nutrients and oxygen to cells in the bulk. In the embryo, the primary capillary plexus is formed in which 'blood islands' of endothelial progenitor cells (EPCs) and angioblasts migrate and join together to form a homogenous capillary bed, which then forms into a hierarchical structure consisting of arteries, veins, and capillaries [2]. This process is known as vasculogenesis and only occurs in the embryo.

While arteries and veins expand radially to increase transport of metabolites to growing tissues, capillaries undergo the process of angiogenesis in which new capillaries form off existing ones; this remodelling leads to the formation of more complex networks which are more effective at meeting the metabolic requirements of nearby cells [23, 2]. Endothelial cells are thus capable of remodelling existing tissue extensively via physiological angiogenesis. For example, hypoxic conditions cause bulk cells to produce various signalling molecules which, along molecular gradients, are detected and acted upon by endothelial and perivascular cells to induce an angiogenic response. The result of this is the formation of a new capillary closer to the hypoxic cells which thus provides an increased supply of oxygen to that region. A specific endothelial cell differentiates into a tip cell, which degrades the local basement membrane and migrates into the bulk forming a new sprout. Endothelial cells subsequently proliferate behind it and pericytes are recruited to the new vessel. With the production of new basement membrane and further remodelling of the extra-cellular matrix, a new capillary is formed joined to an existing one. Most of the time a non-sprouting endothelium is maintained and regulated by a tight pericyte interaction [23, 2]. Tissues generally only undergo physiological angiogenesis in specific instances, such as tissue development and growth, menstruation, and fracture and wound healing. As such, endothelial cells are normally in a quiescent state [23, 2]. Pathological angiogenesis is implicated in several diseases, including the development of solid tumors, and ocular diseases such as retinopathy and macular degeneration [23].

Both vasculogenesis and angiogenesis involve a complex interplay of a number of different cell types, matrix components, growth factors, and proteolytic mechanisms. The field is an active area of research given the importance of angiogenesis to a significant number of pathologies, and to understanding fundamental biological mechanisms. The ability to exercise fine control of these processes *in vitro* would enable a fully vascularized construct to be fabricated; a network of capillaries approximately 400 μm apart should be able to support therapeutic concentrations of parenchymal and/or stromal cell types, in the bulk of the device.

4.3 Vasculogenic Approaches

A widely reported approach for the formation of a capillary-like network is to co-culture endothelial (or endothelial progenitor) cells with a supporting cell type; these include retinal and brain pericytes (PCs), smooth muscle cells (SMCs), fibroblasts (in particular normal human lung fibroblasts (NHLFs) and human dermal fibroblasts (HDFs)), human osteoblasts,

and progenitor cells, such as mesenchymal stromal cells (MSCs) (see Table 4.2 at the end of the chapter for a summary of literature).

This process is somewhat different from the vasculogenesis found in the embryo but since the capillary-like network is forming *de novo* (rather than sprouting off existing channels) and involves cells migrating towards each other and forming multi-cellular cords, it is considered vasculogenic. Table 4.1 summarizes small molecules commonly used in the literature for fabricating angiogenic or vasculogenic capillary networks. A wide range of pro-angiogenic growth factors are reported to induce the endothelial cells to form capillary-like structures, with vascular endothelial growth factor (VEGF) and basic fibroblast growth factor (bFGF) playing a key role [127].

Once endothelial cells have spread and created tight junctions with other endothelial cells, lumen are formed by intracellular and intercellular vesicle fusion [71]. They then recruit pericytes by releasing PDGF [116] and cellular processes subsequently produce a basement membrane. The supporting cell type produces growth factors to help this process and importantly, is able to stabilize and mature the newly-formed capillaries; for instance by production of Angiopoetin 1, which is a vessel stabilizing protein [116] and an apoptosis survival factor for endothelial cells [86]. This interaction with the perivascular cell stops the endothelial cells from migrating, spreading, regressing, and apoptosing, and thus helps form a more long-lived structure [116].

One notable paper [41] states a predictable sequence of phenotypic changes that occur within vasculogenic-like capillary formation. These are: (i) a loss of endothelial cell proliferation in favour of morphogenesis; (ii) pathfinding cell migration; (iii) adherens junction formation between endothelial cells; (iv) branching morphogenesis and network formation; (v) basement membrane formation consisting of collagen IV and XVIII; (vi) patent lumen formation; (vii) anastomosis; and (viii) network stabilization [41].

Table 4.1 Summary of pro-angiogenic small molecules (growth factors, cytokines, chemokines) and their functions in angiogenesis.

Growth Factor	Functions in Capillary Morphogenesis
VEGF (Vascular endothelial growth factor)	Pro-angiogenic growth factor [127, 16]. Stimulates angiogenesis, vasculogenesis [16], increases vascular permeability [162, 16], and leukocyte adhesion [16]. EC mitogen [157], and cell survival factor [98].
bFGF (Basic fibroblast growth factor)	Pro-angiogenic growth factor [127, 16]. Potent mitogen for a range of cell types, including ECs and fibroblasts [142].
Ang-1 (Angiopoietin 1)	Stabilizes vessels, inhibits vascular permeability [16]. Involved in maintenance and growth of vessels [127].
PDGF (Platelet-derived growth factor)	Pro-angiogenic growth factor [127, 124]. Recruits SMCs [16]. Mural cell mitogen and chemoattractrant [150]. Induces SMC and PC proliferation and migration [157].
TGF-α (Transforming growth factor alpha)	Pro-angiogenic growth factor [93]. Induces migration of HMVECs but not HUVECs [162].
TGF-β1 (Transforming growth factor beta)	Stimulates ECM production [16]. Both pro-angiogenic effects at low doses (upregulating angiogenic factors and proteases) and anti-angiogenic at high doses (inhibits EC proliferation and migration of ECs) [127, 157]. Promotes basement membrane reformation and stimulates SMC differentiation and recruitment [127].
SDF-1α (Stromal cell-derived factor 1 alpha)	Pro-angiogenic growth factor [16]. Induces tube-like structure formation and migration [72].
S1P (Sphingosine-1-phosphate)	Pro-angiogenic growth factor. Stimulates EC migration, survival, and proliferation, adherens junction assembly, morphogenesis, enhances invasion, and lumen formation [12].
PMA (Phorbol 12-myristate 13-acetate)	Pro-angiogenic growth factor and tumor promoter. Induces invasion of endothelial cells and angiogenesis [112].
IL-1α (Interleukin 1 alpha)	Induces expression of pro-inflammatory genes in stromal and inflammatory cells [164]. Potential inhibitor of angiogenesis [124].
TNF-α (Tumor necrosis factor alpha)	Pro-angiogenic growth factor [92]. Induces expression of pro-inflammatory genes in stromal and inflammatory cells [164].
EGF (Epidermal growth factor)	Pro-angiogenic growth factor [162]. Regulates PC recruitment to EC tubes. Induces migration of HMVECs but not HUVECs [162].
HGF (Hepatocyte growth factor)	Pro-angiogenic growth factor [16]
SCF (Stem cell factor)	Pro-angiogenic growth factor [151]
IGF-1 (Insulin-like growth factor 1)	Pro-angiogenic growth factor [124, 16]

4.4 Two vs Three Dimensional Vasculogenic Capillaries

The concentration and ratio of endothelial and supporting cells seeded onto a surface is critical for producing a capillary bed, as opposed to simple confluent monolayer of cells. The literature has a number of examples where groups are able to elicit capillary morphogenesis by mixing the right concentrations of endothelial and supporting cell in two dimensions, such as on tissue culture plastic; a good example is shown in Figure 4.1a [41]. Here, two endothelial cell types (HUVEC, HMVEC) interact together to form a single extensive network, in the presence of smooth muscle cells (SMCs) [41].

In three dimensions, one can encapsulate the cells in a matrix material, such as collagen, fibrin, or Matrigel. Shown in Figure 4.1b is an example of an endothelial network in a three-dimensional gel [91]. By incorporating an extra-cellular matrix material into the system, cells are provided with a range of biochemical and mechanical cues for development which would otherwise be lacking, and survival of cells is enhanced by reducing apoptosis [44]. The main consituent protein of the extra cellular matrix is collagen and as such, is widely used by experimenters as an excellent substrate. Fibrin, as the main polymeric component of the wound healing response, is thought to have a range of pro-angiogenic effects on the cells that other substrates lack, such as binding domains for angiogenic factors, including VEGF and bFGF. Matrigel, comprised of solubilized basement membrane proteins, is also able to induce capillary morphogenesis.

Forming a network in matrix material is generally a slower process than in two dimensions since it relies heavily on the rate of proteolysis of the matrix material by the cells, in particular with matrix metalloproteinases (MMPs) and serine proteases (e.g. plasmin). With high numbers of fibroblasts alongside HUVECs, it has been shown that relatively high fibrin concentrations (10 mg/mL) can be used to generate capillary networks over 7 days, as shown in Figure 4.1c [19]. The cells start by spreading and migrating towards one another and then form larger, more stable structures.

One other approach, between two and three dimensions, is to culture pericytes in a three dimensional gel, such as densified collagen, and grow endothelial cells (HUVECs) on tissue culture plastic underneath [4]. This enables rapid development of capillary-like structures, which are not impeded by the matrix material, and enables the endothelial cells to later sprout into the gel when more mature structures have formed [4].

The addition of a parenchymal cell type (hepatoblast) to a co-culture of HUVECs and MSCs was shown to produce organ-like (liver) vasculature; MSCs behaved as pericytes to a complex vascular network of endothelial cells, which supported the hepatic cell type [153]. Thus it is clear that the addition of a third, tissue-specific cell has the potential to influence the capillaries by modulating the morphology of the network. Shown in Figure 4.1d is the

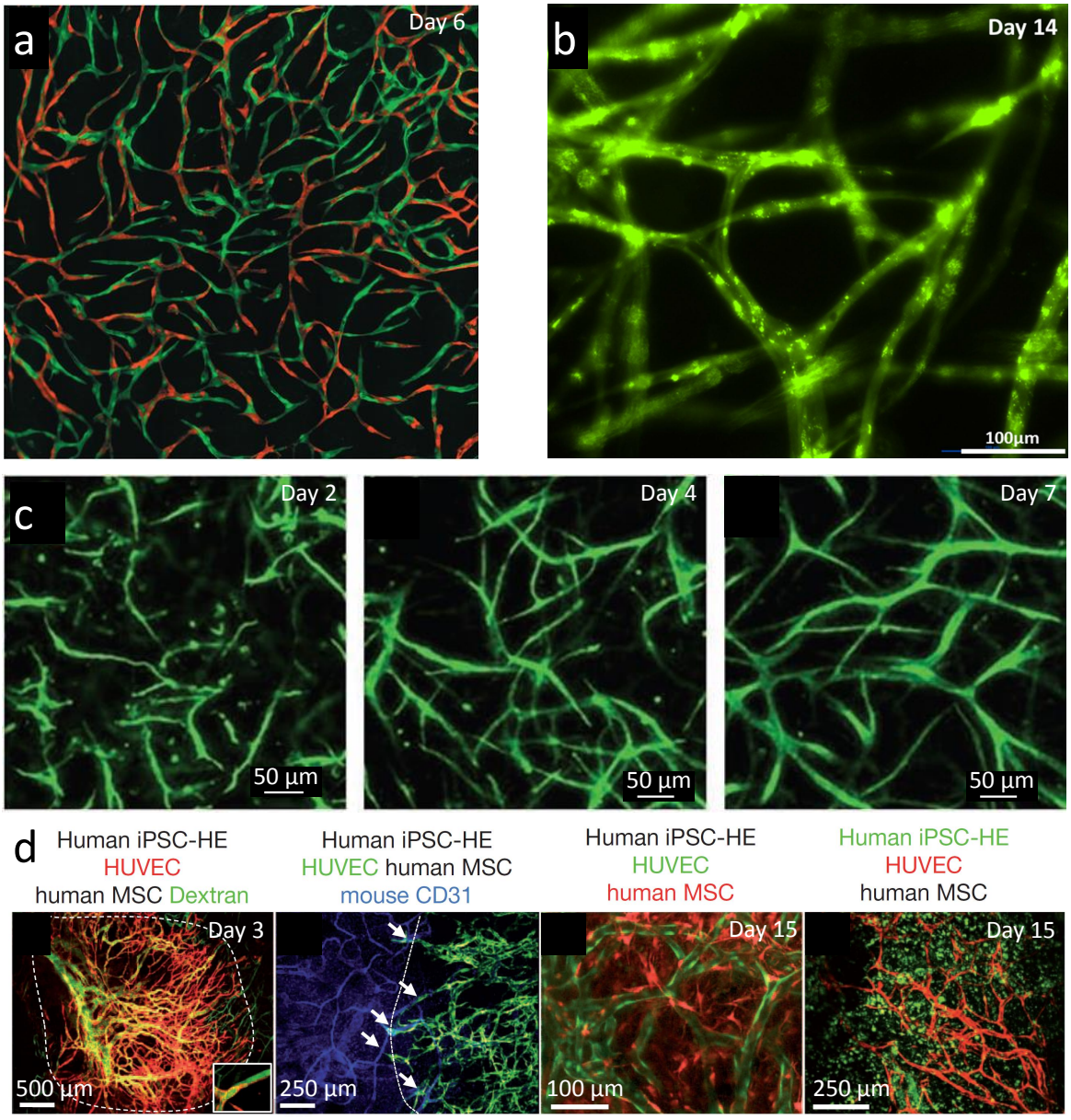

Fig. 4.1 (a) Two dimensional co-culture of endothelial and smooth muscle cell types on tissue culture plastic - green and red stain two different types of endothelial cell [41]. (b) Three-dimensional co-culture of HUVEC and NHLFs in 10 mg/mL fibrin hydrogel [91]. (c) Development of endothelial network over 7 days. [19]. In both (b) and (c) high levels of fibroblasts were used (2×10^6 NHLFs/mL) alongside endothelial cells (1×10^6 HUVECs/mL) which allows for capillary morphogenesis in 10 mg/mL fibrin gel. (d) Liver-like vasculature can be achieved by culturing HUVECs and MSCs alongside hepatic cells [153]. Here, following 72 h of culture *in vitro*, constructs were transplanted into mice and grown *in vivo*. Note MSCs behaving like perivascular cells in the 3rd image. Arrows show connections from HUVECs (green) to host vessels (blue) [153].

liver-like network produced by culturing HUVECs, MSCs, and hepatic cells induced from iPSCs, for 72 h *in vitro* followed by transplantation into mice for two weeks.

4.5 Angiogenic Approaches

Angiogenesis can be achieved by coating endothelial cells onto the surface of microcarrier beads, as shown in Figure 4.2a [116]. Such a method is excellent for studying the process of angiogenesis and optimizing conditions in which long capillaries form within a three dimensional matrix.

Similarly, endothelial cells can be made to form multi-cellular spheroids which also undergo angiogenic sprouting under the right conditions. The outer layer of these spheroids acts like an endothelial monolayer, which sprouts into the bulk [116]. Figure 4.2b shows a gel in which spheroids have been seeded in three dimensions. Following several weeks *in vivo*, the construct exhibited a complex network of capillaries, which had anastomosed to the native vasculature [88]. This approach was considered in this project as a method to produce capillaries *in vitro* and the details of our experiments are described in Chapter 5. Note that a surprisingly low number of cells is required to produce a full network like this, when using multi-cellular spheroids *in vivo* (i.e. 1×10^5 ECs/mL) [88].

Lab-on-chip systems, which were discussed earlier, are excellent platforms for studying angiogenesis and vasculogenesis *in vitro*. By seeding endothelial cells into one channel and a supporting cell type into another, across a matrix-like gel, one observes angiogenic sprouting of endothelial cells [78]. Over time, complex networks can form in that space, as shown in Figure 4.2c [78]. Further, lab-on-chip systems can be designed to set up molecular gradients of growth factors; useful in understanding and optimizing capillary growth.

Capillaries can be formed by angiogenic processes from a confluent layer of endothelial cells, arranged into a tube-like structure as just described, but also from a monolayer on a hydrogel surface [38]. Sprouting of an endothelial cell monolayer into a bulk matrix material below is reported to take place in the presence of tumor promoters such as phorbol esters (e.g. PMA), which is similar to pathological sprouting from large-scale vessels *in vivo* [112]. This has significance when attempting to connect a large cell-lined channel or surface to a vasculogenic capillary bed [38].

Finally, native tissue can be used to induce angiogenic sprouting in lab-based constructs. A mouse aortic ring assay is described in the literature in which sections of the aorta are embedded in a matrix (collagen, fibrin, Matrigel) along with various growth factors (e.g. VEGF, bFGF), as shown in Figure 4.2e [10]. Angiogenic sprouts form rapidly off this already mature structure. In similar work, short sections of microvessels are embedded

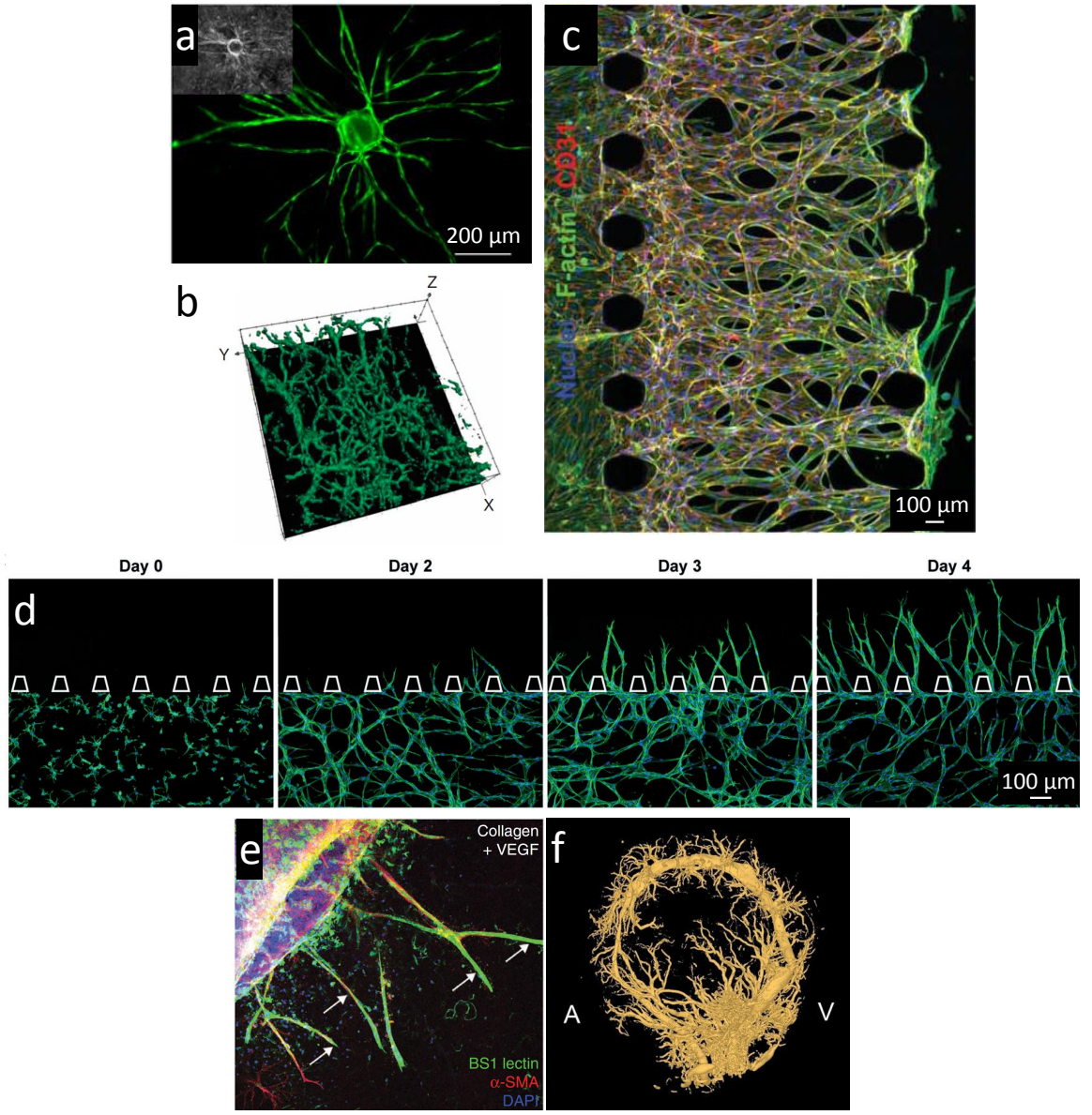

Fig. 4.2 (a) Microcarrier beads, seeded with endothelial cells on their surface, are an excellent way of studying angiogenesis; shown here are HUVECs in 2.5 mg/mL fibrin gel at day 7, with an overlying fibroblast monolayer [45]. (b) Multi-cellular spheroids, consisting of large number number of endothelial cells, can be used in a similar way, and have been shown to yield complex networks of capillaries *in vivo* [88]. (c) Lab-on-chip systems enable fine control of the environment which enables both angiogenic and vasculogenic networks to be formed [78]. (d) Time lapse of lab-on-chip system [77]. Vasculogenic capillaries form in the lower chamber, from 5×10^6 HUVECs/mL and 7.5×10^6 NHLFs/mL in 2.5 mg/mL fibrin. Angiogenic sprouting then takes place into acellular region of the gel. (e) *In vivo* approaches to angiogenic capillary formation include an aortic ring assay [10]. Section of aortic ring is shown in the top left and angiogenic sprouting can be seen into a collagen gel [10]. (f) Arteriovenous loops are also used to vascularise a scaffold rapidly [42]. Shown here is a micro-CT image of a perfused arteriovenous loop in a rat model, where A and V denote the arterial and venous sides respectively [42].

in matrix materials; the cells proliferate and undergo angiogenesis [53, 58, 140]. Finally, arteriovenous loops and arteriovenous bundles are employed *in vivo* in which a length of existing (and connected) vessel is embedded into a gel matrix construct [42, 80, 100, 154]. Shown in Figure 4.2f is a micro-CT image of one such loop in a fibrin matrix [42]. This rapidly yields highly vascularized tissue. All three methods take advantage of native vasculature which comprises the correct layers of cell types, along with basement membrane.

All the above methods have the advantage that the endothelial cells are in constant contact with neighbouring cells, unlike the vasculogenic approach. Single endothelial cells seeded in a suspension culture rapidly undergo apoptosis [85]. Thus, the constant contact from a monolayer or spheroid *in vitro* reflects how endothelial cells are organised in physiological tissue and thus improves their chances for survival. It has been shown that organising endothelial cells into multicellular spheroids prevents apoptosis and induces their differentiation [85]. One paper states that cell-cell junctions in endothelial cells may also transfer intracellular signals that regulate contact-induced inhibition of cell growth, apoptosis, gene expression, and new vessel formation, providing a range of effects on vascular homeostasis [35].

4.6 Substrates for Capillary Morphogenesis

Certain biopolymers are suited for capillary morphogenesis, in particular collagen and fibrin, as they are able to provide molecular binding sites for endothelial and perivascular cells but also are able to bind specific growth factors, encouraging spatial localization of the various factors necessary for capillary morphogenesis to occur.

The matrix properties are very important for inducing capillary morphogenesis; the concentration is key since new capillaries are formed by the degradation of surrounding matrix. A high concentration, while improving the mechanical properties of the gel, will slow down the rate of matrix degradation by proteolysis (matrix metalloproteases (MMPs) and serine proteases are implicated in the degradation of collagen and fibrin) and so, the rate of capillary formation. Commonly found substrates in the capillary morphogenesis literature are 2.5 mg/mL collagen gels and 2.5-10 mg/mL fibrin gels (see Table 4.2). Alternative matrices have also been shown capable of producing capillaries under co-culture conditions, such as glycosaminoglycan (GAG)-based hydrogels [24] and Matrigel [76]. Other components of the native extra-cellular matrix are likely to aid in the development of tissue structures, including basement membrane components, such as collagen IV and laminin, and hyaluronic acid [129].

One particular matrix composition of note that is used for *in vivo* studies is 1.5 mg/mL collagen with 90 μg/mL fibronectin. Fibronectin is an adhesive glycoprotein which aids cellular adhesion and plays an important role in tissue development [143]. One particular paper shows that fibronectin can have a dramatic influence on cell proliferation and microtissue formation, with the morphology of the microtissues dependent on the fibronectin concentration [143]. Further, physiological angiogenesis occurs predominantly in the wound healing environment which consists of fibrin, fibronectin, and vitronectin [64]. Thus, the inclusion of fibronectin into either a fibrin or collagen gel is likely to improve conditions for capillary morphogenesis.

The incorporation of heparin has also been shown to be useful in regulating growth factor release from the matrix material, such as fibrin [134], and heparin has been reported to play an important role in the regulation of VEGF and bFGF signalling, and the wider process of angiogenesis [62, 25].

Only certain matrix types are degradable by the cells. For instance, in the case of a calcium alginate, cells lack the specific enzyme required (alginase) to break it down and as such, are unable to remodel the hydrogel construct, and maintain a spherical morphology. An alignment of ECM fibrils and a particular stiffness can also encourage the formation of a capillary bed due to the mechanical cues imparted to the cells, whilst also enabling efficient migration.

A high concentration of matrix material greatly diminishes the ability of the cells to migrate and form cell-cell junctions, necessary for preventing apoptosis and also for forming a contiguous network of capillaries. Also, matrix concentration affects the rate of diffusion of signalling molecules acting between cells [40]. On the other hand, a matrix of low concentration can be degraded too rapidly by cells before collagen deposition and remodelling has had a chance to stabilize the structure.

The thickness and concentration of the gels used in three dimensional capillary morphogenic systems *in vitro* are thus important variables. Generally, cell medium is deposited on top of a gel and, since oxygen and nutrients will reach the cells by diffusion only, a thick construct limits the volume of oxygen that can reach cells at the bottom of the gel. Oxygen consumption is a faster process than oxygen diffusion and as such, most systems are oxygen limited [5]. Thus, in systems that do not contain vasculature, or are above a threshold of cell concentration, a thin gel of low concentration is generally the only option. One alternative is to introduce interstitial flow which, as well as being a mechanical cue for angiogenesis, can replenish the oxygen levels in a thick and dense construct. Several papers show that even in high concentration gels (i.e. 10 mg/mL fibrin), the application of interstitial flow to the construct yields capillary structures [60, 122, 54, 59]. When combined with VEGF,

interstitial flow is reported to enhance capillary morphogenesis through setting up gradients of the growth factor and is better than either parameter used separately [54].

Collagen deposition is another aspect of the matrix development which needs to be considered, and is a key component of the wound healing process. As the initial fibrin or collagen matrix is broken down by proteolytic mechanisms, newly organised matrix materials need to be deposited by the cells in a way which supports further growth and improves the mechanical properties of the tissue or tissue construct. This is important for producing a tissue-engineered construct with sufficient strength for implantation.

Crosslinking of the matrix material, by physical, chemical, or enzymatic means, is likely to have an effect on capillary morphogenesis. Crosslinking will generally enhance the mechanical properties of the construct (useful in clinical applications), but can have a beneficial or detrimental effect on angiogenesis. For example, covalent linkages between the polymers, formed by crosslinking, can prevent or slow down the degradation of the matrix by proteolysis, thereby making it harder for endothelial cell migration and remodelling of the surrounding matrix. However, it may also improve conditions for capillary formation by stabilizing a construct and slowing its degradation rate. In the case of fibrin, the addition of the enzyme transglutaminase (factor XIII), which is part of the normal coagulation cascade and which further stabilizes the fibrin matrix by forming amide bonds between fibrin molecules, has been shown in the literature to be beneficial to capillary morphogenesis [90].

Table 4.2 Literature on capillary morphogenesis in three dimensional hydrogel systems.

	Reference	Year	Angiogenic/ Vasculogenic	*In Vitro/ In Vivo*	Substrate, Concentration	Endothelial Cell Type, Concentration	Supporting Cell Type, Concentration	Growth Factors and Medium
1	*Angiogenic sprouting and capillary lumen formation modeled by human umbilical vein endothelial cells (HUVEC) in fibrin gels:* textitthe role of fibroblasts and Angiopoietin-1 [119]	2003	Angiogenic (beads)	*In vitro*	2.5 mg/mL Fibrin, pH 7.4	HUVEC (beads)	Skin fibroblasts, (20,000 on top of gel)	EGM2 medium
2	*An Optimized Three-Dimensional In Vitro Model for the Analysis of Angiogenesis [118]*	2008	Angiogenic (beads)	*In vitro*	2 mg/mL (1 U/mL) Fibrin	HUVEC (1×10^5 on beads)	Lung fibroblasts (20,000 on top of gel)	EGM2 medium (2 day medium changes)
3	*The Effect of Matrix Density on the Regulation of 3-D Capillary Morphogenesis [45]*	2008	Angiogenic (beads)	*In vitro*	2.5-10 mg/mL Fibrin	HUVEC (4×10^5 on beads)	NHLF, MSCs (1×10^5 NHLF/mL)	EGM2 medium
4	*Mesenchymal cells stimulate capillary morphogenesis via distinct proteolytic mechanisms [46]*	2010	Angiogenic (beads)	*In vitro*	2.5 mg/mL (1 U/mL) Fibrin	HUVEC (4×10^5 on beads)	NHLF, MSCs (1×10^5 NHLF/mL)	EGM2 medium
5	*Assessing the Permeability of Engineered Capillary Networks in a 3D Culture [50]*	2011	Angiogenic (beads)	*In vitro*	2.5 mg/mL (1 U/mL) Fibrin	HUVEC (4×10^5 on beads)	NHLF, MSCs (25,000 on top of gel)	EGM2 medium
6	*Engineering of In Vitro 3D Capillary Beds by Self-Directed Angiogenic Sprouting [17]*	2012	Angiogenic (channels)	*In vitro*	2.5 mg/mL Collagen, pH 7.4 (with Alginate beads)	HMVEC, 2×10^6 cells/mL (from side channel)	Human dermal fibroblasts (HDF, though not in same study)	50 ng/mL VEGF, EGM2 medium
7	*Biomimetic model to reconstitute angiogenic sprouting morphogenesis in vitro [123]*	2013	Angiogenic (channels)	*In vitro*	2.5 mg/mL Collagen	HUVECs, HMVECs - 1×10^7 ECs/mL (in side channels)	-	Large range of factors, EGM2, EGM2-MV
8	*Complementary effects of ciclopirox olamine, a prolyl hydroxylase inhibitor and sphingosine 1-phosphate on fibroblasts and endothelial cells in driving capillary sprouting [94]*	2013	Angiogenic (channels)	*In vitro*	Collagen	HUVEC, 2.5×10^6 HUVECs (in side channels)	IMR-90 fibroblasts, 25×10^6 cells/mL (in side channels)	EGM2-MV, 20 ng/ml VEGF, also CPX, S1P
9	*Spheroid-based human endothelial cell microvessel formation in vivo [88]*	2008	Angiogenic (spheroids)	*In vivo*	2 mg/mL (0.4 U/mL) Fibrin with Matrigel	HUVEC Spheroids (1×10^5 HUVECs/mL)	1×10^5 HDF/mL	500 ng/mL VEGF, bFGF, PDGF-BB
10	*Dense type I collagen matrices that support cellular remodeling and microfabrication for studies of tumor angiogenesis and vasculogenesis in vitro [27]*	2010	Both	*In vitro*	3-8 mg/mL Collagen, pH 7	HUVEC, 6×10^6 HUVECs/mL	-	40 ng/mL VEGF, 40 ng/mL bFGF, 50 ng/mL TPA
11	*Engineering of functional, perfusable 3D microvascular networks on a chip [78]*	2013	Both	In vitro	2.5 mg/mL (0.5 U/mL) Fibrin + 0.2 mg/ml Collagen	HUVEC, 2-3×10^6 HUVECs/mL	NHLF, 5×10^6 NHLFs/mL	EGM2 (daily medium changes)
12	*Generation of Multi-scale Vascular Network System Within 3D Hydrogel Using 3D Bio-printing Technology [91]*	2014	Both	*In vitro*	10 mg/mL (3 U/mL) Fibrin	HUVEC, 1×10^6 HUVECs/mL	Normal human lung fibroblasts (NHLFs), 2×10^6 NHLFs/mL	EGM2 medium
13	*Endothelial cell dynamics during anastomosis in vitro [38]*	2015	Both	*In vitro*	6 mg/mL Collagen, pH 7.4	HUVEC, 1-2×10^6 HUVECs/mL	Human Brain Vascular Pericytes (HBVPs), 0-2×10^5 PCs/mL	40 ng/mL VEGF, 40 ng/mL bFGF, 50 ng/mL TPA, 50 μg/mL L-ascorbic acid
14	*Interstitial flow regulates the angiogenic response and phenotype of endothelial cells in a 3D culture model [77]*	2016	Both	*In vitro*	2.5 mg/mL (1 U/mL) Fibrin	HUVECs, 5×10^6 HUVECs/mL	NHLF, 7.5×10^6 NHLFs/mL	100 ng/mL VEGF, 1 μM Sphingosine-1-phosphate (S1P), EGM2 medium
15	*Tissue engineering: Creation of long-lasting blood vessels [83]*	2004	Vasculogenic	*In vivo*	1.5 mg/mL Collagen with 90 μg/mL Fibronectin, pH 7.4	HUVEC, 0.8-1×10^6 HUVECs/mL	10T1/2, 2×10^5 PCs/mL	-
16	*Bone marrow–derived mesenchymal stem cells facilitate engineering of long-lasting functional vasculature [6]*	2008	Vasculogenic	*In vivo*	1.5 mg/mL Collagen with 90 μg/mL Fibronectin, pH 7.4 (25mM HEPES-buffered EGM medium)	HUVEC, 1×10^6 HUVECs/mL	MSC, 10T1/2 - 2×10^5 PCs/mL	-
17	*Engineered vascularized bone grafts [158]*	2010	Vasculogenic	*In vivo*	1.5 mg/mL Collagen with 90 μg/mL Fibronectin, pH 7.4	HUVEC, 1×10^6 HUVECs/mL	MSC, 2.5×10^5 MSCs/mL	EGM2 medium
18	*Effects of Extracellular Matrix Density and Mesenchymal Stem Cells on Neovascularization In Vivo [81]*	2011	Vasculogenic	*In vivo*	5-15 mg/mL (1 U/mL) Fibrin (serum-free EGM2 medium)	HUVEC, 5×10^6 HUVECs/mL	MSC, 5×10^6 MSCs/mL	-
19	*Endothelial cells derived from human embryonic stem cells form durable blood vessels in vivo [166]*	2007	Vasculogenic	Both	1.5 mg/mL Collagen with 90 μg/mL Fibronectin, pH 7.4 (25mM HEPES-buffered EGM medium)	ESC-derived CD34+ cells, 1×10^6 ECs/mL	10T1/2, 2×10^5 PCs/mL	EGM medium
20	*A role for VEGF as a negative regulator of pericyte function and vessel maturation [51]*	2008	Vasculogenic	Both	Matrigel	HUVECs, HMVECs, HAECs	HDF, 10T1/2	PDGF-BB, VEGF-165, bFGF at 20 ng/mL, 40 ng/mL, and 50 ng/mL (in vitro)
21	*Prevascularization of a Fibrin-Based Tissue Construct Accelerates the Formation of Functional Anastomosis with Host Vasculature [18]*	2009	Vasculogenic	Both	10 mg/mL (2 U/mL) Fibrin	HUVEC, 0.1-3×10^6 HUVECS/mL	NHLFs, 0.02-0.4×10^6 NHLFs/mL	EGM2 medium
22	*Formation of Human Capillaries In Vitro: The Engineering of Prevascularized Matrices [111]*	2009	Vasculogenic	Both	7-15 mg/mL Fibrin (only 10-11 mg/mL gave lumen structures), 2.5-3.5 mg/mL Collagen	HDMVECs, 1×10^4-2×10^5 ECs/mL, Optimal 3×10^4 ECs/mL	-	EGM2-MV medium
23	*Rapid Anastomosis of Endothelial Progenitor Cell–Derived Vessels with Host Vasculature Is Promoted by a High Density of Cotransplanted Fibroblasts [19]*	2010	Vasculogenic	Both	10 mg/mL (2 U/mL) Fibrin	HUVEC, 1×10^6 HUVECs/mL	NHLFs, 0.2-2×10^6 NHLFs/mL	EGM2 medium

Table 4.2 (cont.) Literature on capillary morphogenesis in three dimensional hydrogel systems.

	Reference	Year	Angiogenic/ Vasculogenic	*In Vitro*/ *In Vivo*	Substrate, Concentration	Endothelial Cell Type, Concentration	Supporting Cell Type, Concentration	Growth Factors and Medium
24	*Cooperation of Endothelial and Smooth Muscle Cells Derived from Human Induced Pluripotent Stem Cells Enhances Neovascularization in Dermal Wounds [76]*	2013	Vasculogenic	Both	Matrigel	hiPSC- and hESC-derived ECs, 1.5×10^5 ECs/mL (without PCs)	SMCs, 6:4 ratio (1.2×10^5:0.8×10^5 EC:SMC/mL)	EGM2 medium
25	*Engineering of human hepatic tissue with functional vascular networks [152]*	2014	Vasculogenic	Both	1.5 mg/mL Collagen with 90 μg/mL Fibronectin, pH 7.4 (25mM HEPES-buffered EGM medium)	HUVEC, 8×10^5 HUVECs/mL. Vessels from HUVECs alone disappeared in vivo after 1 month	MSC, 2×10^5 MSCs/mL (connected to host vessels within 14d). Separate experiment also includes 1×10^6 hFLCs/mL)	EGM medium
26	*Endothelial tubulogenesis within fibrin gels specifically requires the activity of membrane-type matrix metalloproteinases [87]*	2002	Vasculogenic	*In vitro*	2.5 mg/mL Fibrin	HUVEC and HDMVEC, 1.5×10^6 ECs/mL	-	Range of factors: 25 ng/mL VEGF, 10 ng/mL bFGF, 10 ng/mL TNF-α, 1 ng/mL TGF-β1, 50 ng/mL EGF, 10 ng/mL TGF-α, 300 U/mL HGF/SF, 10 ng/mL IL1α, 100 ng/mL angiogenin
27	*Interstitial flow differentially stimulates blood and lymphatic endothelial cell morphogenesis in vitro [122]*	2004	Vasculogenic	*In vitro*	3.5 mg/mL Collagen	Microvascular lymphatic and blood endothelial cells, 1×10^6 ECs/mL	-	50 ng/ml PMA and 20% serum
28	*Synergy between interstitial flow and VEGF directs capillary morphogenesis in vitro through a gradient amplification mechanism [54]*	2005	Vasculogenic	*In vitro*	2 mg/mL (2 U/mL) Fibrin	Human microvascular blood ECs and lymphatic ECs, 1.5×10^6 cells/mL	-	100 ng/mL VEGF121 variant
29	*Pericyte recruitment during vasculogenic tube assembly stimulates endothelial basement membrane matrix formation [149]*	2009	Vasculogenic	*In vitro*	2.5 mg/mL Collagen	HUVECs, HDMVEC	Bovine retinal pericytes and human brain pericytes (20% of HUVEC level)	40 ng/mL bFGF, serum supplement in media, 200 ng/mL stem cell factor, SDF-1α, interleukin-3 in media
30	*Endothelial-derived PDGF-BB and HB-EGF coordinately regulate pericyte recruitment during vasculogenic tube assembly and stabilization [150]*	2010	Vasculogenic	*In vitro*	2.5 mg/mL Collagen	HUVECs, 2×10^6 HUVECs/mL	Human Brain Vascular Pericytes (HBVP), 0.4×10^6 PCs/mL	Culture medium containing reduced serum supplement and 40 ng/mL bFGF. In gel: 200 ng/mL of stem cell factor, SDF-1α, IL-3
31	*Matrix composition regulates three-dimensional network formation by endothelial cells and mesenchymal stem cells in collagen/fibrin materials [135]*	2011	Vasculogenic	*In vitro*	2.5 mg/mL Collagen and Fibrin Mixtures Col:Fib 100:0, 60:40, 50:50, 40:60, 0:100 (best ratio). Also for 40:60, total protein conc 1.25 mg/mL (best), 2.5 mg/mL (best), 5 mg/mL (worst by far)	HUVEC (Ratios: 5:1 (worst), 3:2 (best), 1:1, 2:3, 1:5). Fixed total cell concentration: 6×10^5 cells/mL	MSC	EGM2 medium
32	*A microfluidic platform for generating large-scale nearly identical human microphysiological vascularized tissue arrays [60]*	2013	Vasculogenic	*In vitro*	10 mg/mL (3 U/mL) Fibrin	Endothelial colony forming cell-derived endothelial cells (ECFC-ECs) - 5×10^6 ECs/mL	Normal human lung fibroblasts (NHLFs), 2.5×10^6 NHLFs/mL	EGM2 medium
33	*Aligned human microvessels formed in 3D fibrin gel by constraint of gel contraction [115]*	2013	Vasculogenic	*In vitro*	7.5 mg/mL (2.75 U/mL) Fibrin with 75 μg/ml Fibronectin	HUVECs, 3×10^6 HUVECs/mL	Human brain pericytes, 0.6×10^6 PCs/mL	In gel: 150 ng/mL stem cell factor, interleukin 3, FLT3 ligand, SDF-1α, bFGF. 'Defined medium': M199 with 4 μL/mL RSII, 40 ng/mL bFGF, 50 μg/mL ascorbic acid, 2 KIU/mL aprotinin. 'EGM2+' medium: EGM2 with additional 8% FBS
34	*In Vitro Microvessel Growth and Remodeling within a Three-Dimensional Microfluidic Environment [130]*	2014	Vasculogenic	*In vitro*	2-3 mg/mL Collagen	HUVEC, 3×10^6 HUVEC/mL	-	40 ng/mL VEGF, EGM2-MV medium
35	*Glycosaminoglycan-based hydrogels to modulate heterocellular communication in in vitro angiogenesis models [24]*	2014	Vasculogenic	*In vitro*	StarPEG-Heparin	HUVECs, 6×10^6 HUVECs/mL	MSC, SMC, HDF, 10T1/2, $0.3\text{-}1.5\times10^6$ cells/mL	In gel: 5 μg/mL VEGF, bFGF, SDF-1α. Medium: Low-serum endothelial cell growth medium
36	*Engineered Microvessels with Strong Alignment and High Lumen Density Via Cell-Induced Fibrin Gel Compaction and Interstitial Flow [114]*	2014	Vasculogenic	*In vitro*	2.5 mg/mL (1.25 U/mL) Fibrin	Human blood outgrowth endothelial cells (HBOECs) - 2×10^6 ECs/mL	Human brain pericytes, 0.4×10^6 PCs/mL	In gel: 200 ng/mL SCF, IL-3, SDF-1α. Medium: EGM2 + 8% FBS

4.7 Fibrin vs Collagen as a Substrate for Experiments

Fibrin gels can vary widely between research groups. Fibrinogen, the precursor glycoprotein of fibrin, can come from a wide range of sources. The diameter of the fibrin fibrils, permeability, and porosity of the gel depend greatly upon a number of factors including the concentration of fibrinogen and thrombin (pore size is smaller for higher concentrations of thrombin due to faster gelling time), calcium ion content, ionic strength [120], and temperature of gelation. Further, pH has been shown to have a significant effect of angiogenic sprouting length; gels polymerized at pH 6.8 induced single cell migration whereas gels polymerized at pH 7.0 induced sprout formation [116]. Other work suggests that gels prepared at pH 7.5 (clear gels), rather than pH 7 (turbid gels) are better as there is a greater degree of cell spreading when cells are seeded on the surface [84]. The addition of a basal medium buffer, cytokines, and other ECM molecules (e.g. fibronectin) can further influence the structure of the fibrin gel [116]. Fibrin precursor solutions can be made with relatively low viscosities at concentrations of 2.5-20 mg/mL whilst collagen precursor solutions tend to be much more viscous.

As the provisional matrix of the wound healing process, fibrin is pro-angiogenic [116]. It also promotes the production of extra-cellular matrix proteins such as basement membrane (e.g. collagen IV, laminin) and collagen I, the main structural protein of a tissue [116]. Fibrin has heparin binding domains which bind growth factors. All three growth factors, VEGF, bFGF, and SDF (all heparin-binding proteins), have some binding affinity for fibrin (and fibronectin) through the heparin-binding domain [105, 39].

Collagen-based gels are widely used for capillary morphogenesis since they allow for good cell adhesion [174]. However, collagen gels are not as biodegradable and are potentially antigenic and immunogenic [102, 174]. Fibrin is also significantly cheaper than collagen and more clinically relevant, since fibrinogen and thrombin can be extracted from the blood of the patient and are commonly used in surgical glue.

Fibrin found in wound healing environments has a concentration of around 2.5 mg/mL. However, at such low concentrations, the gels are very weak, undergo significant gel shrinkage, and degrade rapidly by proteolytic mechanisms, requiring higher concentrations to be used. Similarly, collagen at 2.5 mg/mL is very weak since it doesn't have the fibril alignment and organisation present in native tissue. Thus much higher collagen concentrations are also employed.

It has been shown in the literature that concentrations above 2.5 mg/mL are detrimental to capillary morphogenesis, with concentrations of 5 mg/mL showing a significant drop in total network length, when a relatively low concentration of cells is used (6×10^5 cells/mL) [135]. However, examples of vasculogenesis occurring at 10 mg/mL fibrin concentrations

have been reported in the literature, usually in the presence of high fibroblast concentrations (1×10^6 HUVECs/mL, 2×10^6 HNLFs/mL) [91, 19] and also when interstitial flow is introduced [60].

Various protease inhibitors, such as aprotinin, have been added to cell medium for use with fibrin constructs, which prevent the rapid proteolytic degradation by the cells and help to stabilize their development [73, 174]. Aprotinin has also been shown to improve the wound healing response *in vivo* where, in one paper, a significant increase in capillary infiltration was observed and a more fibrous structure formed when aprotinin was added [156]. Aprotinin inhibits serine proteases, such as thrombin and plasmin, whilst other inhibitors can prevent membrane-type MMPs from degrading the matrix. One paper importantly shows that when using MSCs, the use of aprotinin does not prevent vascular network formation [46]. Using specific protease inhibitors for membrane-type MMPs did however prevent capillary formation [46]. For fibroblast-mediated capillary formation, inhibiting either membrane-type MMP proteases or serine proteases separately did not prevent capillary formation, though their simultaneous use did inhibit growth [46].

4.8 Cellular Considerations for Experiments

There are a wide range of combinations of cell types that could be used in co-culture models of angiogenesis and vasculogenesis. Commonly used endothelial cells are human umbilical vein endothelial cells (HUVECs) and human microvascular endothelial cells (HMVECs), alongside a range of supporting cells; human dermal fibroblasts (HDFs), human normal lung fibroblasts (HNLFs), smooth muscle cells (SMCs), mesenchymal stromal cells (MSCs), and pericytes (PCs), as shown in Table 4.2. In our experiments, we choose to use HUVECs alongside either HDF or MSCs for reasons which will be discussed below.

The main role of the supporting cell is to provide stability to the capillary structure; the release of PDGF by the endothelial cells causes the perivascular cells to migrate and interact with the endothelial capillaries; pericyte recruitment triggering the formation of the basement membrane [149]. However, in constructs that lack a parenchymal cell, the supporting cell also signals to the endothelial cells that it is hypoxic or lacking other metabolites.

Whilst endothelial cells are capable of producing capillary structures by themselves, the lack of supporting cell *in vitro* and *in vivo* has been shown to cause microvessels to regress over time [83, 24]. By knocking out PDGF, pericyte recruitment is blocked [116]. When experiments with and without pericytes were compared, it was shown that there is no difference in vessel length or branching. Thus pericytes are only responsible for regulating vascular stability, permeability, and diameter, but not initial micro-vessel patterning [116].

However, high concentrations of supporting cells (MSCs, SMCs) have also been reported to inhibit vasculogenic tube assembly [24, 149, 76]. Since pericytes act to stabilize existing endothelial structures, high concentrations of pericytes could prevent the initial endothelial cell spreading. The literature suggests a co-culture of endothelial cells with 10% MSCs is sufficient to yield a mature and stable network for more than 4 weeks [24].

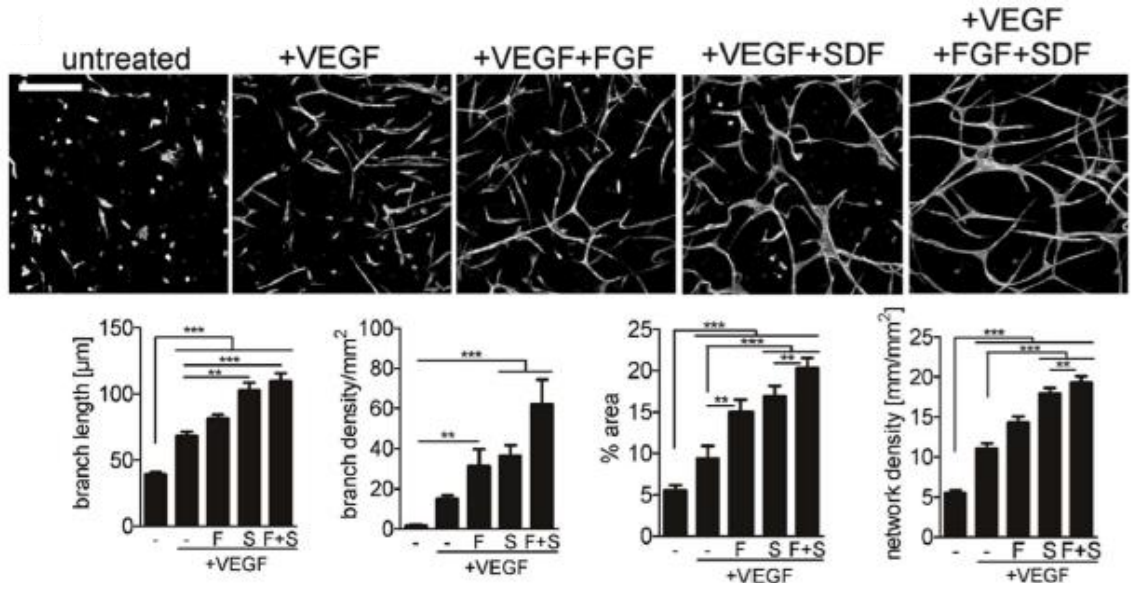

Fig. 4.3 Combination of VEGF, bFGF, and SDF-1α produces a superior capillary network in starPEG-heparin hydrogels [24]. Note that with SDF-1α, only low levels of supporting cell (10% MSCs) were needed to produce a robust network.

The addition of growth factors, as an alternative to high levels of signalling supporting cells, may be suitable. One paper shows that the addition of stromal derived factor (SDF-1α) alongside VEGF and bFGF enhances the formation of vasculogenic capillary-like structures [24]. Figure 4.4 shows that when used together, VEGF, bFGF, and SDF-1α produce an improvement in branch length, branch density, percentage area, and network density [24]. SDF-1α upregulates VEGF-A, VEGF upregulates SDF-1α [132], and SDF-1α induces more migration of HUVECs. Thus the combination of VEGF and SDF-1α is reported to be excellent for inducing angiogenesis [132]. Also, the literature reports that HUVECs and EPCs release a range of pro-angiogenic factors that, along with conditioned medium, can stimulate cell migration, reducing the need for supporting cells [160].

PDGF is another growth factor that one might consider adding to the co-culture system in order to induce angiogenesis. PDGF is reported to induce angiogenesis by priming pericytes and smooth muscle cells into producing pro-angiogenic mediators [51]. It has been used alongside VEGF in several papers, yielding neovascularization [88, 51].

The cell concentration and ratio between endothelial and supporting cell types varies greatly in the literature, which is seen in Table 4.2. As discussed above, the concentration of the matrix material determines the concentration of cells required for a capillary morphogenesis since in denser substrates, diffusion of signalling factors will be slower and with the same rate of proteolysis, cells will take longer to form physical contacts with one another. The colocalization of cells, in particular individual endothelial cells, is necessary for the formation of capillary structures. The passage number of the cells will also determine their ability to proliferate and form structures in the construct, with higher passage cells exhibiting increased senescence and apoptosis.

Finally, since the construct is likely to be oxygen limited in its development, a maximum cell concentration will be determined by the ability to supply oxygen to the cells. Well plate experiments with static medium are likely to have a low concentration threshold for cell survival whilst perfusion experiments, in which the medium is continually being replenished with oxygen, is likely to be able to support a much higher density of cells.

4.9 MSCs vs Fibroblasts

In this project, we use both human dermal fibroblasts (HDFs) and mesenchymal stromal cells (MSCs). Fibroblasts, while suitable as a supporting cell and capable of undertaking significant collagen deposition, can proliferate to high densities, which then compete with endothelial cells for oxygen and nutrients. MSCs have been shown to potentiate VEGF-induced angiogenesis in co-culture [157]. MSCs also exhibit contact inhibition, meaning that they don't overgrow in culture. They also have been shown to turn off endothelial cell proliferation in favour of capillary morphogenesis. The downside to using MSCs is that they may cause signficiantly more gel shrinkage than the HDFs, owing to the contractile smooth muscle and pericyte phenotypes that they develop [24]. Mesenchymal cells have been shown to enhance the wound healing process, when compared to fibroblast-mediated healing [172] and produce Ang-1 and Ang-2, which are capillary stabilizing proteins [172].

High concentrations of fibroblasts enable capillary morphogenesis. Comparisons of experiments using 0.2×10^6 NHLFs/mL and 2×10^6 NHLFs/mL, alongside 1×10^6 HUVECs/mL, showed that the higher concentration of fibroblasts was far better at yielding full networks, even in 10 mg/mL fibrin [91, 19]. However high concentrations of MSCs are reported to inhibit tube formation when used above 25% of the HUVEC concentration (10% was sufficient) [24].

One paper explores the EC-MSC interaction. They found that 1:1 and 3:1 ratios of EC:MSCs inhibited capillary growth, while 10:1 did not [128]. Further, they found that

'MSCs migrated toward the capillaries, intercalated between ECs, established Cx43-based intercellular gap junctional communication (GJC) with ECs, and increased production of reactive oxygen species, which led to EC apoptosis and capillary degeneration' [128]. Another paper found that long-lived vasculature was achievable *in vivo* by culturing HUVEC:MSCs at a 5:1 ratio in collagen-fibronectin gels [6].

The addition of a liver parenchymal cell type, such as hepatoblasts, hepatocytes, and fetal liver cells, to a co-culture of HUVEC and MSC (5:1 HUVEC:MSC) has been reported to yield liver-like vascular structures [152, 153]. Thus, given that the end goal of this research is the formation of useful organ-like vasculature, using MSCs as the supporting cell would appear more appropriate, as fibroblasts would likely overgrow and create a fibrotic tissue.

While fibroblasts appear to not interact with endothelial cells in the same way as MSCs (most notably at higher concentrations of supporting cells), they do produce various factors which enable capillary formation. MSCs, used in lower concentrations, still appear to be the better option, when considering the addition of a parenchymal cell type, preventing cellular overgrowth of the supporting cell type, and getting a better perivascular interaction between the endothelial and supporting cells.

4.10 Perfusion and Anastomosis Mechanisms

One of the primary challenges that follows fabrication of a capillary bed is its perfusion. Angiogenically-formed vessels are easier to perfuse as they are already connected to an existing channel. As such, lab-on-chip systems have been able to show perfusion of angiogenic sprouts which spread from one channel across to another, as shown in Figure 4.4a [123]. Connecting a flow system to a vasculogenically-formed capillary network is more difficult and requires the capillaries to connect to a larger channel system. Various papers show that it is possible to anastomose the angiogenic and vasculogenic forms of capillary morphogenesis in the hope of perfusing the capillary bed, one with [38] and one without [91] the addition of tumor promoters. Note that we are not aware of any literature which attempts to anastomose a capillary bed to an acellular, large-scale channel.

One factor to consider when attempting to perfuse capillaries is their permeability. One paper [50] reports the exclusion of 75 kDa dextran, added to a endothelial-fibroblast co-culture system in 2.5 mg/ml fibrin, from the lumen in the case of mature capillaries (that is, stabilized by supporting cells) but not in the case of immature early sprouts [50]. Since mature capillaries are reported to be impermeable to 65 kDa dextran, this shows that an impermeable layer can be formed by vasculogenic means.

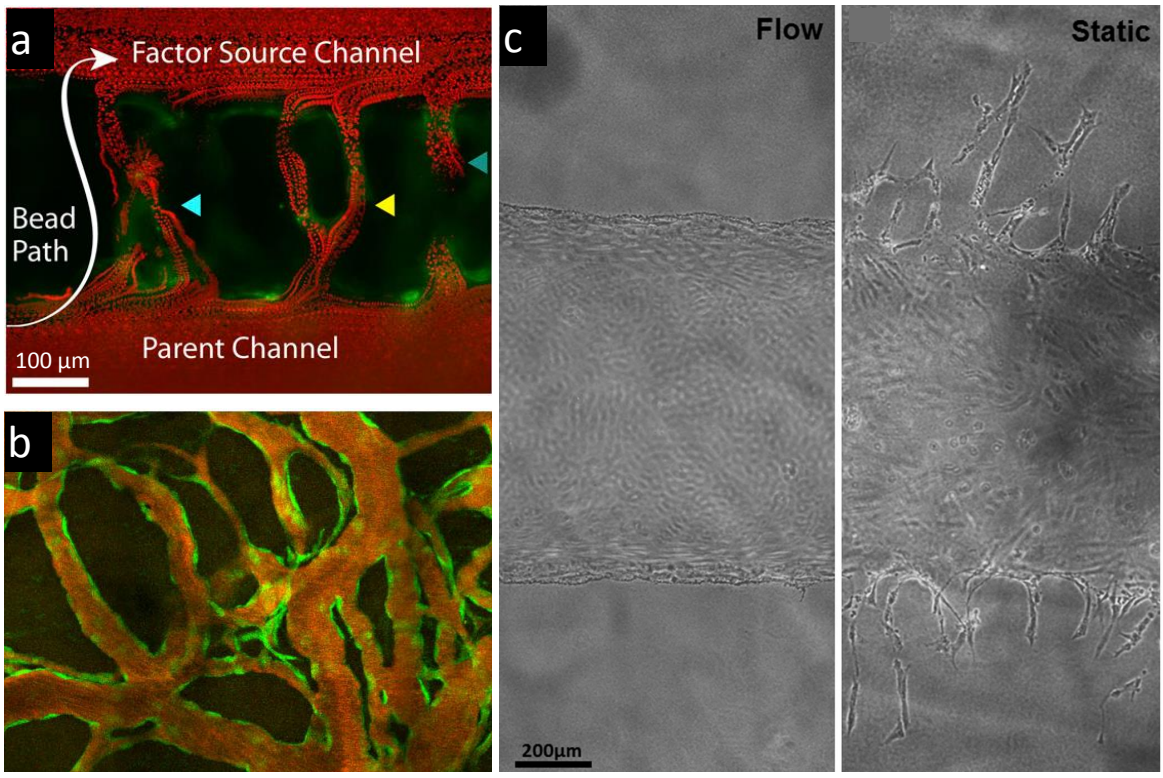

Fig. 4.4 (a) Perfusion between two channels in lab-on-chip system via capillary channel formed via angiogenesis [123]. (b) Long term (130 day) perfusable vasculature was fabricated using *in vivo* techniques with HUVECs and MSCs, in a collagen-fibronectin gel [6]. (c) Paper shows that endothelial-lined channel does not sprout into bulk when flow is applied [91].

There are notable advantages developing vascular constructs *in vivo* as opposed to *in vitro*. The clearest advantage is the anastomosis of a prevascularized construct to the native vasculature, with the subsequent blood perfusion that takes place. This provides the construct with a range of new cues for development, including interaction with macrophages. The downside of *in vivo* work is the lack of control over such a system and the need for an animal in order to conduct the research. One good example of perfusion of a construct *in vivo* is shown in Figure 4.4b [6]. Here, 1×10^6 HUVECs/mL and 2×10^5 MSCs/mL were encapsulated in 1.5 mg/mL collagen containing 90 μg/mL fibronectin. The work is notable for showing the long-lived nature of these vessels (130 days) and that the vessels are entirely perfusable. The application of flow may prevent the large scale vessels from forming angiogenic sprouts, when flow is maintained. One paper [91] shows budding of endothelial cells into the bulk when under static culture conditions, but not under perfusion, as shown in Figure 4.4c.

4.11 Chapter Summary

In this literature review chapter, the cell-based mechanisms of vascular network formation, angiogenesis and vasculogenesis, were examined. The literature describes a wide range of approaches attempting to implement the vasculogenic self-organisation process by which single cells form a capillary bed spontaneously; researchers have investigated this method in both two-dimensions (i.e. on surfaces) and three-dimensions (in gels). Angiogenic approaches have also been described; these include microcarrier beads seeded with endothelial cells, multi-cellular spheroids, a range of lab-on-chip systems, and a number of *in vivo* methods, such as arteriovenous loops and the aortic ring assay. The substrate on which to perform capillary morphogenesis was considered; collagen and fibrin are frequently used to this end due to their bioactive nature, though alternative gels, such as matrigel and glycosaminoglycan-based hydrogels, have also been employed. The choice of using either collagen or fibrin in our experiments was discussed, based on findings from the literature. Further choices of which supporting cell type to use (fibroblast, MSC, smooth muscle) and which growth factors to include were also described, based on published data. Finally, existing examples of perfusion of these systems and potential anastomosis to larger channels were considered.

Chapter 5

Cell-Based Formation of Capillaries - Angiogenic Capillary Formation

5.1 Introduction

The previous chapter established that there exist a wide range of conditions for fabricating capillary networks found in the literature; in this chapter we experimentally investigate capillary formation via angiogenic means, using multi-cellular spheroids.

5.2 Advantages and Limitations of Using Angiogenic Capillary Formation

A co-culture of endothelial and supporting cells types is capable of producing long-lived capillary structures. By forming endothelial cells into multi-cellular spheroids, tight junctions between them can be formed prior to seeding in a gel matrix, enhancing cell survival characteristics and producing a more physiological angiogenesis, as opposed to seeding spatially separated endothelial cells in a gel which have to subsequently colocalize to form capillary structures. Endothelial spheroids are considered a good model for angiogenesis *in vitro* since sprouting behaviour is similar to the physiologically programmed arrangement of endothelial cells in vessels [133].

Spheroids appear to produce much more multi-cellular capillary structures early on when compared to the single cell approach. Single endothelial cells must migrate to their neighbouring endothelial cells, form cord structures, and undergo vesicle formation and fusion to produce lumen. In the case of the angiogenic approach, several endothelial cells migrate behind the tip cell, thereby producing significantly larger lumen early on.

As supported by results reported in the literature [88], it may also be the case that far less endothelial cells are needed to produce an extensive network of capillaries, than would be required for a vasculogenic individual cell approach, due to their colocalized nature, cell survival characteristics, and communication between cells when organised into spheroids.

Multi-cellular spheroids allow for easy comparison of different experimental conditions since the endothelial cells sprout from only a few locations (i.e. the spheroids). Structures can be more easily analyzed for sprout length, sprout diameter, lumen formation, and interconnectedness, than with single cell experiments. Further they produce recognizable capillary structures much more rapidly than the vasculogenic route, which also is harder to analyze since cells are spread uniformly around the gel.

It is possible that cells formed into spheroids may pull less on the surrounding matrix material and thus produce less gel shrinkage, since only cells on the surface of the spheroid are in contact with the matrix, at least initially. Further, the incorporation of supporting cells into spheroids may lower gel shrinkage but more importantly, may produce significantly stronger spatial gradients of pro-angiogenic factors between spheroids, directing capillary growth more strongly than with single cells.

There may also be a better chance of spheroid-based endothelial cells migrating and coating the surface of the larger channels to form a monolayer, owing to the tight junctions already present between the cells. This is important since the large-scale vessels are fabricated by an alternative method (i.e. the multi-casting technique of Chapter 3) and a perfusable link between the two systems is a key challenge.

While it is relatively simple to prepare a low number of spheroids, for the purposes of creating a capillary network, we require the formation of several thousand spheroids and a method for their efficient collection. It has been shown that the ‘hanging drop’ method enables easy spheroid formation and, by pipetting onto a hydrophobic petri dish, large numbers of spheroids can be harvested easily [88].

There are some limitations to using spheroids as the basis of capillary formation. The diameter of the spheroid is limited to less than 400 μm at the very most since this is the defined limit for oxygen diffusion in thick cellularized tissue [7]. Any spheroid larger than this size is likely to have a large necrotic core of cells, which limits the number of cells that can be included in a single spheroid.

Further, the overall number of endothelial cells in a device is more limited than the single cell approach since preparing spheroids is a time-consuming process. Each spheroid is made by depositing a certain number of cells into a droplet. Thus for an experiment with 2.5×10^6 endothelial cells, one requires between 2500-10,000 spheroids, for spheroids containing 250-1000 cells/spheroid.

One key limitation of using multi-cellular spheroids for capillary formation is that they aggregate and are difficult to spread uniformly around the gel; rather they collect at the bottom of the gel, especially if the crosslinking time is long. Another problem is that even with a fast gelling matrix and a uniform distribution of spheroids, the endothelial cells have to migrate significant distances in order to form an interconnected network of capillaries. In the case of the single cell approach, each cell does not need to migrate as far in order to form a network.

5.3 Methods

5.3.1 Reagent Preparation and Cell Culture

VEGF and bFGF (R&D Systems) were resuspended at 100 μg/mL in PBS (no Ca) containing 0.1% BSA, and aliquots frozen at -80°C prior to use. Collagen and fibrin hydrogels were prepared as previously described in Section 3.2.6. Human umbilical vein endothelial cells (HUVEC, Public Health England), human dermal adult fibroblasts (HDFs, Public Health England), and human mesenchymal stromal cells (MSCs, Lonza) were used for the experiments. The cells were trypsinized using TrypLE Express (Life Technologies), centrifuged at 250 g for 5 min, and counted using a Scepter Cell Counter (Millipore). HUVECs were cultured in a T75 flask to 90% confluence, using EGM-2 medium (Lonza), MSCs were cultured in a T75 flask to 90% confluence, using MSCGM medium (Lonza), and HDFs were cultured in a T75 flask to 90% confluence using high-glucose Dulbecco's modified eagle medium (Life Technologies) containing 10% fetal bovine serum (FBS, Life Technologies). HUVECs, MSCs, and HDFs were used in experiments at passage 5.

HUVECs, MSCs, and HDFs were imaged using CMFDA (green) and CMTPX (red) Cell Tracker dyes (Life Technologies), allowing for immediate imaging and tracking of cell seeding. Lyophilized fluorescent dye was resuspended in dimethyl sulfoxide (DMSO, Sigma) at 10 mM and stored at -20 °C until use. A working solution was prepared in DMEM at 10 μM. Plated cells were washed with phosphate buffered saline (PBS, Life Technologies) and the working solution added. Flasks were incubated at 37 °C for 45 min prior to trypsinization.

5.3.2 Multi-Cellular Spheroid Formation

Multi-cellular spheroids were formed using the 'hanging drop' method. A 1.2% stock methylcellulose (MC) solution was prepared by autoclaving 1.2 g methylcellulose powder in a 100 mL bottle and adding 100 mL of basal medium pre-heated to 60 °C. The solution was magnetically stirred for 20 min at room temperature and then stirred overnight at 4 °C. The solution was subsequently aliquoted into 50 mL Falcon tubes and centrifuged at 3,500 g for 3 h at 4 °C. The solution was then stored at 4 °C until use.

For spheroid formation, cells were resuspended in cell medium and 20% of the methylcellulose solution such that a 10 μL drop contained 250-1000 cells, and the medium cell suspension was poured into a disposable reservoir. Using a 12 channel pipette, 10 μL was pipetted onto a square, non-adherent petri dish (Greiner). Once the dish was full of drops, the lid was replaced, the dish turned upside down (see Figure 5.1a), and placed in an incubator overnight. The process was repeated until all the cell suspension had been used (10-20 dishes).

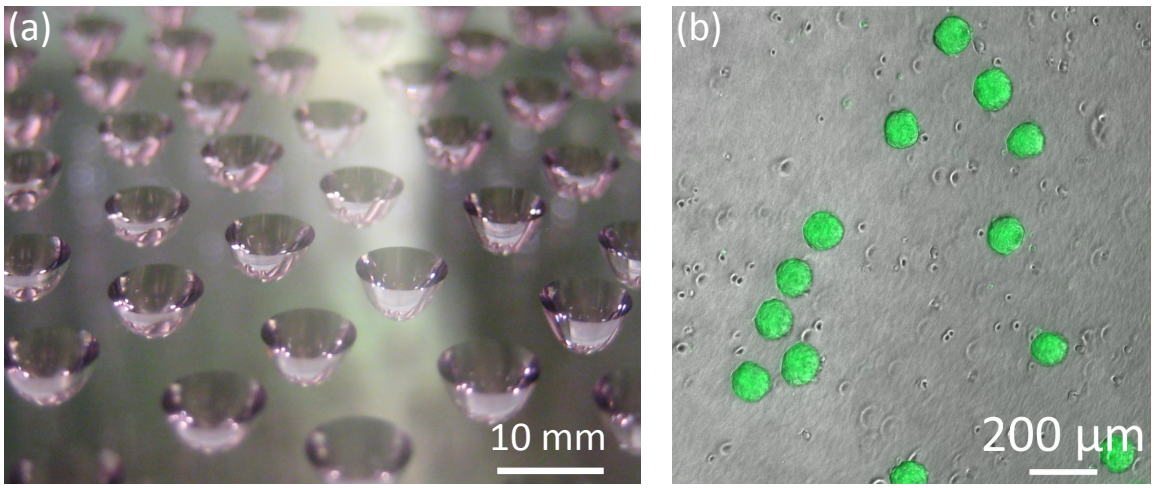

Fig. 5.1 (a) Multi-cellular spheroids form in droplets of cell medium containing methylcellulose when suspended upside-down. (b) Multi-cellular spheroids (green) encapsulated in fibrin gel, alongside single supporting cells, at day 0.

Multi-cellular spheroids were harvested by adding 5 mL cell medium to the petri dish. The solution was subsequently pipetted onto the other petri dishes, thereby collecting all the individual spheroid drops in a 50 mL Falcon tube. Individual cells (e.g. supporting cells) were added at this point and the combined solution centrifuged at 300 g for 5-10 min. The supernatant was removed and the pellet resuspended in the required volume for seeding in collagen and fibrin gels.

5.3.3 Gel Construct Preparation

Collagen and fibrin hydrogels were prepared as described previously (Section 3.2.6). Final concentrations of collagen were 2.5-7.5 mg/mL and final concentrations of fibrin were 5-20 mg/mL, with 20 μg/mL fibronectin added to the precursor solution to improve cell adhesion. The constructs were gelled as either gel sheets (200-1000 μL) as shown in Figure 5.1b, or as small gel drops (50-200 μL) in 24 well plates. Cell concentrations and ratios between cell types were varied between experiments. EGM cell medium (Lonza) containing 20 ng/mL VEGF and 20 ng/mL bFGF was added to the wells. Medium was changed every 2 days.

5.4 Summary of Multi-Cellular Spheroid Experiments

A range of conditions were explored making use of multi-cellular spheroids. We tested a range of different concentration substrates, and combining endothelial cells, supporting cells, and even both together into multi-cellular spheroids, to determine any specific conditions which may be useful when used alongside the 3D printed channels and perfusion. Table 5.1 summarizes the parameters and observations of a number of experiments, and allows comparison between them; the following sections explicitly reference this table and provide the scientific rationale for the undertaking of each experiment.

Table 5.1 Spheroid Experiments

	Cell Description	Number of Cells per Spheroid	Substrate, Concentration	Gel Volume	Ratio	HUVEC Cell Concentration (cells/mL)	Supporting Cell Concentration (cells/mL)	Growth Factors	Duration (days)	Comments
1	HUVEC Spheroids, HDF Single Cell	500	10 mg/mL and 20 mg/mL Fibrin with 20 μg/mL Fibronectin	1 mL and 200 μL gels in 24 well plate	2:1	1×10^6	0.5×10^6	20 ng/mL VEGF, bFGF in medium	75	High number of long sprouts, multicellular, lumen formation, interconnected network, long term stability, CD31 and DAPI staining.
2	HUVEC Spheroids, HDF Single Cell	1000	7.5 mg/mL Collagen	200 μL gels in 24 well plate	3:1	1.5×10^6	0.5×10^6	20 ng/mL VEGF, bFGF in medium	14	Long sprouts, lumen formation, multicellular, very high diameter capillaries.
3	HUVEC Spheroids, MSC Single Cell	500	5 mg/mL and 10 mg/mL Fibrin	200 μL gel sheets in 24 well plate	1:2	1×10^6	2×10^6	20 ng/mL VEGF, bFGF in medium	12	Sprouting in both 5 mg/mL and 10 mg/mL gels. High concentration of MSCs appears to aid sprouting.
4	HUVEC Spheroids, HDF Single Cell	500	10 mg/mL Fibrin with 20 μg/mL Fibronectin or 7.5 mg/mL Collagen	200 μL gel sheets and drops in 24 well plate	5:1	1.5×10^6	0.3×10^6	20 ng/mL VEGF, bFGF in medium	14	Limited number of spheroids visible. Fibrin: High number of sprouts, shorter and multi-cellular. Lumen visible by day 4. Collagen: High number of sprouts, long and multi-cellular. Clear lumen visible by day 4.
5	HUVEC Spheroids, HDF Single Cell	500	5-10 mg/mL Fibrin or 2.5-7.5 mg/mL Collagen	200 μL gel sheets in 24 well plate	5:1	1×10^6	0.2×10^6	20 ng/mL VEGF, bFGF in medium	10	5 mg/mL was best at this concentration of HDF
6	Mixed HUVEC-HDF Spheroids	500	10 mg/mL Fibrin with 20 μg/mL Fibronectin	200 μL, 300 μL, 500 μL gels in 24 well plate	2:1	3×10^6	1.5×10^6	20 ng/mL VEGF, bFGF in medium	8	HUVEC media disrupted some gels leading to multicellular sprouts, significant sprouting
7	Mixed HUVEC-HDF Spheroids	500	10 mg/mL Fibrin with 0.2% TG and 20 μg/mL Fibronectin	Gel drops in 24 well plate	2:1	2×10^6	1×10^6	20 ng/mL VEGF, bFGF in medium	6	High number of sprouts, shorter in length.
8	Mixed HUVEC-MSC Spheroids	1000	5 mg/mL and 7.5 mg/mL Fibrin with 20 μg/mL Fibronectin	400 μL gel sheets in 12 well plate	3:1	2.4×10^6	0.8×10^6	20 ng/mL VEGF, bFGF in medium	4	HUVECs coated outside of spheroids, MSCs inside, MSCs spread from spheroids, HUVEC sprouts formed with MSCs as they spread out. However no sprouts beyond MSC range.
9	HUVEC Spheroids - with and without HDF or MSC Spheroids	500	7.5 mg/mL Fibrin	200 μL gel sheets in 24 well plate	3:1	1.5×10^6	0.5×10^6	20 ng/mL VEGF, bFGF in medium	14	HUVECs sprouted long distance towards supporting cell spheroids. By day 6, all MSC spheroids had been penetrated by HUVEC sprouts. MSCs appeared to coat HUVEC capillaries better than HDFs.
10	HUVEC Single Cell, MSC Spheroids	500	5 mg/mL and 7.5 mg/mL Fibrin	200 μL gel sheets in 24 well plate	1:1	1×10^6	1×10^6	20 ng/mL VEGF, bFGF in medium	14	HUVECs remained round. HUVECs briefly formed networks near MSC spheroids but degraded rapidly. MSCs spreading from spheroids.

5.5 Spheroid Capillary Formation - HUVEC Spheroids with HDF Single Cells

Preliminary experiments were conducted using fibroblasts as the supporting cell (see Experiments 1 and 2 in Table 5.1). Both 10 mg/mL and 20 mg/mL fibrin gels were investigated at relatively low cell concentrations (1×10^6 HUVECs/mL and 0.5×10^6 HDFs/mL) in order to evaluate spheroid sprouting and the stability of these networks in the long term (75 days). While cells in the 20 mg/mL fibrin gels were found to be relatively inactive, in 10 mg/mL fibrin, the initially round spheroids were detected to have formed a significant number of sprouts by day 2 (Figure 5.2a), displaying thin strands protruding out into the bulk gel. By day 4 (5.2b), these sprouts had matured into noticeably wider structures with visibly clear lumen.

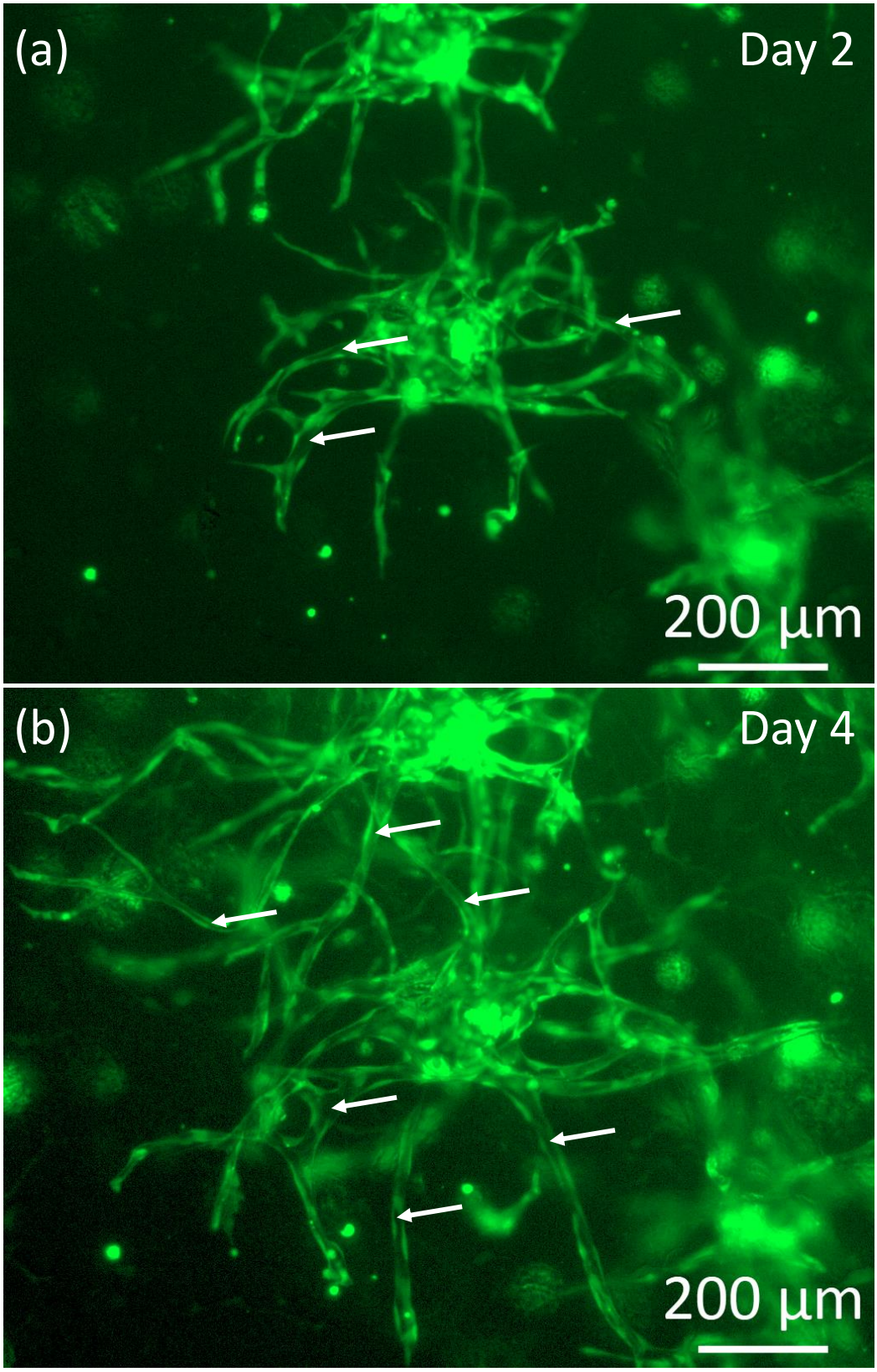

Fig. 5.2 (a) HUVEC multi-cellular spheroid, in the presence of HDFs, and 20 ng/mL VEGF and bFGF growth factors, in 10 mg/mL fibrin exhibited sprouting as early as day 2. (b) After 4 days, the same spheroid had extended its sprouts into the bulk hydrogel and multiple lumen are clearly visible. Arrows denote examples of lumen structures.

After 75 days, the gels were fixed and stained for CD-31 and DAPI, which displayed large networks over the whole of the gel, as shown in Figures 5.3a and 5.3b. An equivalent experiment was performed using collagen, extracted from rat-tail tendon. While collagen is not considered pro-angiogenic in the same way as fibrin, the unpurified collagen likely contained a range of other matrix materials (e.g. laminin, collagen IV, elastin) which enhanced capillary formation. Thus after 14 days, large structures, as shown in Figure 5.3c and 5.3d, and large lumen were observed, as shown in Figure 5.3e. It seems to be the case that between 14 and 75 days, the spheroid structures disappear and a more interconnected network forms in which the original spheroid structures are no longer recognizable.

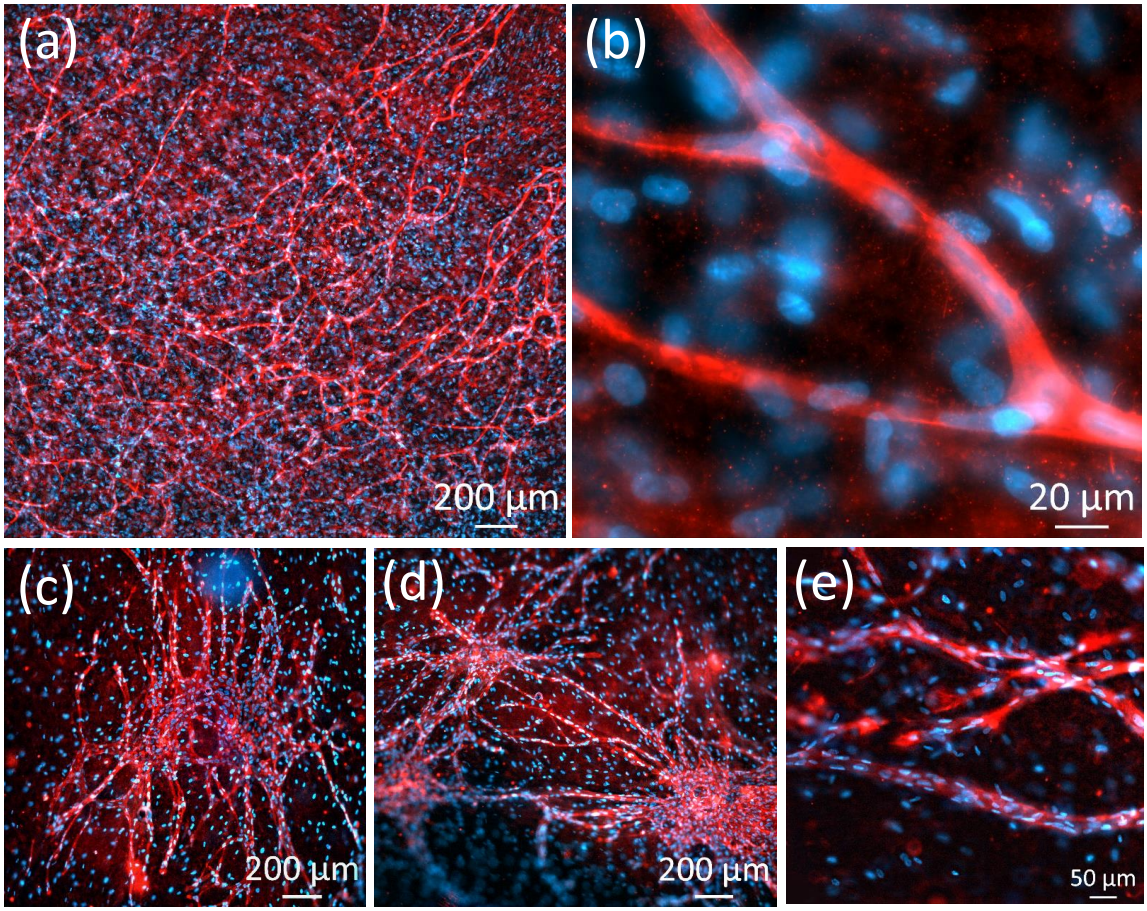

Fig. 5.3 (a,b) After 75 days, large networks of capillary-like structures were observed in rat-tail tendon collagen, as shown by CD-31 staining (red) and DAPI nuclear stain (blue). (c,d) When rat-tail tendon collagen is used, large vessels were produced (day 14). (e) Highly multi-cellular structures were observed, with large lumen (day 14).

5.6 Spheroid Capillary Formation - HUVEC Spheroids with MSC Single Cells

Mesenchymal stromal cells, with their ability to differentiate into both pericytes and smooth muscle cells [34], should provide a more physiological interaction with the endothelial cells, wrapping around the nascent capillary structures and supporting their development. In this experiment (Experiment 3 in Table 5.1 and Figure 5.4), we compare 5 mg/mL and 10 mg/mL fibrin gels containing HUVEC spheroids (1×10^6 HUVECs/mL) with MSC single cells (2×10^6 MSCs/mL). It does appear as though MSCs do closely interact with the HUVEC capillary structures as seen by the (red) MSCs wrapping around the (green) HUVEC sprouts (an example is shown by the asterisk and figure insert in Figure 5.4f). Also, HUVECs in 5 mg/mL fibrin produce longer sprouts than 10 mg/mL fibrin. This is expected since a higher density of gel means more matrix material must be broken down for the sprouts to grow.

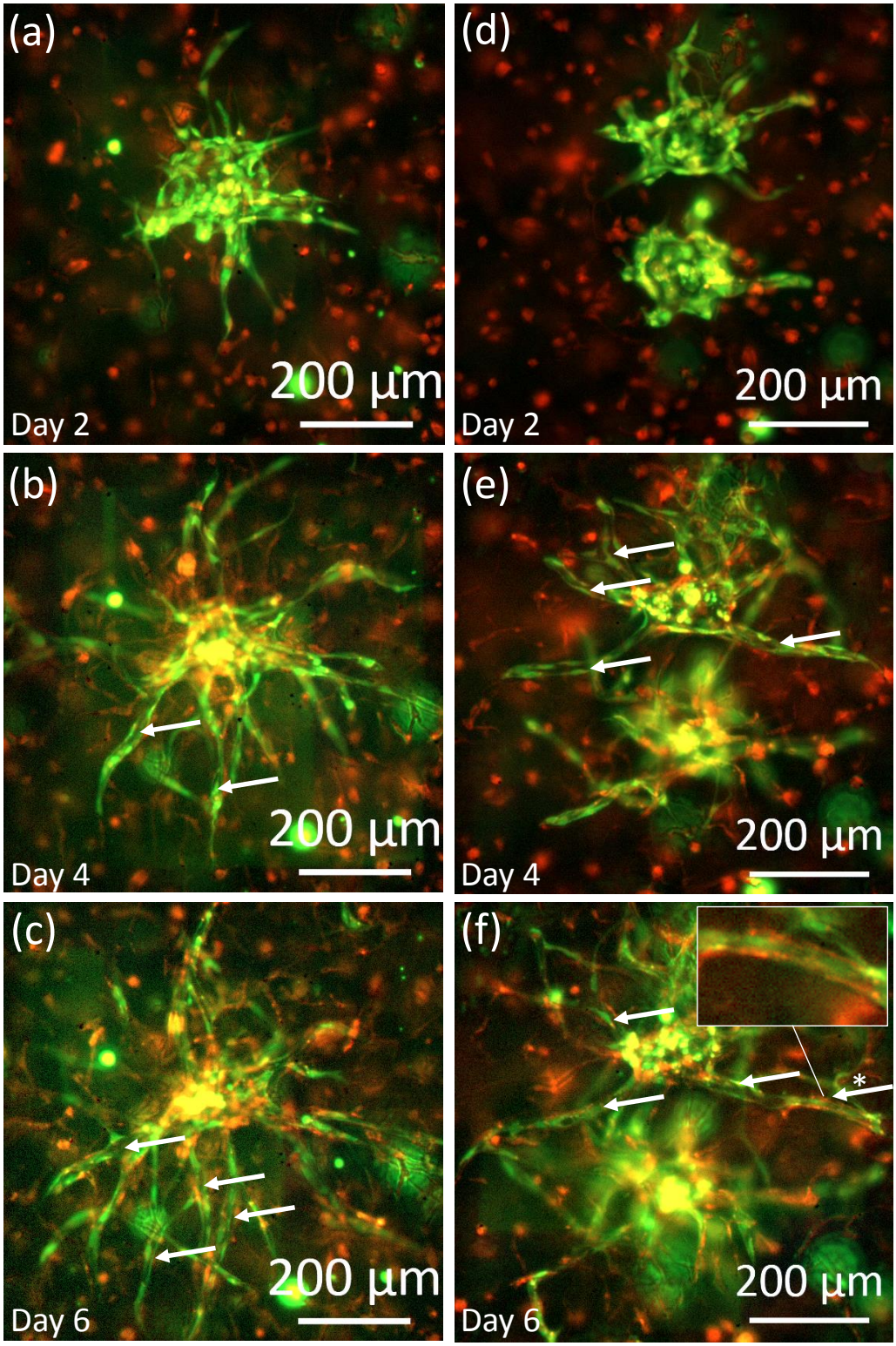

Fig. 5.4 HUVEC spheroids (green) sprouting in the presence of MSCs (red) and 20 ng/mL VEGF and bFGF growth factors, in (a-c) 5 mg/mL and (d-f) 10 mg/mL fibrin gels. Note that MSCs are thought to interact more closely with nascent capillary structures owing to their ability to develop a perivascular phenotype. Arrows denote examples of lumen structures. Asterisk and insert show example of interaction of (red) MSCs with (green) HUVEC structure.

5.7 Variation of Substrate and Substrate Concentration

A set of experiments was conducted to compare different substrates and substrate concentrations, using collagen and fibrin (see Experiments 4 and 5 in Table 5.1). It was found that spheroids embedded in 2.5 mg/mL collagen expanded in diameter with a few sprouts. No noticeable differences were observed between 5 and 7.5 mg/mL collagen. However significant differences were observed between 5, 7.5, and 10 mg/mL fibrin. 5 mg/mL fibrin produced the longest sprouts whilst 10 mg/mL fibrin produced short but wide diameter sprouts, as shown in Figure 5.5.

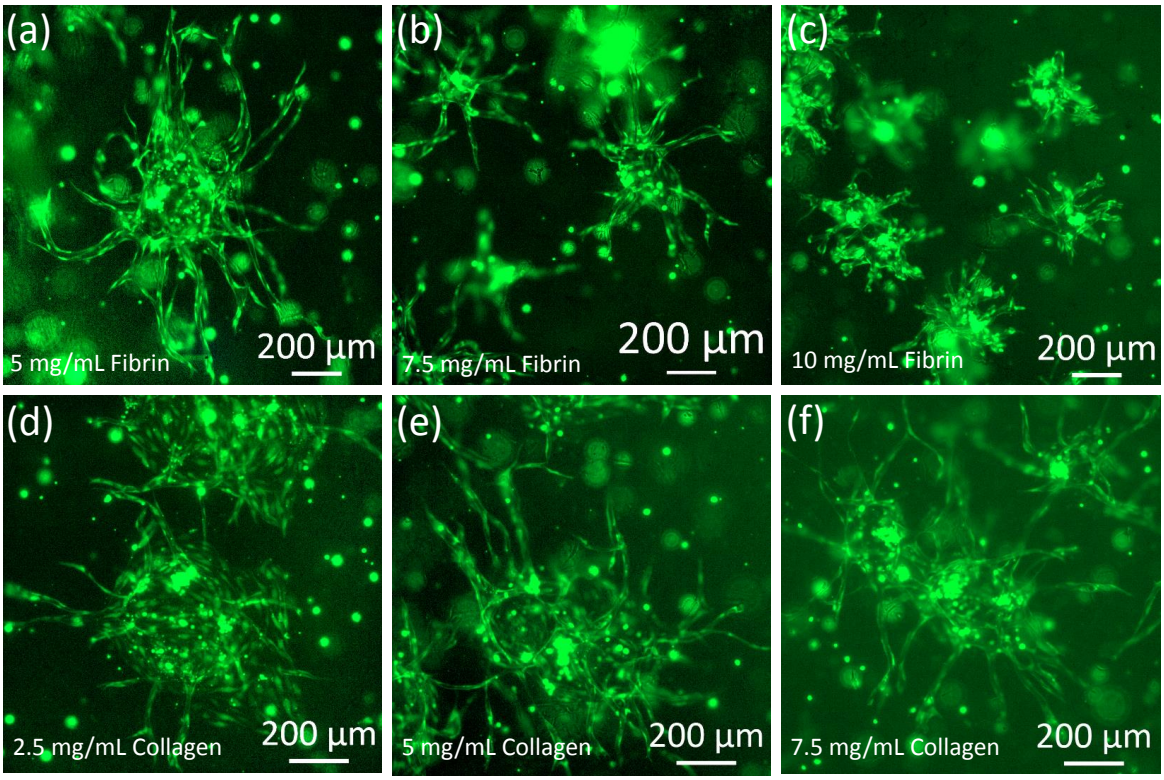

Fig. 5.5 Comparison of concentrations of (a-c) fibrin and (d-f) collagen substrates, for HUVEC cells in spheroids (green) in the presence of HDF single cells (not shown). Shown is day 4.

5.8 Mixed Cell Type Spheroids

A study looked for any beneficial effects of localizing the supporting and endothelial cell types to the same spheroid (see Experiments 6-8 in Table 5.1). These heterogeneous spheroids, consisting of HUVECs and either HDFs or MSCs, meant that cells producing pro-angiogenic

factors (i.e. fibroblasts or mesenchymal stromal cells) were in high density and close proximity to the sprouting endothelial cells. Thus it was thought that this may enhance sprouting. It was observed that in the case of MSCs as the supporting cell, the cells organised themselves such that the MSCs were in the center of the spheroid and the endothelial cells were in a shell around them. Both fibroblast and MSC cell types could be seen migrating into the gel by day 2. However, it was found that the endothelial cells only spread as far as the supporting cell had migrated into the bulk gel, with and without the presence of VEGF and bFGF in the cell medium, and looked much migratory in form than when individual supporting cells were seeded in the bulk. This can be compared to the organisation and lumen structures observed in Figure 5.3 where long multi-cellular sprouts were observed; the sprouts in the mixed spheroid case remained thin by day 4. Thus it was concluded that this was not a viable way of producing a good coverage of the gel with capillary-like structures.

5.9 Supporting Cells Organised as Spheroids

A series of experiments were performed where both endothelial cells and supporting cells were prepared into separate multi-cellular spheroids (see Experiment 9 in Table 5.1). In the mixed spheroid approach, a high concentration of supporting cells was added to the same spheroid as the endothelial cells so as to provide a boost to the development of the capillaries by producing various pro-angiogenic factors. This was not found to yield large networks. As an alternative, supporting cells were placed in distinct spheroids and spatially separated from the endothelial spheroids. In doing so, it was thought that pro-angiogenic factors would be produced in high concentrations around the supporting cell spheroids and provide strong gradients in the gels for the HUVEC cells to follow, over relatively long distances. We were able to show that the endothelial capillary sprouts were indeed directed towards the supporting cell spheroids. Further, they were able to penetrate the supporting cell spheroid and continue spreading. This was true when using either MSCs or HDFs as shown in Figure 5.6.

When no supporting cell is present but the cell medium still contains 20 ng/mL VEGF and bFGF, the HUVECs produce a migratory response and do not form significant sprouts, thereby showing that the supporting cell is a necessary component; as shown in Figure 5.7(a,b). When the 20 ng/mL VEGF and bFGF growth factors are removed from the cell medium, the HUVEC spheroids neither migrate nor form angiogenic sprouts. This is shown in Figure 5.7(c) and 5.7(d) for MSCs and HDFs respectively. Thus, both a supporting cell type and sufficient growth factors in the medium are required for angiogenic sprouting.

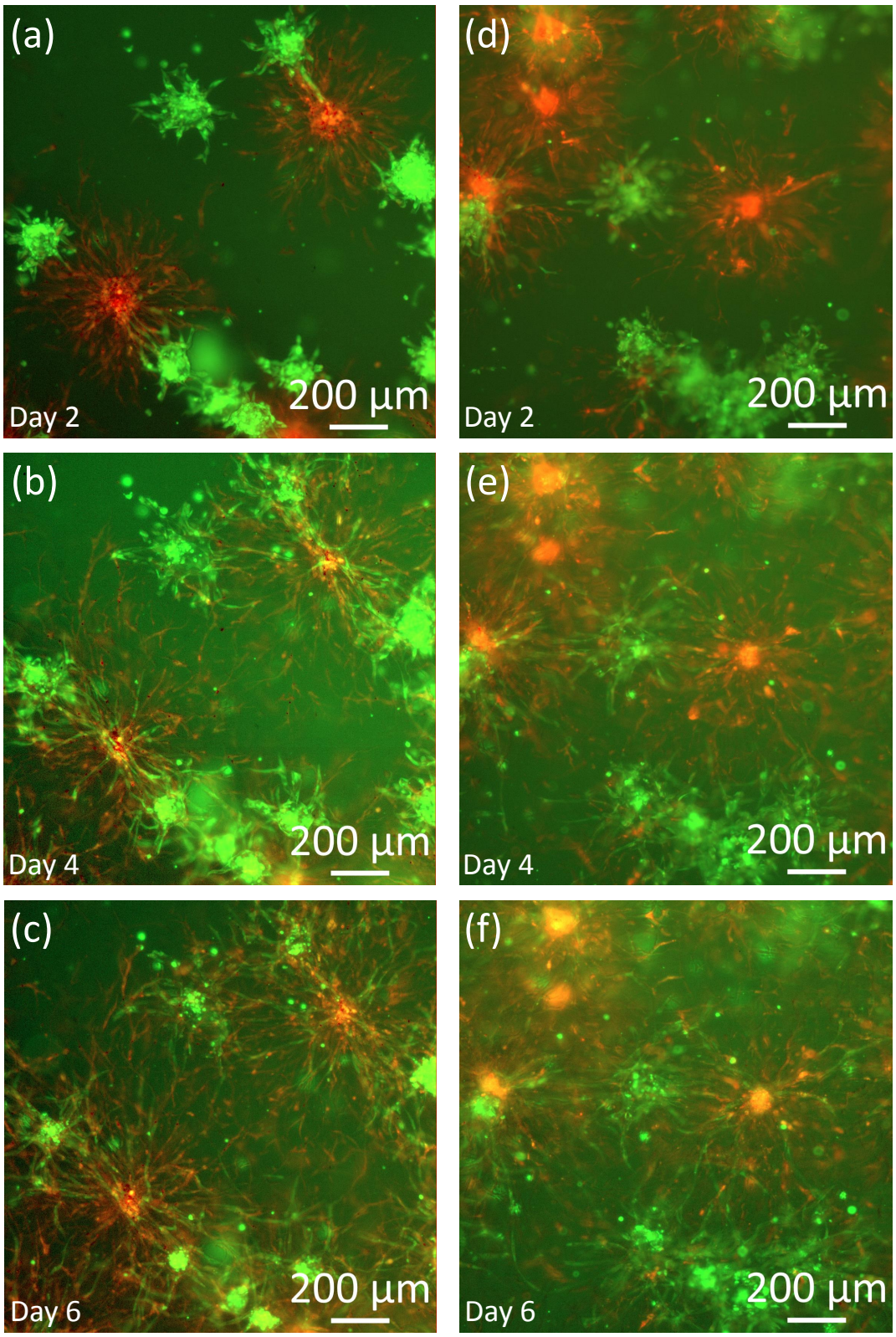

Fig. 5.6 Multi-cellular spheroids of HUVEC (green) in the presence of supporting cell spheroids. (a-c) MSCs and (d-f) HDFs (red), in a 7.5 mg/mL fibrin gel.

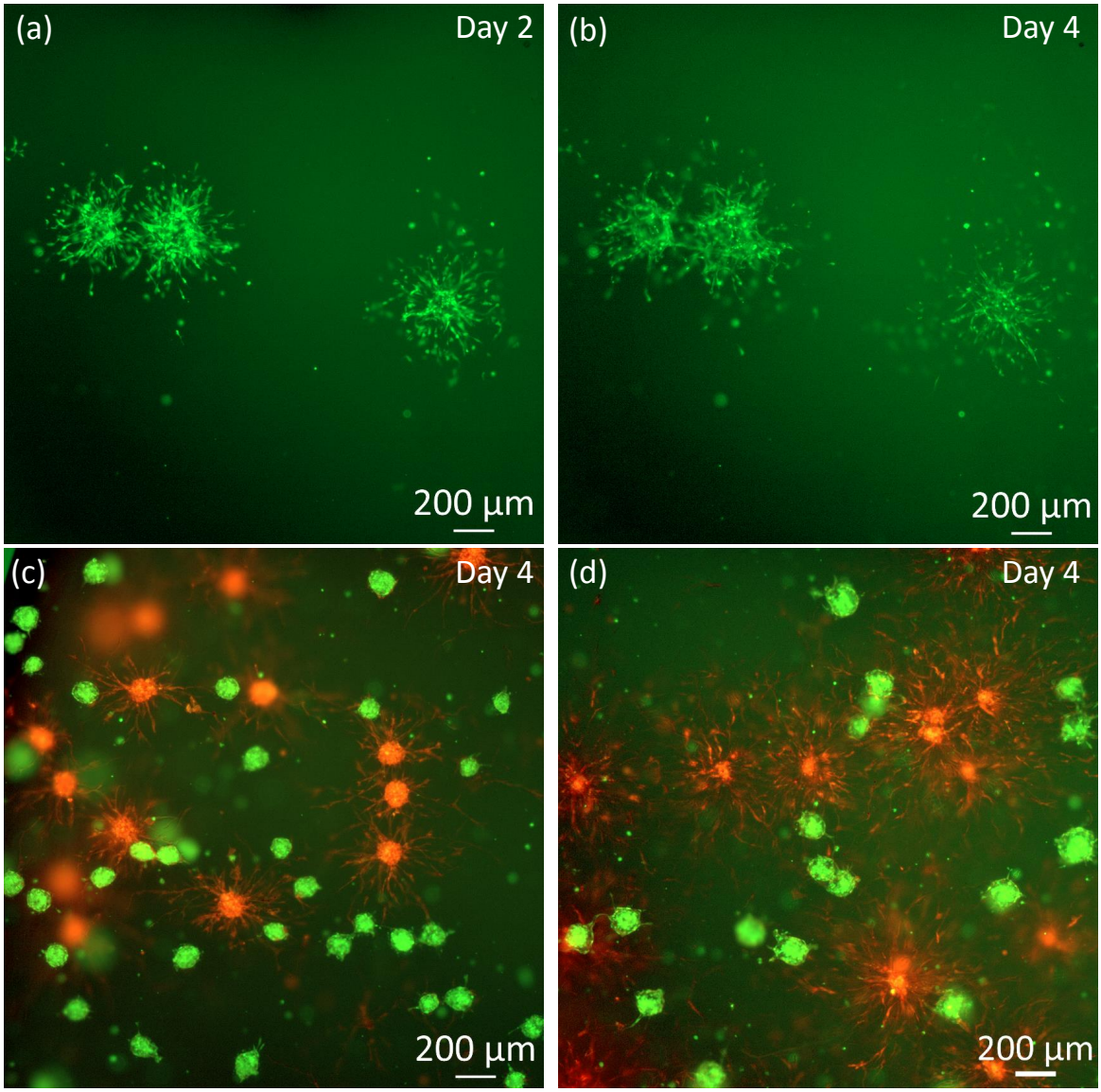

Fig. 5.7 (a,b) HUVEC spheroids without a supporting cell type undergo a migratory response, rather than forming capillary-like sprouts. In the presence of (c) MSC spheroids (red) or (d) HDF spheroids (red), but without 20 ng/mL VEGF and bFGF in the cell medium, HUVEC spheroids (green) do not undergo either migration or capillary sprouting. Shown is day 4.

Finally, we tested single cell HUVECs alongside spheroids of MSCs (see Experiment 10 in Table 5.1). It was thought that, like the above, supporting cells arranged into spheroids would yield strong spatial gradients of growth factors which should induce the endothelial cells to form capillary-like structures. As shown in Figure 5.8, no significant capillary formation was observed in this experiment. At day 4, it is possible to see some spreading of HUVECs nearby to the MSC spheroids, though the cells quickly regress back to a spherical morphology.

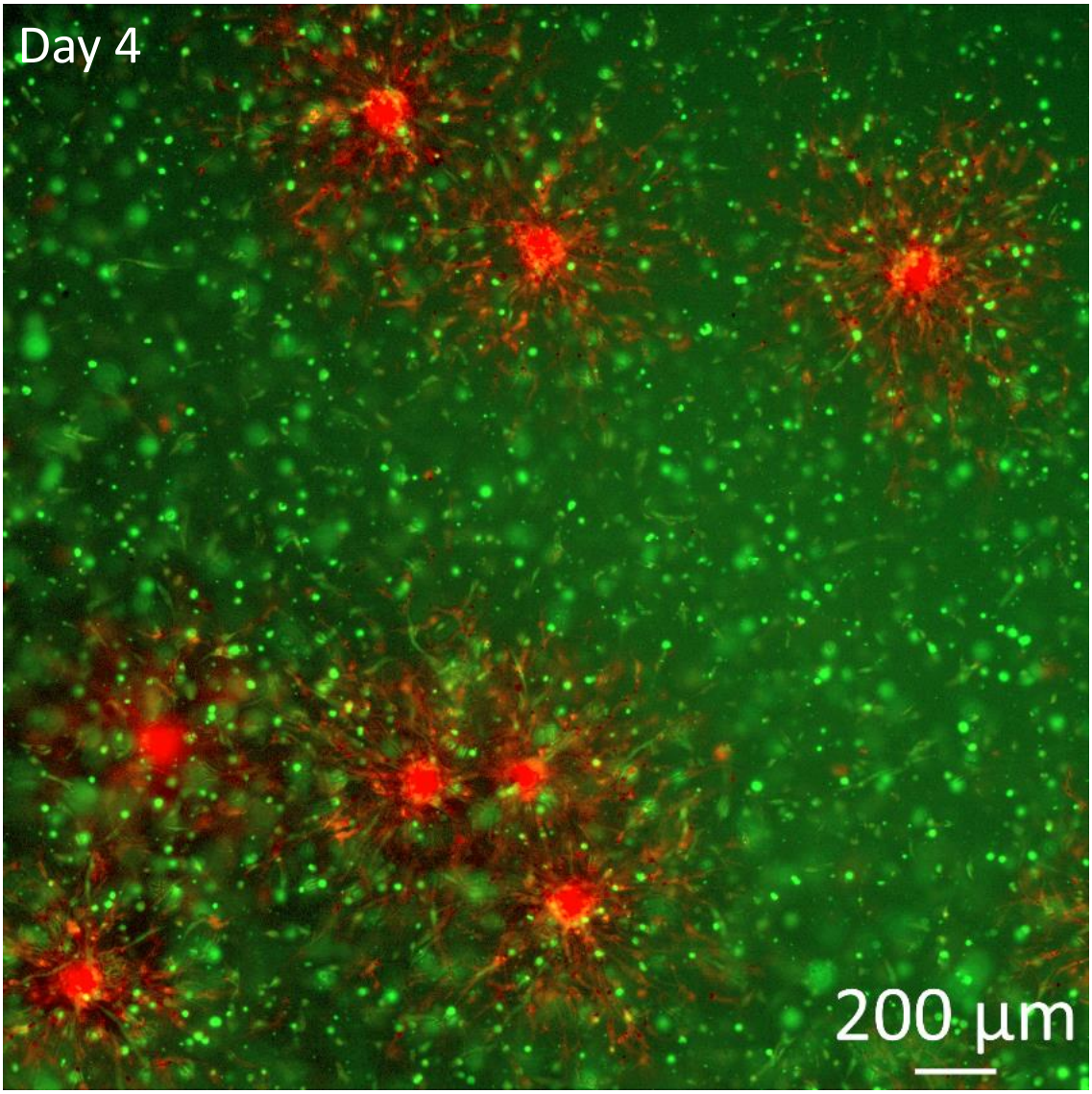

Fig. 5.8 Single cell HUVECs (green) alongside MSC multi-cellular spheroids (red), in 7.5 mg/mL fibrin gel. No noticeable spreading of HUVECs was observed in this setup.

As described in Chapter 4, high concentrations of mesenchymal stromal cells have been reported to prevent the formation of capillaries by intercalating between the endothelial cells and causing the endothelial cells to apoptose. In the reported case, the MSCs were also single cells and the literature puts a 25% threshold of MSC concentration (to HUVEC concentration) above which the HUVEC capillary structures are not stable [24]. Here, we hypothesize that near to the MSC spheroids, the high concentration of MSCs first enables structures to form. However, as the MSCs migrate out from the spheroid, they cause any nascent capillary structures to degrade. In the cases where the endothelial cells were also formed into spheroids, as in Figure 5.6, the endothelial cells already have formed tight junctions with one another and thus the MSCs could not intercalate between them. Thus the endothelial cell sprouts were able to penetrate dense regions of cells, such as the MSC spheroids, without their capillary structures degrading.

Note that in the multi-cellular spheroids work, no stromal derived factor (SDF-1α) was used, as opposed to the single cell vasculogenic approach where it was found to be necessary, since low concentrations of MSCs, relative to HUVECs, were required. If it was to be used in the spheroid experiments alongside MSCs, one may observe a useful increase in sprouting though this is an experiment for future work.

5.10 Multi-Cellular Spheroid Cells Coat Internal Surfaces

Spheroid-based endothelial cells were observed to coat the surface of air bubbles in fibrin gels, which rapidly formed a monolayer of cells, as shown in Figure 5.9(a-c). These findings suggested the idea of coating the inside of large channels fabricated via the multi-casting approach of Chapter 3. A network was prepared and set up for a perfusion experiment in which HUVEC spheroids and HDF single cells were seeded into the bulk of a 7.5 mg/mL fibrin gel. In Figure 5.9(d), one can see that some of the large channel (to the right of the image) had been coated with endothelial cells (stained with Cell Tracker Green). It was noted that the rest of the channel remained acellular due to the presence of an air bubble which had infiltrated the system, preventing the formation of an endothelial lining. While capillary-like structures had formed in the gel as well (discernable by the green in the background), they remained unperfusable after 7 days.

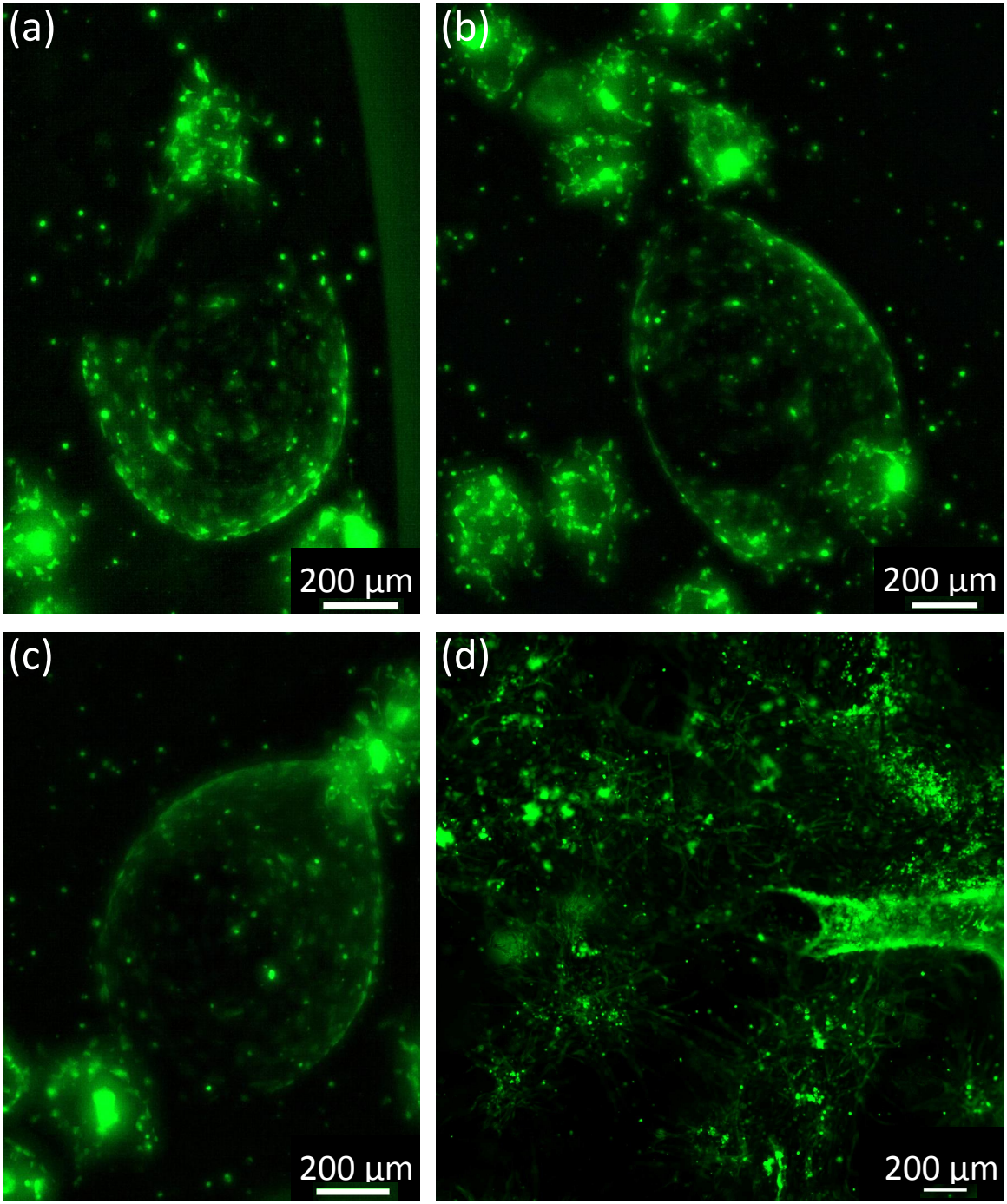

Fig. 5.9 (a-c) Multi-cellular spheroid cells, stained with Cell Tracker Green, quickly coat the surface of bubbles trapped in fibrin gel, shown in the center of the images (shown is Day 2). (d) When multi-cellular spheroids are added to a gel containing large channels produced via the multi-casting technique and subsequently perfused with cell medium, they coat some of the 3D printed channels with cells (shown middle-right of the image). However, capillary bed was unperfusable by day 7 (shown in the background).

5.11 Chapter Summary

In this results chapter, multi-cellular spheroids were used to produce capillary-like structures. It was thought that an angiogenic approach would be preferable due to tight junctions between endothelial cells being present from the beginning of the experiment leading to better cell survival and function, and the fact that this angiogenic approach more closely mimics the normal physiological process. A series of experiments investigated their use, including a comparison of fibroblasts or MSCs as the supporting cell type, the influence of matrix concentration upon spheroid sprouting, and several experiments looking at incorporating the supporting cell type into a multi-cellular spheroid form.

Multi-cellular spheroids produce long-lived capillary-like structures with large lumen early on and have the potential to coat the large-scale, 3D printed vessels. However, they suffer from several limitations; most notably a lack of uniformity achievable (when using 500 cells/spheroid), the time-consuming nature of their preparation, and the limit in the number of cells which can be realistically added to a culture system. Thus, it was concluded that the single cell vasculogenic approach would be pursued, which overcomes each of these limitations.

Chapter 6

Cell-Based Formation of Capillaries - Vasculogenic Capillary Formation

6.1 Introduction

The previous chapter explored the possibility of generating blood vessel networks via an angiogenic approach using multi-cellular spheroids. Here we investigate the possibility of seeding individual cells into a bulk matrix and having them undergo vasculogenic-like capillary formation.

6.2 Advantages and Limitations of Using Vasculogenic Capillary Formation

Through the process of vasculogenesis, angioblasts migrate and differentiate into endothelial and blood cells, aggregating and forming into cords to form a capillary plexus [161]. The seeding of individual mature endothelial cells into a gel matrix is considered a vasculogenic form of capillary formation since single cells migrate and form cords to produce vessels *de novo*.

Single cells are advantageous as they enable an unlimited number of cells to be encapsulated in the matrix material with little prior work. They also produce a much more uniform distribution of cells throughout the gel matrix than spheroids. All cells are in immediate contact with the surrounding matrix material which should enable rapid degradation of the tissue-engineered gel and replacement with extracellular matrix components.

However, single cells are harder to maintain in a matrix since they are more likely to apoptose as they have to re-establish tight junctions between endothelial cells. Gel shrinking

may also be more of a problem for single cells as all cells will apply forces directly upon the matrix. Further, the formation of lumen is by the process of vesicle formation and fusion (as described in Section 4.3) which means only small lumen will be possible early on.

6.3 Methods

6.3.1 Reagent Preparation and Cell Culture

VEGF, bFGF, and SDF-1α (R&D Systems) were resuspended at 100 μg/mL in PBS (no Ca) containing 0.1% BSA, and aliquots frozen at -80°C prior to use. Collagen and fibrin hydrogels were prepared as previously described in Section 3.2.6. Cell culture was performed as previously described (Section 5.3.1). MSCs were used as the supporting cell type alongside HUVECs. The HUVEC cell type was stained with Cell Tracker prior to addition to the gel precursor solution (Section 5.3.1).

6.3.2 Gel Preparation

Capillary experiments were performed in adherent well plates or in specially fabricated PDMS wells, using the same approach as Chapter 3; fibrin hydrogels were also prepared as described previously. Final concentrations of fibrin were 2.5-10 mg/mL fibrinogen (0.5-2 U/mL thrombin), prepared in pH 7.5 endothelial growth medium (EGM2-MV, Lonza), and 20 μg/mL fibronectin was added to the precursor solution to improve cell adhesion. Cellularized fibrin was gelled as either gel sheets (100-200 μL), as small gel drops (25-100 μL) in well plates, or in PDMS wells which allows for a flat gel surface. Cell concentrations and ratios between cell types were varied between experiments. Endothelial growth medium (EGM2, Lonza), containing 20 ng/mL of growth factors (VEGF, bFGF, SDF-1α), was added on top of the gels typically with a volume of 400 μL which was changed every other day. For variation between experiments, see Table 6.1.

Single cell HUVEC-MSC experiments were formed in 2.5-10 mg/mL fibrin gels. 2.5 mg/mL fibrin is near to the physiological concentration though produces significantly weak gels, prone to gel shrinking. 10 mg/mL fibrin gels are significantly stronger and resist gel shrinkage, though cells are less able to spread and migrate in them since there is more matrix material to degrade and metabolite diffusion is slower. 20 μg/mL fibronectin was added to the precursor solution since fibronectin enhances cell adhesion and helps induce tissue formation [143].

Ideally we wish to use high concentrations of endothelial cells (i.e. 3×10^6 HUVECs/mL) as the endothelial cells would then have less distance to migrate to one another and, by

interaction with each other, would form larger lumen early on, rather than requiring significant cell proliferation. Further, it was thought that high concentrations of cells would negate the effect of using 10 mg/mL fibrin, rather than 2.5 mg/mL fibrin. However, since well plate experiments rely on diffusion of nutrients and oxygen from the surface of the gel to the cells, and since cells compete for oxygen consumption, lower concentrations of $1-2\times10^6$ HUVECs/mL (with relative concentrations of MSCs) were also tested. As described in Section 4.9, the literature suggests that a 10-20% concentration of MSCs relative to HUVECs is sufficient for the stabilizing influence that they impart upon the nascent capillary structures [24].

Fibrin gel formation is reported to be highly sensitive to the pH of the precursor solution [120]. It was thought that using cell medium as the primary buffer for the precursor solution would be beneficial in supporting the cells while fibrin formation takes place and, in the case of using 3D printed channels, the removal of the gelatin template material. Further, we required a cell medium that did not contain heparin as this is known to inactivate thrombin, which would yield poorly formed fibrin gels. Thus, the proprietary medium, EGM2-MV was used which contains no heparin. Whilst this medium is defined for microvascular endothelial cells and not larger vessel HUVECs, the contents are similar, also containing low concentrations of VEGF and bFGF which are useful as survival factors against apoptosis early on. EGM2-MV was found to have a pH of 7.9 and so, to adjust the gel precursor solution to pH 7.5, the cell medium pH was set using 0.1M HCl and the pH of the fibrinogen stock solution was raised as well, prior to its addition into the gel precursor solution.

To induce capillary formation with relatively low concentrations of supporting cells, we used 20 ng/mL VEGF, bFGF, and SDF-1α growth factors, added to endothelial cell growth medium. It was found that adding 20 ng/mL of VEGF, bFGF, and SDF-1α growth factors was in fact a necessary condition for forming capillary structures; the low levels of VEGF and bFGF found in the EGM2 medium, used to culture the gels, were not capable of inducing a noticeable vasculogenic response from the cells, at least using our supporting cell concentrations.

6.4 Summary of Single Cell Experiments

A range of conditions were tested in a series of experiments in well plates, in order to help determine suitable parameters for future experiments combining 3D printed channels and capillary networks. Table 6.1 summarizes the conditions and briefly comments on the observations from each experiment. The experiments are organised with the most recent (and successful) experiments at the top of the table. The purpose of the table is to present

a range of experiments that had both positive and negative results; the following sections subsequently use this data to attempt to find ideal conditions for use in a perfusion experiment (which is thought to require a higher concentration of fibrin gel).

A large number of parameters were found to be important to the success or failure of a particular experiment. Firstly, the fibrin gel concentration played a key role with lower concentration gels generally producing more complete networks. This was thought to be due to increased cell migration, cell spreading, and cell remodelling of the scaffold, as well as a higher rate of diffusion of nutrients and oxygen from the cell medium surrounding the gel. Various cell concentrations, and ratios between endothelial cells and MSCs, were attempted with the rationale that higher concentrations would mean that cells would be closer together. Thus in higher concentration gels, the cells would have less fibrin to break down and shorter migration distances in order to form vessels. However, at high cell concentrations, cells would also compete for oxygen and nutrients, and limit their transfer to the gel center. Gel volume was found to be important as larger gels contained a higher number of cells (for a fixed cell concentration), and so have higher requirements for oxygen and nutrients from the medium. Further, the shape of the gel was found to be important; if the gel was too flat, cells would not form structures; if the gel was too round, insufficient oxygen and nutrients reached the center of the gel meaning only the edges of the gel yielded any capillary-like structures. The buffer medium of the precursor solution was eventually optimized to best meet conditions ideal for maintaining the cell popuation during the gelation process (as opposed to using PBS as the buffer); the use of EGM2-MV, adjusted to pH 7.5, appeared the best solution as it provides a suitable pH for fibrin gel formation and is free from heparin (which can inhibit thrombin crosslinking of fibrinogen). The volume of medium that would be added on top of the gels was assessed; too little medium would starve a large cell popuation, whilst excessive cell medium would block significant oxygen diffusion from the medium surface. Further, the frequency of medium changes was examined; too frequent medium changes would remove potential cell-derived factors necessary for capillary morphogenesis and use up significant volumes of costly growth factors, whilst infrequent medium changes led to cell starvation and poor capillary formation. Consideration was put into where to add the growth factors; it was generally the case that growth factors were added to the medium on top of the gel as they could be replenished with every medium change. Growth factors added to the gel prior to gelation were thought to be washed out with each medium change and thus did not act sufficiently upon the cells for capillary formation.

Table 6.1 Single Cell Experiments

	Substrate, Concentration	Gel Volume	Buffer in Gel Precursor	Cell Ratio	HUVEC Cell Concentration (cells/mL)	Supporting Cell Concentration (cells/mL)	Medium Volume	Growth Factors	Duration (days)	Comments
1	2.5 mg/mL (0.5 U/mL) and 10 mg/mL (2 U/mL) Fibrin with 20 μg/mL Fibronectin	50 μL gels in PDMS chambers (not pre-wetted) and 100 μL gel drops (not pre-wetted) in 48 well plate	EGM2-MV medium adjusted to pH 7.5	3:0.6, 2:0.4, 1:0.2	1-3$\times10^6$	0.2-0.6$\times10^6$	400 μL EGM2 (2 day changes)	With and without 20 ng/mL VEGF, bFGF, SDF-1α in medium	8	Gel drop 2.5 mg/mL: Less spreading in 3:0.6, but 2:0.4 and 1:0.2 produce dense networks. Gel drop 10 mg/mL: Only spreading at edges of 3:0.6 and 2:0.4. PDMS 2.5 mg/mL: 3:0.6 shows large structures, only some spreading in 2:0.4, same dense structures as gel drop seen in 1:0.2. PDMS 10 mg/mL: No spreading in 3:0.6, significant spreading in 2:0.4, very limited spreading in 1:0.2.
2	2.5 mg/mL (0.5 U/mL) and 10 mg/mL (2 U/mL) Fibrin with 20 μg/mL Fibronectin	25 μL, 50 μL gel drops (not pre-wetted) and 100 μL gel drops (pre-wetted) in 48 well plate	EGM2-MV medium adjusted to pH 7.5	3:0.6, 2:0.4, 1:0.2	1-3$\times10^6$	0.2-0.6$\times10^6$	400 μL EGM2 with and without 20 μg/mL Aprotinin (2 day changes)	20 ng/mL VEGF, bFGF, SDF-1α in medium	8	2.5 mg/mL: No structures in 3:0.6, average network in 2:0.4, dense network in 1:0.2. 10 mg/mL: No structures in 3:0.6 apart from 100 μL gels. Minimal structures in 2:0.4 apart from 100 μL gels. Significant networks in all 1:0.2 gels. No difference with aprotinin.
3	2.5 mg/mL (0.5 U/mL) with 20 μg/mL Fibronectin	25 μL, 50 μL, 100 μL gel drops (not pre-wetted) in 48 well plate	EGM2-MV medium adjusted to pH 7.5	3:1	3$\times10^6$	1$\times10^6$	200 μL, 400 μL EGM2 with and without 20 μg/mL Aprotinin (2 day changes)	20 ng/mL VEGF, bFGF, SDF-1α in medium or 200 ng/mL VEGF, bFGF, SDF-1α in gel	14	GFs in medium: Dense networks in gels. Clearly visible lumen in center of 100 μL gels but not in 25 μL or 50 μL gels. GFs in gel: round cells in 25 μL, 50 μL, structures in 100 μL gels but regressed by day 6.
4	5 mg/mL (1 U/mL) or 10 mg/mL (2 U/mL) Fibrin with 20 μg/mL Fibronectin and 0.2% TG	100 μL gels (pre-wetted) in 48 well plate	EGM2-MV medium	2:1, 1:1, 1:0.5	1-2$\times10^6$	0.5-1$\times10^6$	400 μL or 1000 μL EGM (daily or 2 day changes)	200 ng/mL VEGF, bFGF in gel	10	2:1: spreading of cells up to day 6, regressed after then. 1:1: Areas of higher density cells in 1:1 produced large capillary-like structures within 4 days. 1:0.5: No structures.
5	2.5 mg/mL (0.5 U/mL) with 20 μg/mL Fibronectin	100 μL, 200 μL gels (pre-wetted) in 48 well plate and 100 μL gels in PDMS wells (pre-wetted)	EGM2-MV medium	3:0.3, 3:0.6, 1.5:0.15, 1.5:0.3	1.5-3$\times10^6$	0.15-0.6$\times10^6$	400 μL EGM2 in well plate and 1000 μL EGM2 in PDMS wells (2 day changes)	200 ng/mL VEGF, bFGF, SDF-1α in gel	4	Cells remained round for duration of experiment.
6	2.5 mg/mL (0.5 U/mL) or 10 mg/mL (2 U/mL) Fibrin with 20 μg/mL Fibronectin	100 μL gels (pre-wetted) in 48 well plate	EGM2-MV medium	3:0.3, 5:0.5	3-5$\times10^6$	0.3-0.5$\times10^6$	400 μL EGM2-MV (2 day changes)	200 ng/mL VEGF, bFGF in gel with and without SDF-1α	4	Cells remained round for duration of experiment.
7	5 mg/mL (1 U/mL) or 10 mg/mL (2 U/mL) Fibrin with 20 μg/mL Fibronectin and 0.2% TG	100 μL gels (pre-wetted) in 48 well plate	EGM2-MV medium	5:1, 5:2.5, 3:1.5	3-5$\times10^6$	1-2.5$\times10^6$	400 μL EGM2-MV (daily or 2 day changes)	200 ng/mL VEGF, bFGF in gel	6	Cells remained round for duration of experiment, except for 3:1.5 in 5 mg/mL fibrin, which lost structure by day 6.
8	5 mg/mL (1 U/mL) or 10 mg/mL (2 U/mL) Fibrin with 20 μg/mL Fibronectin and 0.2% TG	50 μL and 100 μL gels (pre-wetted) in 48 well plate	EGM2-MV medium	2:1, 1:1, 1:2	1-2$\times10^6$	1-2$\times10^6$	200 μL (daily changes) or 400 μL EGM (2 day changes)	20 ng/mL VEGF, bFGF in medium	10	2:1 structures formed but regressed by day 6. Limited spreading in 1:1 and 1:2. 50 μL better than 100 μL gels. 5 mg/mL better than 10 mg/mL gels. 400 μL better than 200 μL medium.
9	5 mg/mL (1 U/mL) or 10 mg/mL (2 U/mL) Fibrin with 20 μg/mL Fibronectin and 0.2% TG	150 μL gels (pre-wetted) in 48 well plate	EGM2-MV medium	2:1, 1:1, 1:2	1-2$\times10^6$	1-2$\times10^6$	400 μL EGM (daily or 2 day changes)	20 ng/mL VEGF, bFGF in medium	8	5 mg/mL: 1:1 better than 2:1 and 1:2. Lumen visible in 1:1 by day 6. Most structures regressed by day 8. 10 mg/mL: regions of higher cell density yielded significant structure. Marginally better changing medium every day than every 2 days.
10	5 mg/mL (1 U/mL) Fibrin with 20 μg/mL Fibronectin and 0.2% TG	150 μL gels (pre-wetted) in 48 well plate	EGM2-MV medium	1:1, 1:0.5, 1:0.2	1$\times10^6$	0.2-1$\times10^6$	200 μL or 400 μL EGM or EGM2-MV (2 day changes)	20 ng/mL VEGF, bFGF in EGM medium	12	Day 4: 1:1, 1:0.5, 1:0.2 all displaying structure. Day 6: 1:1 retained structure better than 1:0.5, which was better than 1:0.2. 400 μL better than 200 μL medium. Day 8: Only 1:1 maintained structure.
11	5 mg/mL (0.5 U/mL) Fibrin with 20 μg/mL Fibronectin and 0.2% TG	150 μL gels (pre-wetted) in 48 well plate	EGM2-MV medium	0.3:1.5, 0.3:0.6, 0.3:0.3, 0.3:0.15, 0.3:0.06	0.3$\times10^6$	0.06-1.5$\times10^6$	200 μL EGM or EGM2-MV (3 day changes)	20 ng/mL VEGF, bFGF in EGM medium	10	Limited disconnected structures in 1:2 and 1:1. Others show no structure.
12	5 mg/mL Fibrin with 20 μg/mL Fibronectin and 0.2% TG	150 μL gels in 48 well plate	MSC medium	1:2, 1:0.33, 1:0.2	1$\times10^6$	0.2-2$\times10^6$	250 μL or 1000 μL EGM, EGM2-MV (3 day changes)	With or without 20 ng/mL VEGF, bFGF in medium	8	Limited spreading of cells, though 1:2 marginally better.
13	5 mg/mL or 10 mg/mL Fibrin	200 μL gels in 24 well plate	MSC medium	1:2	1$\times10^6$	2$\times10^6$	2000 μL EGM (2 day half medium changes)	With or without 20 ng/mL VEGF, bFGF in medium	12	Limited spreading of cells.

6.5 Capillary Formation under Optimal Conditions

The optimal condition for interconnected capillary growth throughout the fibrin gels was found using 2.5 mg/mL fibrin gels, using relatively low levels of cells overall, with a 5:1 ratio between HUVECs (1×10^6 HUVECs/mL) and supporting MSC cells (0.2×10^6 MSCs/mL). Figure 6.1 shows gel drops (more spherical gels) in a 48 well plate (100 μL gel volume). 400 μL of endothelial cell growth medium (EGM2) was added to the wells on top of the gels, containing 20 ng/mL VEGF, bFGF, and SDF-1α growth factors.

By day 2, a high degree of cell spreading was observed. By day 6, a large number of connections appeared to have been made between endothelial cells. While lumen may indeed have formed, they are hard to discern in this dataset.

Note however that the vessels produced in this way, despite producing complex networks of cells, still have small diameter lumen. This is thought to be down to the limited concentration of endothelial cells which are cultured in this experiment. Thus in order to enable perfusion through this structure, a higher cell concentration is thought to be required. Further, we consider 2.5 mg/mL fibrin gels to be too susceptible to gel contraction present with higher cell concentrations and not ideal for running with a high flow rate perfusion experiment. Thus, in the following sections, we look to increasing both the matrix concentration and the cell concentration to yield a structure more suitable for a perfusion experiment.

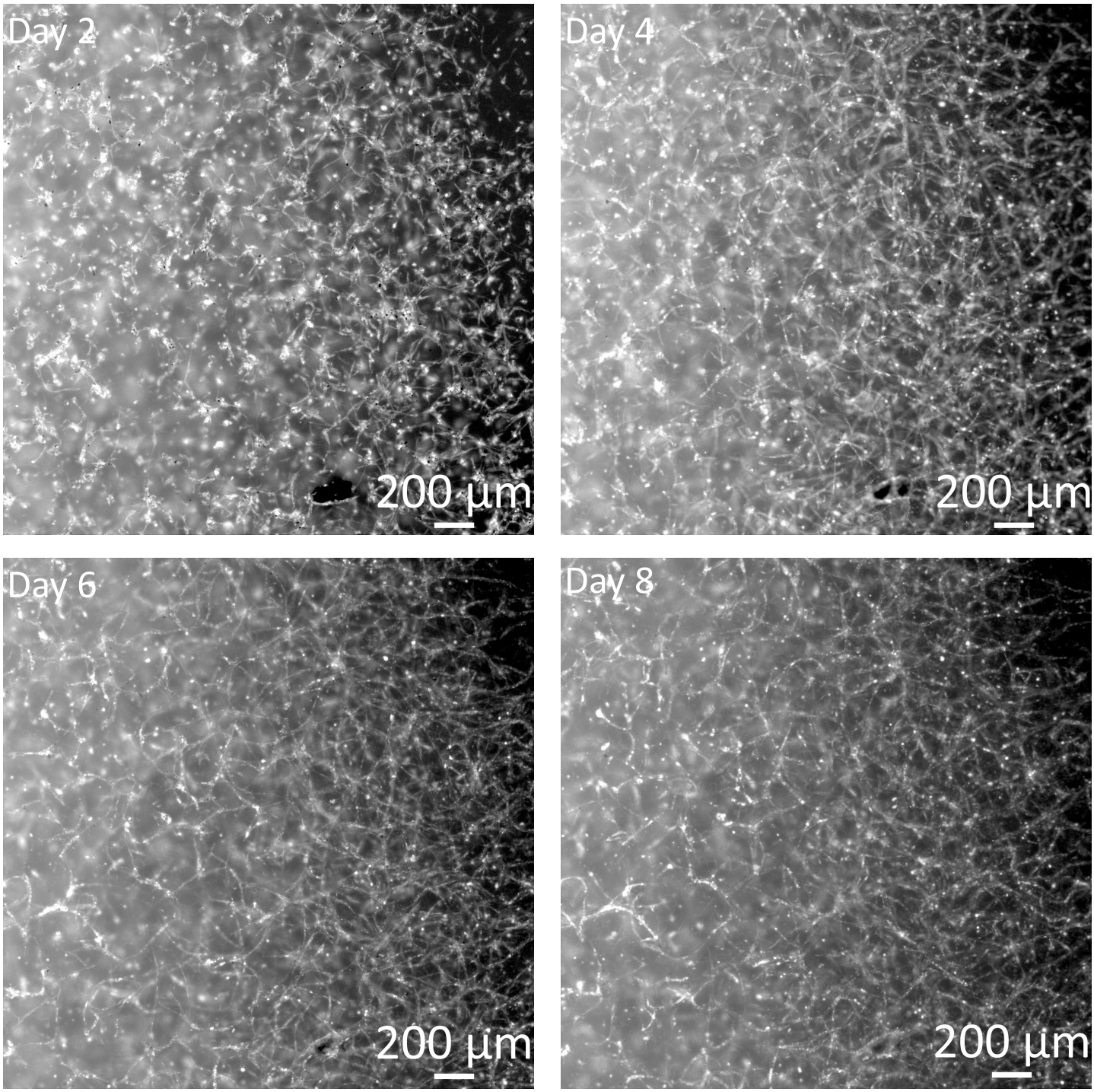

Fig. 6.1 Fibrin gel droplets (2.5 mg/mL) with 1×10^6 HUVECs/mL and 0.2×10^6 MSCs/m, for days 2-8. 20 ng/mL VEGF, bFGF, and SDF-1α growth factors were added to 400 μL cell medium on top of the gels. Images show single droplets; the center of the drop is to the left of the image and the edge of the drop is to the right. Shown in white are the endothelial cells.

6.6 Effect of Increasing Matrix Concentration

With increasing matrix concentration, the length and degree of interconnectedness of capillary structures decreased. Over the course of the single cell experiments in well plates, fibrin concentrations of 2.5-10 mg/mL were tested. 2.5 mg/mL gels, while optimal for capillary growth, were not considered capable of supporting high flow rate perfusion, due to the associated high shear and pulsatile flow, and were less capable of resisting cell-mediated gel shrinkage. Both perfusion and preventing gel shrinkage were necessary conditions for the addition of 3D printed networks and so higher concentration fibrin gels were tested.

Figure 6.2 shows a comparison of 2.5 mg/mL and 10 mg/mL fibrin gels organised as 50 μL gel droplets, over days 2-6. Both matrix concentrations show extensive network formation but 2.5 mg/mL forms a significantly higher density of structures. 10 mg/mL fibrin gels appear to have a more delayed formation of capillary structures and a less dense network formed by day 6. This is expected as the cells in 10 mg/mL fibrin have significantly more matrix to digest prior to be able to spread and connect to other endothelial cells. Also, the diffusion of nutrients, oxygen, and growth factors will be greatly slowed in 10 mg/mL fibrin, compared to 2.5 mg/ml fibrin gels. This appears to have an effect on the proliferation and cell survival rates of the endothelial cells, as shown by the increased cell number in 2.5 mg/mL fibrin (Figure 6.2(a)) and reduced cell number in 10 mg/mL fibrin (Figure 6.2(d)) by day 2.

However, the fact that 10 mg/mL fibrin gels do indeed form networks means the higher concentration fibrin can be used alongside perfusion and 3D printed channels. Further, perfusion is likely to be a far more effective system of delivering metabolites than static cell medium since perfusion involves both diffusion from the channel and bulk movement of fluid (advection).

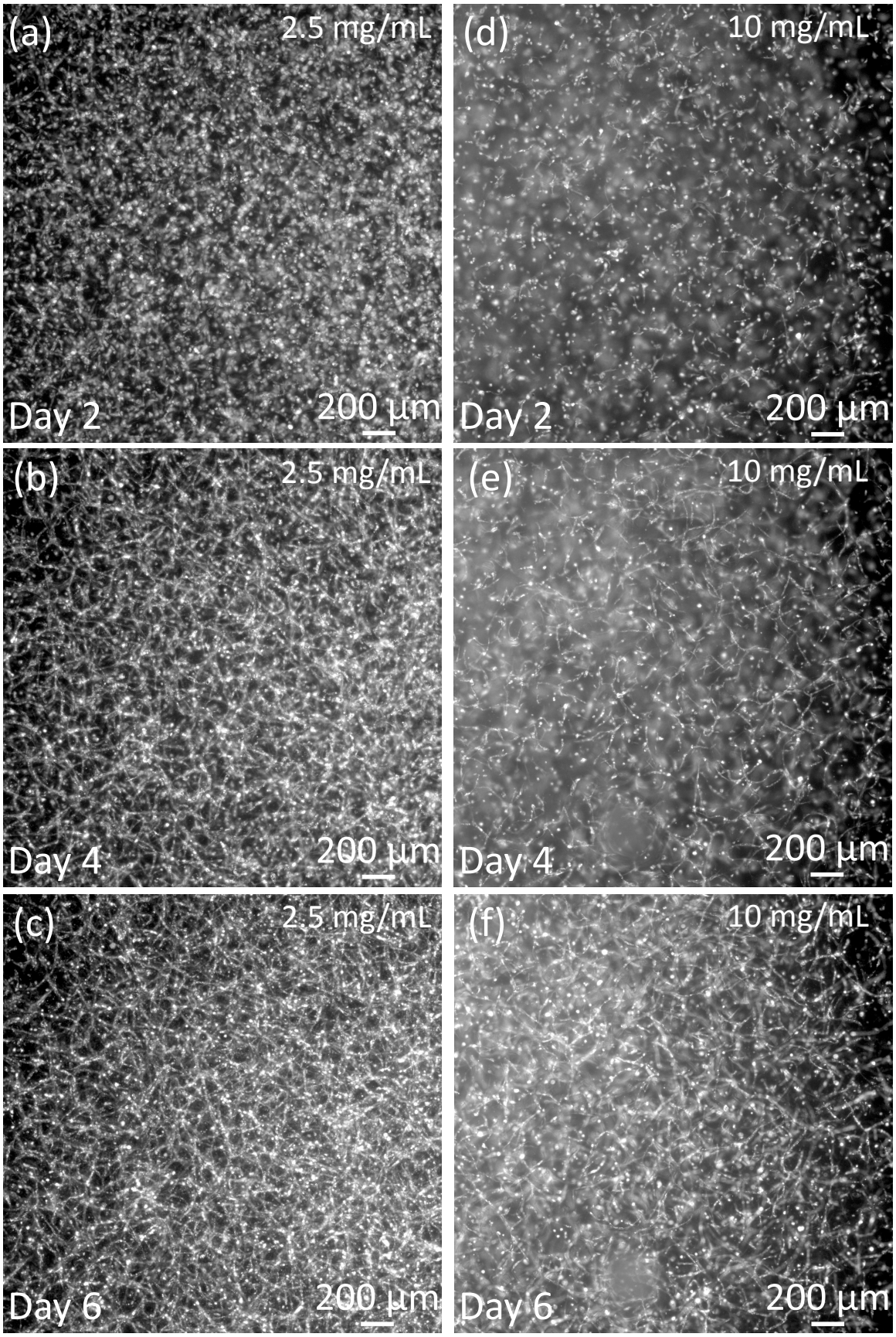

Fig. 6.2 Matrix concentration comparison of (a-c) 2.5 mg/mL and (d-f) 10 mg/mL fibrin gels, using 1×10^6 HUVECs/mL and 0.2×10^6 MSCs/mL, for days 2-6. 20 ng/mL VEGF, bFGF, and SDF-1α growth factors were added to 400 μL cell medium on top of the gels.

6.7 Regions of Higher Cell Density Yield Rapid Capillary Formation

Having shown that it is indeed possible to form networks in 10 mg/mL fibrin gels, we looked to improving the formation of the capillary-like structures and larger lumen. In experiments using 5 mg/mL fibrin gels (between 2.5 and 10 mg/mL gels), with 1×10^6 HUVECs/mL and 1×10^6 MSCs/mL, it was found that regions with a locally higher density of cells produced large capillary structures very rapidly, with clear signs of lumen formation by day 4, as shown in Figure 6.3. As stated previously, with single cell capillary morphogenesis, lumen are formed by intracellular vesicle formation and fusion, meaning the lumen are significantly thinner and less well developed than spheroid-formed lumen at the same time-point, and more susceptible to movement (compare with Figure 5.2 and Figure 5.4 for angiogenic lumen formation).

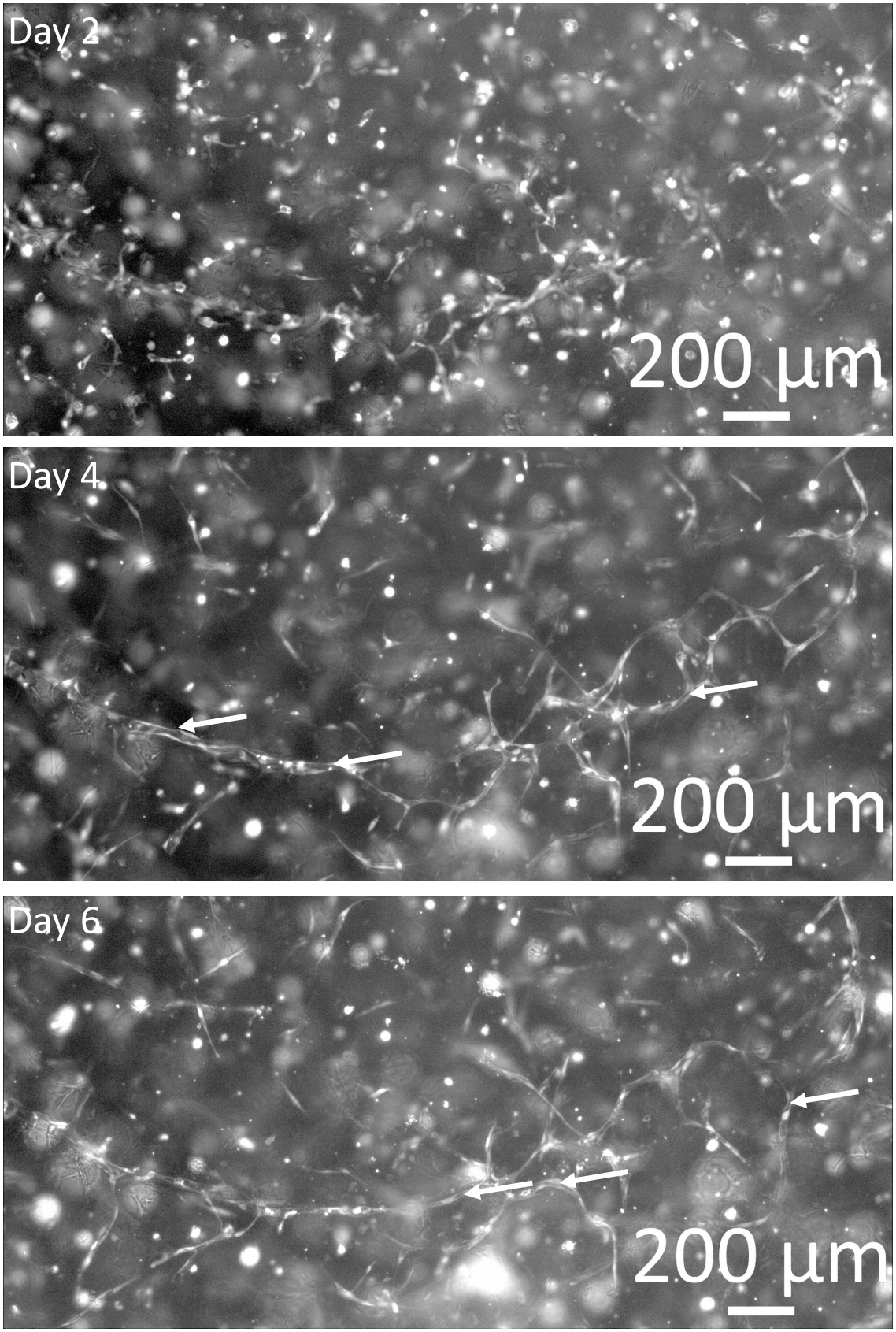

Fig. 6.3 Regions that by chance had a higher density of cells yielded capillary-like structures as early as day 4. Here, 5 mg/mL fibrin gel was used with 1×10^6 HUVECs/mL and 1×10^6 MSCs/mL (1:1). Arrows show examples of early lumen formation.

6.8 Increased Cell Concentrations in 10 mg/mL Fibrin Gels

Having established that a higher density of cells enables rapid capillary structures to form with relatively large lumen, we looked to increasing the concentration of cells throughout the whole gel, with the aim of improving capillary formation. Further, it was thought that in higher matrix concentrations, a higher density of endothelial cells would mean that they would have less distance to migrate to form junctions with one another and would each have less matrix to degrade to form capillary structures, thereby reducing the effect of matrix concentration upon capillary morphogenesis.

Thus we tried raising the HUVEC concentration (up to 3×10^6 HUVECs/mL), whilst maintaining a ratio of HUVEC:MSC at 5:1, in 10 mg/mL fibrin gels, as shown in Figure 6.4. Cell spreading was observed in both 2×10^6 HUVECs/mL and 3×10^6 HUVECs/mL, though the spreading was limited to the edge of gel droplets, which was thought to be due to a reduced diffusion distance of metabolites through a higher concentration matrix (as described in Section 6.6), but also due to increased cellular competition for oxygen and nutrients, now present with higher cell densities. To maximize supply of metabolites to the cells in the well plate static culture conditions, gel drops were formed which were relatively low volume (100 μL), the data for which is shown in Figure 6.4.

Thick gels were also explored, using wells fabricated out of PDMS. By tailoring the dimensions of a chamber in the bottom of the well, a gel of the same volume (100 μL) can be fabricated with a known depth (2 mm) and with a flat surface, leading to a uniform gel thickness, not present in the gel drops. The results of these experiments are shown in Figure 6.5. Gels of 2.5 mg/mL fibrin yielded network structures at both 3×10^6 and 1×10^6 HUVECs/mL, with the lower concentration producing noticeably thinner structures (shown at day 6). The equivalent in 10 mg/mL fibrin gels yielded no noticeable structures for 3×10^6 HUVECs/mL and only a disconnected network for 1×10^6 HUVECs/mL. Differences in observed cell number at day 6 suggest that the reduced diffusion distance produced a nutrient-limited experiment for the 10 mg/mL fibrin gels.

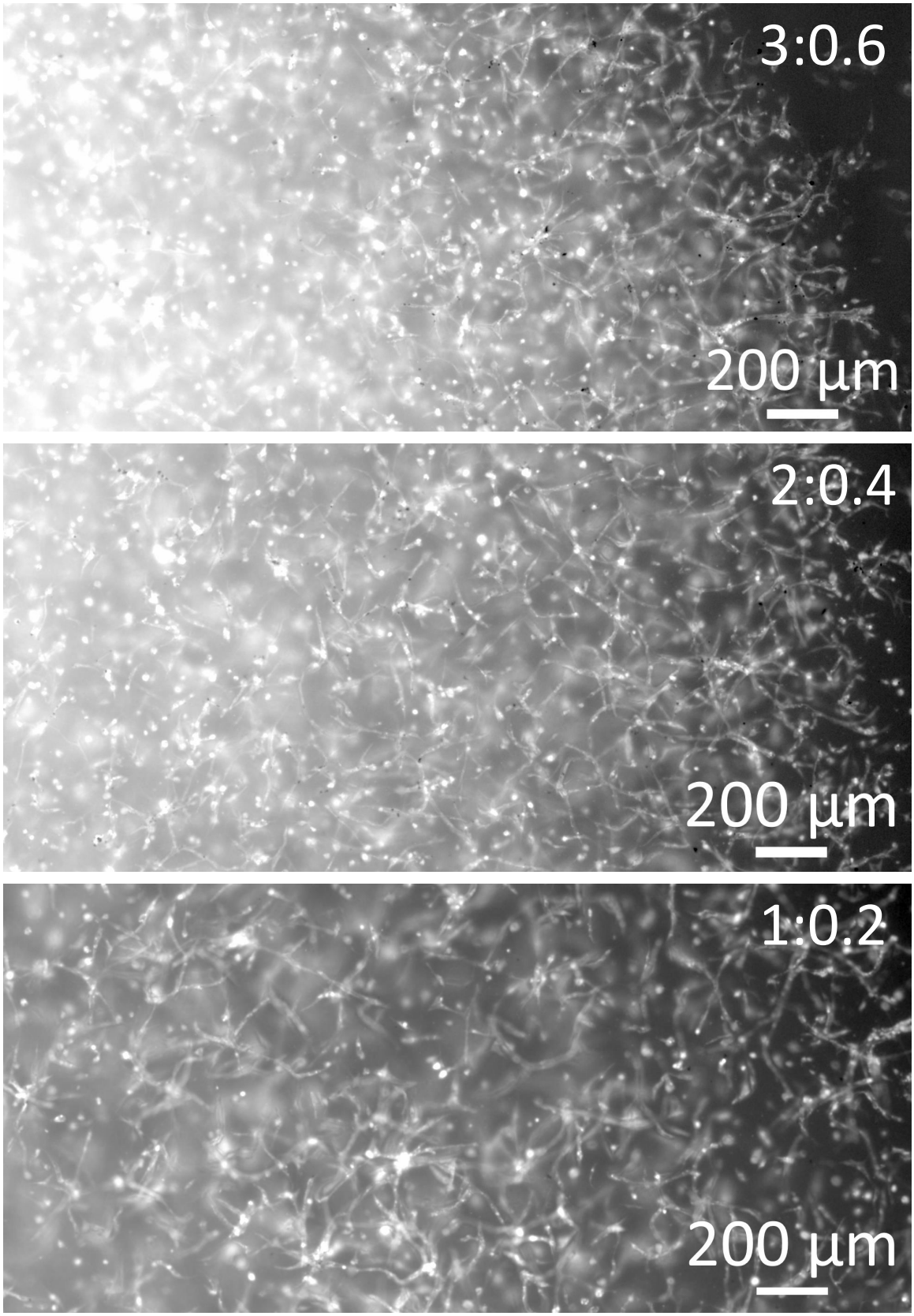

Fig. 6.4 Comparison of different cell concentrations in thin (100 μL) gel drops (day 4). Shown is 1-3$\times 10^6$ HUVECs/mL with 0.2-0.6$\times 10^6$ MSCs/mL respectively (5:1 ratio maintained), in 10 mg/mL fibrin gel. Grown with 20 ng/mL VEGF, bFGF and SDF-1α growth factors added to cell medium. Note that with decreasing cell concentration, cell spreading is observed increasingly further from the gel surface, thought to be due to increased penetration of metabolites and growth factors as cell competition is lower.

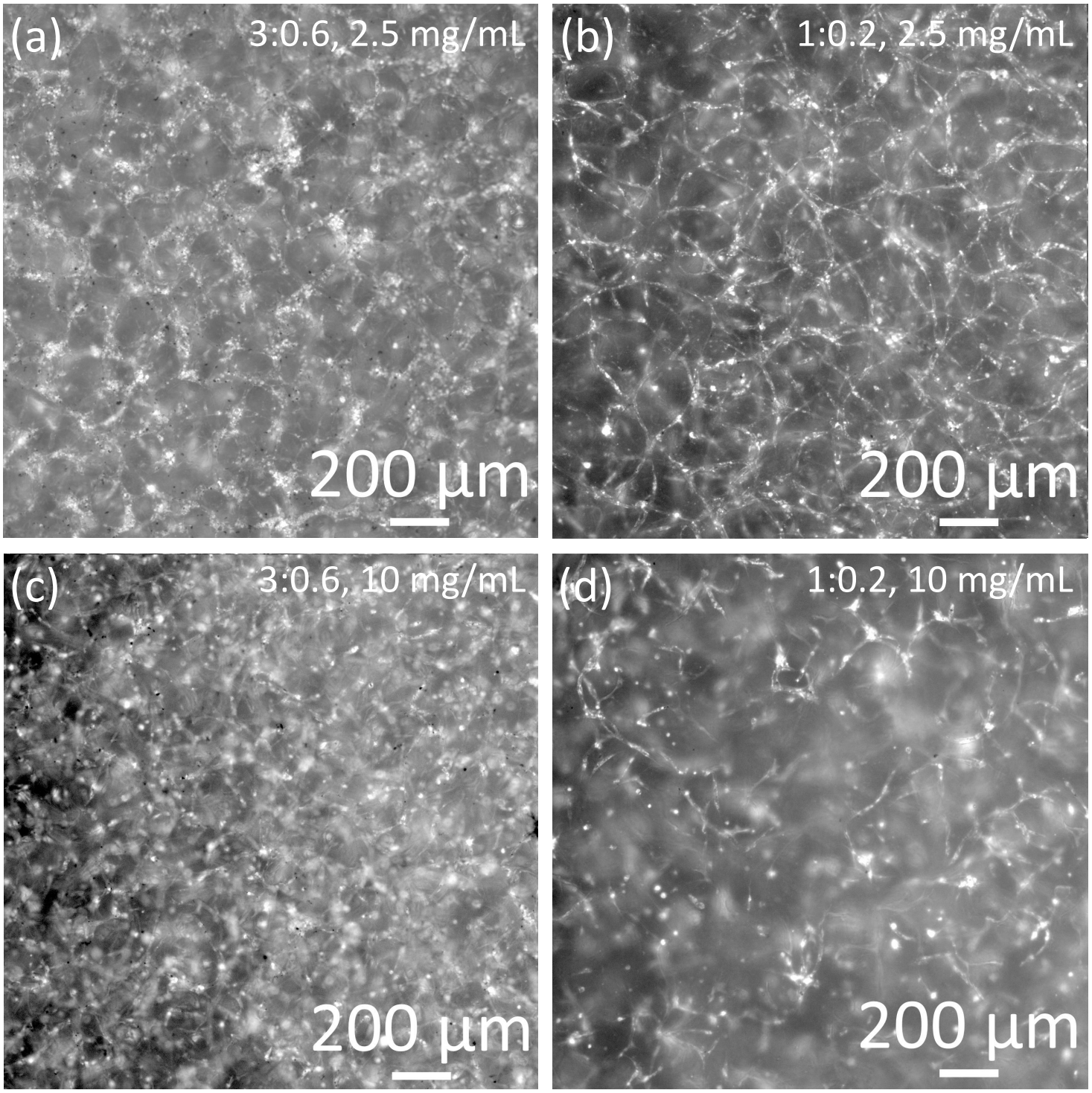

Fig. 6.5 Comparison of different cell concentrations in thick (2 mm deep) PDMS wells in 2.5 mg/mL and 10 mg/mL fibrin gels (day 6). 2.5 mg/mL fibrin gels, (a) 3×10^6 HUVECs/mL and (b) 1×10^6 HUVECs/mL, yield networks. Lower concentrations of cells yielded thinner features. 10 mg/mL fibrin gels, with (c) 3×10^6 HUVECs/mL and (d) 1×10^6 HUVECs/mL, did not produce networks. Lower concentrations of cells formed disconnected strands. Grown with 20 ng/mL VEGF, bFGF, and SDF-1α growth factors added to cell medium.

6.9 Variation in MSC Concentration

We also investigated any potential effects of increasing the MSC concentration, relative to the HUVEC concentration. In the case of fibroblasts, the literature suggests a high concentration is preferable as they produce a significant number of pro-angiogenic factors and undergo collagen deposition [159]. In the case of MSCs, the literature suggests that a high concentration of the cell type inhibits capillary formation as they intercalate between the endothelial cells and cause their apoptosis [24]. As shown in Figure 6.6, we compared cell ratios either side of the 25% threshold stated in the literature, testing HUVEC:MSC ratios of (a) 3:1 (33%) and (b) 3:0.6 (20%). The difference was slight but the 3:1 version seemed marginally better in terms of interconnectness and lumen formation. This could be explained by increased presence of MSC-derived factors which aid in the capillary development, though it conflicts with the threshold stated in the literature.

Both HUVEC:MSC 3:1 and 3:0.6 were grown in the presence of stromal derived factor (SDF-1α). The use of SDF-1α alongside relatively low levels of MSC (HUVEC:MSC 5:1) means that the oxygen and nutrient requirements of the cell-ladened gel are significantly lower than would otherwise be needed for high supporting cell concentrations (i.e. with fibroblasts) and SDF-1α is able to replace some of the factors produced by the supporting cell type. This could be beneficial for the perfused gel system as less exogenous growth factors will need to be added to the perfusate. However, MSCs are still required for other factors and for stabilizing the nascent capillary structures.

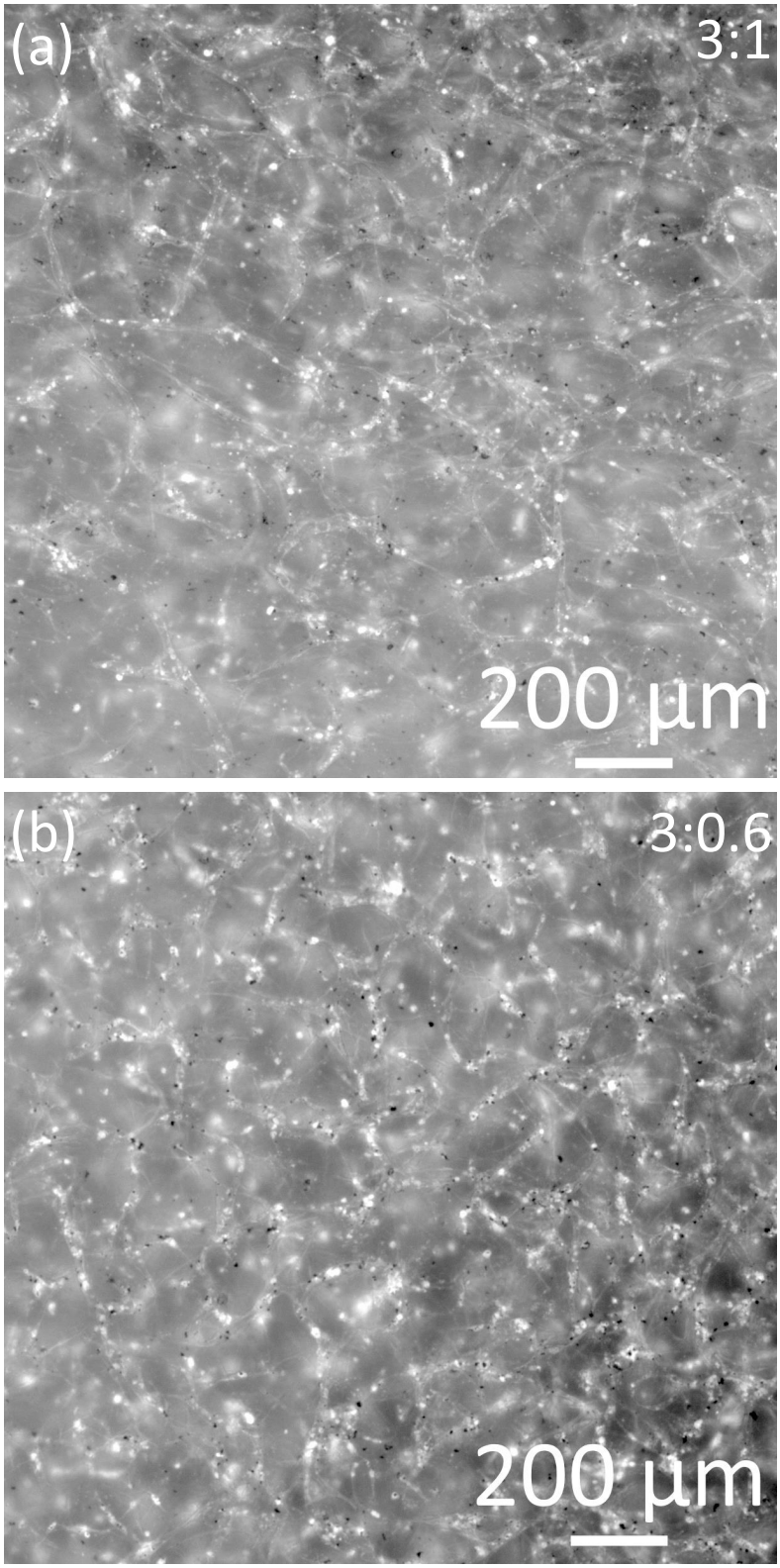

Fig. 6.6 Variation in MSC concentration with fixed HUVEC concentration of 3×10^6 HUVECs/mL in 2.5 mg/mL fibrin gels, at day 6. (a) 1×10^6 MSCs/mL (3:1) and (b) 0.6×10^6 MSCs/mL (3:0.6). Grown with 20 ng/mL VEGF, bFGF, and SDF-1α in cell medium. 3:1 appears slightly better than 3:0.6 in terms of connected networks and lumen.

6.10 Location of Growth Factors and Incorporation of Aprotinin

We investigated placing the growth factors in the gel precursor solution, thereby inducing growth factor binding to the fibrinogen and fibronectin, via their heparin-binding domains. The aim here was to present bound growth factors (i.e. 200 ng/mL bound to the gel matrix) to the cells rather than soluble growth factors added to the cell medium (20 ng/mL). These bound growth factors could then be broken down by the cells over the course of the experiment to provide spatial cues for capillary development. Further, the binding of growth factors into the gel would mean that growth factors would not need to be added to the cell medium. The use of significantly larger gels containing the 3D printed channels requires a proportionally larger volume of cell medium to maintain the cell population, including an increase in the usage of growth factors. Thus were we able to add growth factors to the gels, the cost of the experiment would be reduced and high volumes of cell medium could be employed, for delivery of higher levels of nutrients.

However, growth factors added to the precursor solution were thought to be rapidly washed out since regression of any nascent capillary structures was observed by day 8, suggesting the growth factors had not bound to the matrix material and were free to diffuse through the gel matrix. Figure 6.7 shows 200 ng/mL VEGF, bFGF, and SDF-1α growth factors added to the gel precursor solution and deposited in well plates as 25 μL and 100 μL gel drops, with a cell concentration of HUVEC:MSC 3:1. As one would expect if the growth factors were free to diffuse away into the surrounding medium, the cells in the smaller 25 μL droplets (Figure 6.7a,b) remained completely round (as did the 50 μL drops (not shown)). However, the cells in the larger 100 μL droplets did sprout and form structures by day 4 (Figure 6.7c). However these structures had regressed by day 8 (Figure 6.7d). Thus, these results support the hypothesis that the growth factors were diffusing out of the gel; diffusion from the larger gel taking longer to complete.

Under perfusion conditions, these factors are likely to be washed out even more rapidly and so unless a method can be found to bind growth factors into the matrix, we must continue to add growth factors to the cell medium rather than to the gel precursor solution.

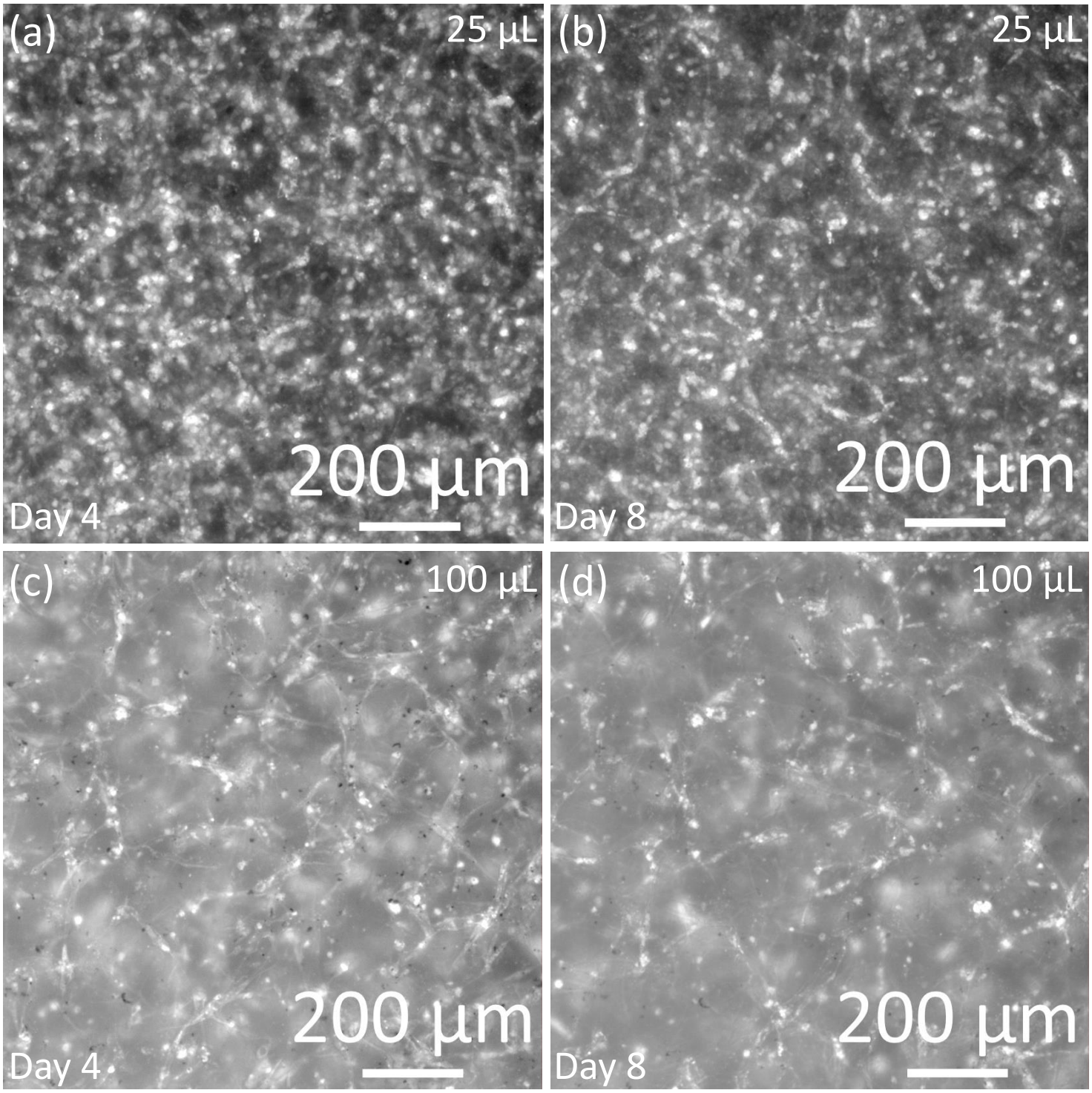

Fig. 6.7 VEGF, bFGF, and SDF-1α growth factors added to gel precursor solution at 200 ng/mL did not yield long-lived capillary-like structures. Cells in (a,b) 25 μL gel drops remained spherical for duration of experiment and 100 μL gel drops sprouts and formed structure by day 4 (c), but by day 8 (d), had lost most of its structures. Shown here is 3×10^6 HUVECs/mL and 1×10^6 MSCs/mL in 2.5 mg/mL fibrin gel.

Findings in the literature do suggest that modifying the current process of gel formation may enable growth factors to be bound to fibrinogen (which are reported to have a high affinity for certain growth factors [105]) and thus incorporated into the gel structure. Growth factors bound in this way may produce spatial cues for vascular development, as well as providing an inexpensive way of delivering growth factors to cells (as opposed to adding growth factors to cell medium). However, on the other hand, growth factors added to the cell medium, which is delivered via the channel network, may set up spatial gradients which enhance capillary formation and anastomosis with the larger channels.

The literature suggests that bFGF binds strongly to fibrin, but standard VEGF-A121 and VEGF-A165 do not [105]. Thus, it is likely that the VEGF is being washed out of the gels. The solution found in the literature is to fuse a particular peptide sequence, which is a substrate for the transglutaminase factor XIIIa, to the N-terminus of either VEGF-A164 [137] or VEGF-A121 [54, 176]. The transglutaminase (with bound growth factors) then covalently binds to the fibrin during the crosslinking reaction, thus binding the VEGF to the fibrin network, which can only be released under enzymatic cleavage [137].

An alternative approach may be to bind growth factors to fibronectin, prior to its addition into the gel precursor solution. Fibronectin is reported to have a high binding affinity for VEGF-A165 and VEGF-B, but not to VEGF-A121 [106]. Comparing experiments from two papers [105, 106], fibronectin appears to have double the binding affinity for VEGF-A165 and VEGF-B to that of fibrinogen. Further, the conformational state of fibronectin may be important to the degree of VEGF binding, due to the presentation of binding sites in the fibrillar state (through decreased extracellular pH which is an indication of deficient vascularization or the presence of heparin) [110, 47]. Fibronectin binds reversibly to fibrin and can subsequently be covalently cross-linked to the fibrin by the transglutaminase factor XIIIa [104]. Though perhaps not as effective, this may be a simpler way to incorporate VEGF into the fibrin gel matrix than via the addition of a peptide sequence.

We also investigated the use of aprotinin, added to the cell medium, as it has been reported in the literature to produce better organized gels, whilst not inhibiting capillary growth in HUVEC and MSC co-cultures. Our findings corroborate the finding that aprotinin does not inhibit capillary formation (similar structures were observed, not shown) though no advantage was found in its addition. Further, we looked at adding 0.2% transglutaminase which has also been reported to improve fibrin structure, mechanical strength and gel transparency [84]. In these limited experiments (not shown), we did not see any significant improvement when using transglutaminase (a degree of gel shrinking was still observed with 2.5 mg/ml fibrin gels) and so it was not included in subsequent experiments since it adds complexity to the method without significant advantage.

6.11 Synthesis of 3D Printed Channel Network and Vasculogenic Capillaries

One of the limitations of well plate and PDMS well experiments is that the nutrients and oxygen are delivered to the cells via diffusion from the gel surface, and cells compete for these metabolites. In the case of perfusion experiments, oxygen and nutrients are more actively delivered both by diffusion from the capillaries and by interstitial flow in the bulk gel (advection). Further, since there are potentially significantly more metabolites available to a gel under perfusion than in a well plate experiment, the cells may be much more proliferative and metabolically active, and as such require a significantly larger volume of medium to support capillary formation. Thus, the experiments of this chapter only provide a starting point for determining the best conditions for perfusion experiments.

6.12 Chapter Summary

Having established the limitations of using a spheroid-based system for producing a capillary network, this chapter investigated the use of a single cell approach. A large number of parameters were found to be important for success, including the matrix concentration, the volume and shape of the gels, and cell concentrations and ratios between endothelial and MSC cell types. Whilst a successful protocol was established for vessel formation in low concentration gels, it was thought that for perfusion, a higher concentration fibrin gel would be necessary to resist perfusion-related stresses and prevent gel shrinking from large numbers of metabolically active cells. Thus a series of experiments attempted to find suitable parameters for capillary morphogenesis in a relatively high concentration gel.

The key difference of perfusion experiments is the ability to support high concentrations of cells, if desired. When performed in well plate experiments, an increase in cell concentration (either endothelial cell or MSCs) led to poorer capillary formation and could lead to rapid regression of the capillary structures, as shown in Figure 6.4. However, since higher endothelial cell concentrations will help produce capillary structures earlier, and with larger lumen, as shown in Figure 6.3, and likely produce more interconnected networks, using a cell concentration of 3×10^6 HUVECs/mL and 0.6×10^6 MSCs/mL, with the additional SDF-1α growth factor in the cell medium, seems the preferred condition on which to begin synthesis of the two vascular network approaches, when employing single cell capillary formation.

Chapter 7

Conclusions and Future Work

7.1 Conclusions

Vascular network formation is a key challenge in the pursuit of forming thick tissue-engineered cellular constructs. As can be seen by the range of techniques reported in the literature, no one method is yet capable of producing the three-dimensionality, hierarchy, and perfusion of a vascular system with sufficient complexity and architecture to support therapeutic levels of cells, in materials ideal for tissue engineering.

Techniques for forming vascular channel networks included materials-based approaches, including lithography, bioprinting, and sacrificial 3D printing, and cell-based approaches, using co-culture systems of endothelial and supporting cell types to produce a vessel network via biological self-organization processes. A thorough literature review of materials-based approaches (Chapter 2) to vascularisation revealed that no one technique is currently able to meet the requirements for a vascular system, limited by the length-scale of channel that can be produced, by a lack of three-dimensionality that is achievable from the particular technique, a lack of scalability, or the complexity of the structures that can be fabricated.

In this project, we have assembled the building blocks of a full vascular system, capable of being deployed in ideal tissue engineering materials, such as collagen and fibrin hydrogels. A novel 3D printing-based approach has been invented in order to produce vascular networks which are hierarchical, three-dimensional, and perfusable with culture medium (Chapter 3). Templates made from standard 3D printed thermoplastic materials were converted into gelatin gel, via an alginate gel intermediary, which allows us to make use of intricate and reproducible 3D printed network designs in materials ideal for tissue engineering, and which can be pre-loaded with cells to produce scaffolds with high and uniform cell densities.

Further, these three-dimensional and hierarchical gelatin templates were cast in collagen (extracellular matrix-like) and fibrin (wound healing-like) gels and removed rapidly under

physiological conditions (i.e. 37 °C), making them ideal for use as a vascular template. This multi-casting process is a key finding of this project and enables large-scale and three dimensional tissue constructs to be fabricated in the lab.

A series of pilot cell experiments were performed as a preliminary evaluation of these vascular networks. By seeding fibroblasts into the bulk of the gel matrix and perfusing the channel network with cell culture medium, we investigated how the cell viability was dependent upon the flow rate, and a regime was found in which the vast majority of fibroblasts were alive (i.e. above 10 mL/hr). It was observed that increasing the flow rate further caused the cell morphology to change from being round to highly elongated; this is suggestive that the cells were more metabolically active. Thus we were able to maintain a high cell viability in a thick and densely populated scaffold.

Further to this work, the channels were seeded with endothelial cells so as to form a nascent endothelium. It was found that by perfusing at a very low flow rate, the endothelial cells would remain attached and would proliferate to cover the whole surface of the channels. Increasing the flow rate led to poor cell attachment, thought due to high shear stresses associated with pulsatile flow from the peristaltic pump.

Thus this novel process allows 3D printing technology to be used to produce hydrogel templates without the requirement for a custom-made machine and using relatively inexpensive materials. Further improvements to the method were then undertaken. The addition of a custom-made PDMS chamber (fabricated using another 3D printed cast) and a surface coating of PEI enabled a more stable alginate casting step to be performed, improving the relaibility of the method and a more customizable device to be fabricated.

Limitations in 3D printing technology at this time led us to investigate forming micro-scale vasculature via cellular processes. A literature review of three-dimensional capillary experiments (Chapter 4) found no consensus on the best approach to their formation.

Thus two primary methods were investigated as a means to form a capillary-like vascular network. An angiogenic approach using multi-cellular spheroids was first considered, in well plate experiments (Chapter 5). The use of spheroids, in which high numbers of endothelial cells are in immediate contact prior to encapsulating the gel matrix, yielded long, multi-cellular structures with visible and large lumen, and were capable of creating long-lived and interconnected networks.

Experiments were carried out using both fibroblasts and mesenchymal stromal cells as the supporting cell type, and over a range of substrate concentrations. Furthermore, experiments were also carried out which investigated incorporating the supporting cell type into the same spheroid as the endothelial cell or into distinct spheroids themselves, though no particular advantage was found in these approaches. Further, it was found that cells from spheroids

were able to coat the inside of the large-scale, 3D printed channels, which may provide a means of connecting the two systems together. However, deficiencies in this method were found in the lack of uniformity of the spheroids in the gels, the time-consuming nature of their fabrication, and importantly the limits on the number of cells which can be realistically incorporated into the device.

A vasculogenic single-cell approach was investigated (Chapter 6) which would overcome the limitations associated with the angiogenic, multi-cellular spheroid method. Optimal conditions were identified in which cells seeded individually into a low concentration gel matrix were able to form capillary-like structures. However, a large number of parameters were observed to affect capillary morphogenesis in the well plate experiments.

In order to undertake perfusion experiments involving the addition of the 3D printed channels, it was thought necessary to investigate capillary formation in higher matrix concentrations. The results suggested that networks were possible in these higher concentration gels, suitable for perfusion experiments by using higher concentrations of cells, and that capillary-like vessels would form with large lumen early on. However difficulties were encountered in sustaining the high populations of cells by diffusion-based medium culture alone, as was the case in the well plate and PDMS chamber experiments.

The findings of these experiments guide future work, in which the challenge will be to incorporate the cellular co-culture techniques with the 3D printed channels approach, thereby producing a vascular network over the full range of length-scales found in nature. At this point, we should be able to support the survival of liver parenchymal cells which would add functionality to the tissue construct.

7.2 Future Work

7.2.1 Perfusion Experiments with 3D Printed and Cell-Based Vascular Networks

The next part of this work is to combine the large-scale channels produced by the 3D printing method with the capillary vessels produced by vasculogenic co-culture of endothelial and mesenchymal stromal cell types, in 10 mg/ml fibrin gels and with higher concentrations of cells, thereby producing perfusable lumen.

Based on the results of perfusion experiments performed with fibroblasts alongside the 3D printed channels, it should not be too difficult to induce a similar degree of spreading of both endothelial cells and MSCs, at similar flow rates. The challenge will be to optimize conditions under medium perfusion such that an interconnected network forms between the capillary bed and the large-scale 3D printed channels. Flow of cell medium, carrying nutrients and oxygen, through the capillaries is a pre-requisite for further cellular work incorporating liver parenchymal cells.

7.2.2 Incorporation of Growth Factors into Gel Matrix

The binding of growth factors into the gel matrix itself, rather than as supplements to the cell medium, is thought would enhance the formation of capillary structures and is preferable as an inexpensive means of stimulating the cells. Two methods were described for doing this; via the addition of a peptide sequence which allows the growth factors to be covalently bound into the matrix, or by using the affinity of the growth factors to fibronectin, which itself can be bound into the fibrin matrix. Both methods will be investigated in future.

7.2.3 Optimization of Gel Matrix Concentration

We also wish to improve the robustness of the gels, allowing them to be handled, whilst maintaining the ability of the endothelial cells to form capillary networks. Further, a self-supporting gel into which tubes can be attached directly would be beneficial. Thus a 20 mg/mL fibrin gel, rather than the 2.5-10 mg/mL concentrations employed in this project, would produce a rigid structure capable of being handled. The main hurdle against using high concentration gels is that the cells have to break down significantly more matrix to migrate and spread, and that diffusion of metabolites and signaling factors is diminished considerably.

In this project we have shown cell spreading in 10 mg/mL fibrin gels despite being denser than the optimal 2.5 mg/mL fibrin gels. Thus, increasing the flow rate to increase interstitial flow, increasing cell concentration to lower cell-cell distances, and tailoring the 3D printed channel structure to incorporate a reduced diffusion distance may mitigate the effects of using high concentration fibrin as the matrix material. The ideal outcome would be a construct with a solid outer shell and a soft internal structure formed by the degradation of the matrix by cells. This will be investigated in future experiments.

7.2.4 Addition of Hepatoblasts to Add Funtionality to the Scaffold

The end goal of this research is a solid organ structure capable of supporting high densities of parenchymal cells. Thus, once it has been shown that a full hierarchy of vascular channels has been produced, hepatoblasts will be incorporated into the precursor solution, alongside endothelial cells and MSCs. The literature has suggested that hepatoblasts are able to modulate the capillary network formed by co-culture of HUVECs and MSCs, to form a more liver-like vasculature [152, 153]. Thus the addition of the hepatoblast to our system would greatly help in forming a more functional tissue construct.

References

[1] 3ders (2012). Solidscape launches high precision fully automated 3z pro 3d printer.

[2] Adams, R. H. and Alitalo, K. (2007). Molecular regulation of angiogenesis and lymphangiogenesis. *Nature reviews Molecular cell biology*, 8(6):464–478.

[3] Ahmed, T. A., Dare, E. V., and Hincke, M. (2008). Fibrin: a versatile scaffold for tissue engineering applications. *Tissue Engineering Part B: Reviews*, 14(2):199–215.

[4] Alekseeva, T., Unger, R. E., Brochhausen, C., Brown, R. A., and Kirkpatrick, J. C. (2014). Engineering a microvascular capillary bed in a tissue-like collagen construct. *Tissue Engineering Part A*, 20(19-20):2656–2665.

[5] Ardakani, A. G., Cheema, U., Brown, R. A., and Shipley, R. J. (2014). Quantifying the correlation between spatially defined oxygen gradients and cell fate in an engineered three-dimensional culture model. *Journal of The Royal Society Interface*, 11(98):20140501.

[6] Au, P., Tam, J., Fukumura, D., and Jain, R. K. (2008). Bone marrow–derived mesenchymal stem cells facilitate engineering of long-lasting functional vasculature. *Blood*, 111(9):4551–4558.

[7] Auger, F. A., Gibot, L., and Lacroix, D. (2013). The pivotal role of vascularization in tissue engineering. *Annual review of biomedical engineering*, 15:177–200.

[8] Bae, H., Puranik, A. S., Gauvin, R., Edalat, F., Carrillo-Conde, B., Peppas, N. A., and Khademhosseini, A. (2012). Building vascular networks. *Science translational medicine*, 4(160):160ps23–160ps23.

[9] Baier Leach, J., Bivens, K. A., Patrick Jr, C. W., and Schmidt, C. E. (2003). Photocrosslinked hyaluronic acid hydrogels: natural, biodegradable tissue engineering scaffolds. *Biotechnology and bioengineering*, 82(5):578–589.

[10] Baker, M., Robinson, S. D., Lechertier, T., Barber, P. R., Tavora, B., D'amico, G., Jones, D. T., Vojnovic, B., and Hodivala-Dilke, K. (2012). Use of the mouse aortic ring assay to study angiogenesis. *Nature protocols*, 7(1):89–104.

[11] Barber, R., Cie, K., Emerson, D., et al. (2006). Using murray's law to design artificial vascular microfluidic networks. *WIT Trans. Ecol. Envir.*, 87:245–254.

[12] Bayless, K. J. and Davis, G. E. (2003). Sphingosine-1-phosphate markedly induces matrix metalloproteinase and integrin-dependent human endothelial cell invasion and lumen formation in three-dimensional collagen and fibrin matrices. *Biochemical and biophysical research communications*, 312(4):903–913.

[13] Bertassoni, L. E., Cardoso, J. C., Manoharan, V., Cristino, A. L., Bhise, N. S., Araujo, W. A., Zorlutuna, P., Vrana, N. E., Ghaemmaghami, A. M., Dokmeci, M. R., et al. (2014a). Direct-write bioprinting of cell-laden methacrylated gelatin hydrogels. *Biofabrication*, 6(2):024105.

[14] Bertassoni, L. E., Cecconi, M., Manoharan, V., Nikkhah, M., Hjortnaes, J., Cristino, A. L., Barabaschi, G., Demarchi, D., Dokmeci, M. R., Yang, Y., et al. (2014b). Hydrogel bioprinted microchannel networks for vascularization of tissue engineering constructs. *Lab on a Chip*, 14(13):2202–2211.

[15] Blaeser, A., Duarte Campos, D. F., Puster, U., Richtering, W., Stevens, M. M., and Fischer, H. (2016). Controlling shear stress in 3d bioprinting is a key factor to balance printing resolution and stem cell integrity. *Advanced healthcare materials*, 5(3):326–333.

[16] Carmeliet, P. and Jain, R. K. (2000). Angiogenesis in cancer and other diseases. *Nature*, 407(6801):249–257.

[17] Chan, J. M., Zervantonakis, I. K., Rimchala, T., Polacheck, W. J., Whisler, J., and Kamm, R. D. (2012). Engineering of in vitro 3d capillary beds by self-directed angiogenic sprouting. *PloS one*, 7(12):e50582.

[18] Chen, X., Aledia, A. S., Ghajar, C. M., Griffith, C. K., Putnam, A. J., Hughes, C. C., and George, S. C. (2008). Prevascularization of a fibrin-based tissue construct accelerates the formation of functional anastomosis with host vasculature. *Tissue Engineering Part A*, 15(6):1363–1371.

[19] Chen, X., Aledia, A. S., Popson, S. A., Him, L., Hughes, C. C., and George, S. C. (2009). Rapid anastomosis of endothelial progenitor cell–derived vessels with host vasculature is promoted by a high density of cotransplanted fibroblasts. *Tissue Engineering Part A*, 16(2):585–594.

[20] Choi, N. W., Cabodi, M., Held, B., Gleghorn, J. P., Bonassar, L. J., and Stroock, A. D. (2007). Microfluidic scaffolds for tissue engineering. *Nat. Mater.*, 6(11):908–915.

[21] Chrobak, K. M., Potter, D. R., and Tien, J. (2006). Formation of perfused, functional microvascular tubes in vitro. *Microvasc. Res.*, 71(3):185–196.

[22] Chua, C. K. and Leong, K. F. (2014). *3D Printing and Additive Manufacturing: Principles and Applications (with Companion Media Pack) of Rapid Prototyping Fourth Edition*. World Scientific Publishing Company.

[23] Chung, A. S. and Ferrara, N. (2011). Developmental and pathological angiogenesis. *Annual review of cell and developmental biology*, 27:563–584.

[24] Chwalek, K., Tsurkan, M. V., Freudenberg, U., and Werner, C. (2014). Glycosaminoglycan-based hydrogels to modulate heterocellular communication in in vitro angiogenesis models. *Scientific reports*, 4:4414.

[25] Collen, A., Smorenburg, S. M., Peters, E., Lupu, F., Koolwijk, P., Van Noorden, C., and van Hinsbergh, V. W. (2000). Unfractionated and low molecular weight heparin affect fibrin structure and angiogenesis in vitro. *Cancer Research*, 60(21):6196–6200.

[26] Considine, D. M. (2012). Foods and food production encyclopedia. *Springer Science & Business Media*, page 824.

[27] Cross, V. L., Zheng, Y., Choi, N. W., Verbridge, S. S., Sutermaster, B. A., Bonassar, L. J., Fischbach, C., and Stroock, A. D. (2010). Dense type i collagen matrices that support cellular remodeling and microfabrication for studies of tumor angiogenesis and vasculogenesis in vitro. *Biomaterials*, 31(33):8596–8607.

[28] Cuchiara, M. P., Allen, A. C., Chen, T. M., Miller, J. S., and West, J. L. (2010). Multilayer microfluidic pegda hydrogels. *Biomaterials*, 31(21):5491–5497.

[29] Cui, X. and Boland, T. (2009). Human microvasculature fabrication using thermal inkjet printing technology. *Biomaterials*, 30(31):6221–6227.

[30] Custom Part Net (2008). Additive fabrication. http://www.custompartnet.com/wu/ink-jet-printing.

[31] Damink, L. O., Dijkstra, P. J., Van Luyn, M., Van Wachem, P., Nieuwenhuis, P., and Feijen, J. (1995). Glutaraldehyde as a crosslinking agent for collagen-based biomaterials. *Journal of materials science: materials in medicine*, 6(8):460–472.

[32] Damink, L. O., Dijkstra, P. J., Van Luyn, M., Van Wachem, P., Nieuwenhuis, P., and Feijen, J. (1996). Cross-linking of dermal sheep collagen using a water-soluble carbodiimide. *Biomaterials*, 17(8):765–773.

[33] De Iuliis, G. and Tsuji, L. J. (1991). Alginate impression material. *Collection*, 7(1):38–15.

[34] de Souza, L. E. B., Malta, T. M., Kashima Haddad, S., and Covas, D. T. (2016). Mesenchymal stem cells and pericytes: to what extent are they related? *Stem cells and development*, 25(24):1843–1852.

[35] Dejana, E. (2004). Endothelial cell–cell junctions: happy together. *Nature reviews Molecular cell biology*, 5(4):261–270.

[36] Deng, G., Tang, C., Li, F., Jiang, H., Chen, Y., et al. (2010). Covalent cross-linked polymer gels with reversible sol- gel transition and self-healing properties. *Macromolecules*, 43(3):1191.

[37] Dhariwala, B., Hunt, E., and Boland, T. (2004). Rapid prototyping of tissue-engineering constructs, using photopolymerizable hydrogels and stereolithography. *Tissue engineering*, 10(9-10):1316–1322.

[38] Diaz-Santana, A., Shan, M., and Stroock, A. D. (2015). Endothelial cell dynamics during anastomosis in vitro. *Integrative Biology*, 7(4):454–466.

[39] Dutta, D., Fauer, C., Mulleneux, H., and Stabenfeldt, S. (2015). Tunable controlled release of bioactive sdf-1α via specific protein interactions within fibrin/nanoparticle composites. *Journal of Materials Chemistry B*, 3(40):7963–7973.

[40] Erikson, A., Andersen, H. N., Naess, S. N., Sikorski, P., and Davies, C. d. L. (2008). Physical and chemical modifications of collagen gels: impact on diffusion. *Biopolymers*, 89(2):135–143.

[41] Evensen, L., Micklem, D. R., Blois, A., Berge, S. V., Aarsæther, N., Littlewood-Evans, A., Wood, J., and Lorens, J. B. (2009). Mural cell associated vegf is required for organotypic vessel formation. *PloS one*, 4(6):e5798.

[42] Eweida, A., Nabawi, A., Elhammady, H., Marei, M., Khalil, M., Shawky, M., Arkudas, A., Beier, J., Unglaub, F., Kneser, U., et al. (2012). Axially vascularized bone substitutes: a systematic review of literature and presentation of a novel model. *Archives of orthopaedic and trauma surgery*, 132(9):1353–1362.

[43] Fabbaloo (2014). Solidscape's hold on the 3d printed jewelry market.

[44] Freyer, A. M., Johnson, S. R., and Hall, I. P. (2001). Effects of growth factors and extracellular matrix on survival of human airway smooth muscle cells. *American Journal of Respiratory Cell and Molecular Biology*, 25(5):569–576.

[45] Ghajar, C. M., Chen, X., Harris, J. W., Suresh, V., Hughes, C. C., Jeon, N. L., Putnam, A. J., and George, S. C. (2008). The effect of matrix density on the regulation of 3-d capillary morphogenesis. *Biophysical journal*, 94(5):1930–1941.

[46] Ghajar, C. M., Kachgal, S., Kniazeva, E., Mori, H., Costes, S. V., George, S. C., and Putnam, A. J. (2010). Mesenchymal cells stimulate capillary morphogenesis via distinct proteolytic mechanisms. *Experimental cell research*, 316(5):813–825.

[47] Goerges, A. L. and Nugent, M. A. (2004). ph regulates vascular endothelial growth factor binding to fibronectin a mechanism for control of extracellular matrix storage and release. *Journal of Biological Chemistry*, 279(3):2307–2315.

[48] Goh, C. H., Heng, P. W. S., and Chan, L. W. (2012). Alginates as a useful natural polymer for microencapsulation and therapeutic applications. *Carbohydrate Polymers*, 88(1):1–12.

[49] Golden, A. P. and Tien, J. (2007). Fabrication of microfluidic hydrogels using molded gelatin as a sacrificial element. *Lab Chip*, 7(6):720–725.

[50] Grainger, S. J. and Putnam, A. J. (2011). Assessing the permeability of engineered capillary networks in a 3d culture. *PLoS One*, 6(7):e22086.

[51] Greenberg, J. I., Shields, D. J., Barillas, S. G., Acevedo, L. M., Murphy, E., Huang, J., Scheppke, L., Stockmann, C., Johnson, R. S., Angle, N., et al. (2008). A role for vegf as a negative regulator of pericyte function and vessel maturation. *Nature*, 456(7223):809.

[52] Gutowska, A., Jeong, B., and Jasionowski, M. (2001). Injectable gels for tissue engineering. *The Anatomical Record*, 263(4):342–349.

[53] Hata-Sugi, N., Kawase-Kageyama, R., and Wakabayashi, T. (2002). Characterization of rat aortic fragment within collagen gel as an angiogenesis model; capillary morphology may reflect the action mechanisms of angiogenesis inhibitors. *Biological and Pharmaceutical Bulletin*, 25(4):446–451.

[54] Helm, C.-L. E., Fleury, M. E., Zisch, A. H., Boschetti, F., and Swartz, M. A. (2005). Synergy between interstitial flow and vegf directs capillary morphogenesis in vitro through a gradient amplification mechanism. *Proceedings of the National Academy of Sciences of the United States of America*, 102(44):15779–15784.

[55] Hinton, T. J., Jallerat, Q., Palchesko, R. N., Park, J. H., Grodzicki, M. S., Shue, H.-J., Ramadan, M. H., Hudson, A. R., and Feinberg, A. W. (2015). Three-dimensional printing of complex biological structures by freeform reversible embedding of suspended hydrogels. *Science advances*, 1(9):e1500758.

[56] Hoganson, D. M., Pryor, H. I., and Vacanti, J. P. (2008). Tissue engineering and organ structure: a vascularized approach to liver and lung. *Pediatric research*, 63(5):520–526.

[57] Hollister, S. J. (2005). Porous scaffold design for tissue engineering. *Nature materials*, 4(7):518–524.

[58] Hoying, J. B., Boswell, C. A., and Williams, S. K. (1996). Angiogenic potential of microvessel fragments established in three-dimensional collagen gels. *In Vitro Cellular & Developmental Biology-Animal*, 32(7):409–419.

[59] Hsu, Y.-H., Moya, M. L., Abiri, P., Hughes, C. C., George, S. C., and Lee, A. P. (2013a). Full range physiological mass transport control in 3d tissue cultures. *Lab on a chip*, 13(1):81–89.

[60] Hsu, Y.-H., Moya, M. L., Hughes, C. C., George, S. C., and Lee, A. P. (2013b). A microfluidic platform for generating large-scale nearly identical human microphysiological vascularized tissue arrays. *Lab on a chip*, 13(15):2990–2998.

[61] Huh, D., Torisawa, Y.-S., Hamilton, G. A., Kim, H. J., and Ingber, D. E. (2012). Microengineered physiological biomimicry: organs-on-chips. *Lab on a chip*, 12(12):2156–2164.

[62] Iozzo, R. V. and San Antonio, J. D. (2001). Heparan sulfate proteoglycans: heavy hitters in the angiogenesis arena. *The Journal of clinical investigation*, 108(3):349–355.

[63] Irvine, S. A., Agrawal, A., Lee, B. H., Chua, H. Y., Low, K. Y., Lau, B. C., Machluf, M., and Venkatraman, S. (2015). Printing cell-laden gelatin constructs by free-form fabrication and enzymatic protein crosslinking. *Biomedical microdevices*, 17(1):16.

[64] Isik, F. F., Gibran, N. S., Jang, Y.-C., Sandell, L., and Schwartz, S. M. (1998). Vitronectin decreases microvascular endothelial cell apoptosis. *Journal of cellular physiology*, 175(2):149–155.

[65] Jeong, B., Bae, Y. H., and Kim, S. W. (1999). Thermoreversible gelation of peg- plga-peg triblock copolymer aqueous solutions. *Macromolecules*, 32(21):7064–7069.

[66] Jeong, B. and Gutowska, A. (2002). Lessons from nature: stimuli-responsive polymers and their biomedical applications. *Trends in biotechnology*, 20(7):305–311.

[67] Jeong, B., Kim, S. W., and Bae, Y. H. (2012). Thermosensitive sol–gel reversible hydrogels. *Advanced drug delivery reviews*, 64:154–162.

[68] Jockenhoevel, S., Zund, G., Hoerstrup, S. P., Chalabi, K., Sachweh, J. S., Demircan, L., Messmer, B. J., and Turina, M. (2001). Fibrin gel–advantages of a new scaffold in cardiovascular tissue engineering. *European journal of cardio-thoracic surgery*, 19(4):424–430.

[69] Joo, M. K., Park, M. H., Choi, B. G., and Jeong, B. (2009). Reverse thermogelling biodegradable polymer aqueous solutions. *Journal of Materials Chemistry*, 19(33):5891–5905.

[70] Kadler, K. E., Hill, A., and Canty-Laird, E. G. (2008). Collagen fibrillogenesis: fibronectin, integrins, and minor collagens as organizers and nucleators. *Current opinion in cell biology*, 20(5):495–501.

[71] Kamei, M., Saunders, W. B., Bayless, K. J., Dye, L., Davis, G. E., and Weinstein, B. M. (2006). Endothelial tubes assemble from intracellular vacuoles in vivo. *Nature*, 442(7101):453–456.

[72] Kanda, S., Mochizuki, Y., and Kanetake, H. (2003). Stromal cell-derived factor-1α induces tube-like structure formation of endothelial cells through phosphoinositide 3-kinase. *Journal of Biological Chemistry*, 278(1):257–262.

[73] Kang, H.-W., Lee, S. J., Ko, I. K., Kengla, C., Yoo, J. J., and Atala, A. (2016a). A 3d bioprinting system to produce human-scale tissue constructs with structural integrity. *Nature biotechnology*, 34(3):312–319.

[74] Kang, T.-Y., Hong, J. M., Jung, J. W., Kang, H.-W., and Cho, D.-W. (2016b). Construction of large-volume tissue mimics with 3d functional vascular networks. *PloS one*, 11(5):e0156529.

[75] Kaully, T., Kaufman-Francis, K., Lesman, A., and Levenberg, S. (2009). Vascularization—the conduit to viable engineered tissues. *Tissue Engineering Part B: Reviews*, 15(2):159–169.

[76] Kim, K. L., Song, S.-H., Choi, K.-S., and Suh, W. (2013a). Cooperation of endothelial and smooth muscle cells derived from human induced pluripotent stem cells enhances neovascularization in dermal wounds. *Tissue engineering Part A*, 19(21-22):2478–2485.

[77] Kim, S., Chung, M., Ahn, J., Lee, S., and Jeon, N. L. (2016). Interstitial flow regulates the angiogenic response and phenotype of endothelial cells in a 3d culture model. *Lab on a Chip*, 16(21):4189–4199.

[78] Kim, S., Lee, H., Chung, M., and Jeon, N. L. (2013b). Engineering of functional, perfusable 3d microvascular networks on a chip. *Lab on a Chip*, 13(8):1489–1500.

[79] Kinstlinger, I. S. and Miller, J. S. (2016). 3d-printed fluidic networks as vasculature for engineered tissue. *Lab on a Chip*, 16(11):2025–2043.

[80] Kneser, U., Polykandriotis, E., Ohnolz, J., Heidner, K., Grabinger, L., Euler, S., Amann, K. U., Hess, A., Brune, K., Greil, P., et al. (2006). Engineering of vascularized transplantable bone tissues: induction of axial vascularization in an osteoconductive matrix using an arteriovenous loop. *Tissue engineering*, 12(7):1721–1731.

[81] Kniazeva, E., Kachgal, S., and Putnam, A. J. (2010). Effects of extracellular matrix density and mesenchymal stem cells on neovascularization in vivo. *Tissue engineering Part A*, 17(7-8):905–914.

[82] Ko, H., Milthorpe, B. K., McFarland, C. D., et al. (2007). Engineering thick tissues—the vascularisation problem. *Eur Cell Mater*, 14(1).

[83] Koike, N., Fukumura, D., Gralla, O., Au, P., Schechner, J. S., and Jain, R. K. (2004). Tissue engineering: creation of long-lasting blood vessels. *Nature*, 428(6979):138–139.

[84] Kolesky, D. B., Homan, K. A., Skylar-Scott, M. A., and Lewis, J. A. (2016). Three-dimensional bioprinting of thick vascularized tissues. *Proc. Natl. Acad. Sci. USA*, 113(12):3179–3184.

[85] Korff, T. and Augustin, H. G. (1998). Integration of endothelial cells in multicellular spheroids prevents apoptosis and induces differentiation. *The Journal of cell biology*, 143(5):1341–1352.

[86] Kwak, H. J., So, J.-N., Lee, S. J., Kim, I., and Koh, G. Y. (1999). Angiopoietin-1 is an apoptosis survival factor for endothelial cells. *FEBS letters*, 448(2-3):249–253.

[87] Lafleur, M. A., Handsley, M. M., Knäuper, V., Murphy, G., and Edwards, D. R. (2002). Endothelial tubulogenesis within fibrin gels specifically requires the activity of membrane-type-matrix metalloproteinases (mt-mmps). *Journal of Cell Science*, 115(17):3427–3438.

[88] Laib, A. M., Bartol, A., Alajati, A., Korff, T., Weber, H., and Augustin, H. G. (2009). Spheroid-based human endothelial cell microvessel formation in vivo. *Nature protocols*, 4(8):1202–1215.

[89] Lee, K. Y. and Mooney, D. J. (2012). Alginate: properties and biomedical applications. *Progress in polymer science*, 37(1):106–126.

[90] Lee, P.-F., Bai, Y., Smith, R., Bayless, K., and Yeh, A. (2013). Angiogenic responses are enhanced in mechanically and microscopically characterized, microbial transglutaminase crosslinked collagen matrices with increased stiffness. *Acta biomaterialia*, 9(7):7178–7190.

[91] Lee, V. K., Lanzi, A. M., Ngo, H., Yoo, S.-S., Vincent, P. A., and Dai, G. (2014). Generation of multi-scale vascular network system within 3d hydrogel using 3d bio-printing technology. *Cellular and molecular bioengineering*, 7(3):460–472.

[92] Leibovich, S. J., Polverini, P. J., Shepard, H. M., Wiseman, D. M., Shively, V., and Nuseir, N. (1987). Macrophage-induced angiogenesis is mediated by tumour necrosis factor-α. *Nature*, 329(6140):630–632.

[93] Leker, R. R., Toth, Z. E., Shahar, T., Cassiani-Ingoni, R., Szalayova, I., Key, S., Bratincsák, A., and Mezey, E. (2009). Transforming growth factor α induces angiogenesis and neurogenesis following stroke. *Neuroscience*, 163(1):233–243.

[94] Lim, S. H., Kim, C., Aref, A. R., Kamm, R. D., and Raghunath, M. (2013). Complementary effects of ciclopirox olamine, a prolyl hydroxylase inhibitor and sphingosine 1-phosphate on fibroblasts and endothelial cells in driving capillary sprouting. *Integrative Biology*, 5(12):1474–1484.

[95] Ling, Y., Rubin, J., Deng, Y., Huang, C., Demirci, U., Karp, J. M., and Khademhosseini, A. (2007). A cell-laden microfluidic hydrogel. *Lab Chip*, 7(6):756–762.

[96] Liu, C., Xia, Z., and Czernuszka, J. (2007). Design and development of three-dimensional scaffolds for tissue engineering. *Chemical Engineering Research and Design*, 85(7):1051–1064.

[97] Liu, C., Xia, Z., Han, Z., Hulley, P., Triffitt, J., and Czernuszka, J. (2008). Novel 3d collagen scaffolds fabricated by indirect printing technique for tissue engineering. *J. Biomed. Mater. Res. Part B Appl. Biomater.*, 85(2):519–528.

[98] Liu, W., Ahmad, S., Reinmuth, N., Shaheen, R., Jung, Y., Fan, F., and Ellis, L. (2000). Endothelial cell survival and apoptosis in the tumor vasculature. *Apoptosis*, 5(4):323–328.

[99] Lloyd, G. O. and Steed, J. W. (2009). Anion-tuning of supramolecular gel properties. *Nature chemistry*, 1(6):437–442.

[100] Lokmic, Z., Stillaert, F., Morrison, W. A., Thompson, E. W., and Mitchell, G. M. (2007). An arteriovenous loop in a protected space generates a permanent, highly vascular, tissue-engineered construct. *The FASEB Journal*, 21(2):511–522.

[101] Lovett, M., Lee, K., Edwards, A., and Kaplan, D. L. (2009). Vascularization strategies for tissue engineering. *Tissue Eng.*, 15(3):353–370.

[102] Lynn, A., Yannas, I., and Bonfield, W. (2004). Antigenicity and immunogenicity of collagen. *Journal of Biomedical Materials Research Part B: Applied Biomaterials*, 71(2):343–354.

[103] MacDonald, N. (1983). Trees and networks in biological models.

[104] Makogonenko, E., Tsurupa, G., Ingham, K., and Medved, L. (2002). Interaction of fibrin (ogen) with fibronectin: further characterization and localization of the fibronectin-binding site. *Biochemistry*, 41(25):7907–7913.

[105] Martino, M. M., Briquez, P. S., Ranga, A., Lutolf, M. P., and Hubbell, J. A. (2013). Heparin-binding domain of fibrin (ogen) binds growth factors and promotes tissue repair when incorporated within a synthetic matrix. *Proceedings of the National Academy of Sciences*, 110(12):4563–4568.

[106] Martino, M. M. and Hubbell, J. A. (2010). The 12th–14th type iii repeats of fibronectin function as a highly promiscuous growth factor-binding domain. *The FASEB Journal*, 24(12):4711–4721.

[107] Mathur, A. M., Moorjani, S. K., and Scranton, A. B. (1996). Methods for synthesis of hydrogel networks: A review. *Journal of Macromolecular Science, Part C: Polymer Reviews*, 36(2):405–430.

[108] Miller, J. S. (2014). The billion cell construct: will three-dimensional printing get us there? *PLoS biology*, 12(6):e1001882.

[109] Miller, J. S., Stevens, K. R., Yang, M. T., Baker, B. M., Nguyen, D.-H. T., Cohen, D. M., Toro, E., Chen, A. A., Galie, P. A., Yu, X., et al. (2012). Rapid casting of patterned vascular networks for perfusable engineered three-dimensional tissues. *Nature materials*, 11(9):768–774.

[110] Mitsi, M., Hong, Z., Costello, C. E., and Nugent, M. A. (2006). Heparin-mediated conformational changes in fibronectin expose vascular endothelial growth factor binding sites. *Biochemistry*, 45(34):10319–10328.

[111] Montaño, I., Schiestl, C., Schneider, J., Pontiggia, L., Luginbühl, J., Biedermann, T., Böttcher-Haberzeth, S., Braziulis, E., Meuli, M., and Reichmann, E. (2009). Formation of human capillaries in vitro: the engineering of prevascularized matrices. *Tissue Engineering Part A*, 16(1):269–282.

[112] Montesano, R. and Orci, L. (1987). Phorbol esters induce angiogenesis in vitro from large-vessel endothelial cells. *Journal of cellular physiology*, 130(2):284–291.

[113] Morgan, J. P., Delnero, P. F., Zheng, Y., Verbridge, S. S., Chen, J., Craven, M., Choi, N. W., Diaz-Santana, A., Kermani, P., Hempstead, B., et al. (2013). Formation of microvascular networks in vitro. *Nat. Protoc.*, 8(9):1820–1836.

[114] Morin, K. T., Dries-Devlin, J. L., and Tranquillo, R. T. (2013a). Engineered microvessels with strong alignment and high lumen density via cell-induced fibrin gel compaction and interstitial flow. *Tissue Engineering Part A*, 20(3-4):553–565.

[115] Morin, K. T., Smith, A. O., Davis, G. E., and Tranquillo, R. T. (2013b). Aligned human microvessels formed in 3d fibrin gel by constraint of gel contraction. *Microvascular research*, 90:12–22.

[116] Morin, K. T. and Tranquillo, R. T. (2013). In vitro models of angiogenesis and vasculogenesis in fibrin gel. *Experimental cell research*, 319(16):2409–2417.

[117] Murray, C. D. (1926). The physiological principle of minimum work applied to the angle of branching of arteries. *The Journal of general physiology*, 9(6):835.

[118] Nakatsu, M. N. and Hughes, C. C. (2008). An optimized three-dimensional in vitro model for the analysis of angiogenesis. *Methods in enzymology*, 443:65–82.

[119] Nakatsu, M. N., Sainson, R. C., Aoto, J. N., Taylor, K. L., Aitkenhead, M., Pérez-del Pulgar, S., Carpenter, P. M., and Hughes, C. C. (2003). Angiogenic sprouting and capillary lumen formation modeled by human umbilical vein endothelial cells (huvec) in fibrin gels: the role of fibroblasts and angiopoietin-1. *Microvascular research*, 66(2):102–112.

[120] Nehls, V. and Herrmann, R. (1996). The configuration of fibrin clots determines capillary morphogenesis and endothelial cell migration. *Microvascular research*, 51(3):347–364.

[121] Neumann, T., Nicholson, B. S., and Sanders, J. E. (2003). Tissue engineering of perfused microvessels. *Microvascular research*, 66(1):59–67.

[122] Ng, C. P., Helm, C.-L. E., and Swartz, M. A. (2004). Interstitial flow differentially stimulates blood and lymphatic endothelial cell morphogenesis in vitro. *Microvascular research*, 68(3):258–264.

[123] Nguyen, D.-H. T., Stapleton, S. C., Yang, M. T., Cha, S. S., Choi, C. K., Galie, P. A., and Chen, C. S. (2013). Biomimetic model to reconstitute angiogenic sprouting morphogenesis in vitro. *Proceedings of the National Academy of Sciences*, 110(17):6712–6717.

[124] Nicosia, R. F., Nicosia, S., and Smith, M. (1994). Vascular endothelial growth factor, platelet-derived growth factor, and insulin-like growth factor-1 promote rat aortic angiogenesis in vitro. *The American journal of pathology*, 145(5):1023.

[125] Norotte, C., Marga, F. S., Niklason, L. E., and Forgacs, G. (2009). Scaffold-free vascular tissue engineering using bioprinting. *Biomaterials*, 30(30):5910–5917.

[126] Orban, J. M., Wilson, L. B., Kofroth, J. A., El-Kurdi, M. S., Maul, T. M., and Vorp, D. A. (2004). Crosslinking of collagen gels by transglutaminase. *Journal of biomedical materials research Part A*, 68(4):756–762.

[127] Otrock, Z. K., Mahfouz, R. A., Makarem, J. A., and Shamseddine, A. I. (2007). Understanding the biology of angiogenesis: review of the most important molecular mechanisms. *Blood Cells, Molecules, and Diseases*, 39(2):212–220.

[128] Otsu, K., Das, S., Houser, S. D., Quadri, S. K., Bhattacharya, S., and Bhattacharya, J. (2009). Concentration-dependent inhibition of angiogenesis by mesenchymal stem cells. *Blood*, 113(18):4197–4205.

[129] Pardue, E. L., Ibrahim, S., and Ramamurthi, A. (2008). Role of hyaluronan in angiogenesis and its utility to angiogenic tissue engineering. *Organogenesis*, 4(4):203–214.

[130] Park, Y. K., Tu, T.-Y., Lim, S. H., Clement, I. J., Yang, S. Y., and Kamm, R. D. (2014). In vitro microvessel growth and remodeling within a three-dimensional microfluidic environment. *Cellular and molecular bioengineering*, 7(1):15–25.

[131] Pataky, K., Braschler, T., Negro, A., Renaud, P., Lutolf, M. P., and Brugger, J. (2012). Microdrop printing of hydrogel bioinks into 3d tissue-like geometries. *Advanced Materials*, 24(3):391–396.

[132] Petit, I., Jin, D., and Rafii, S. (2007). The sdf-1–cxcr4 signaling pathway: a molecular hub modulating neo-angiogenesis. *Trends in immunology*, 28(7):299–307.

[133] Pfisterer, L. and Korff, T. (2016). Spheroid-based in vitro angiogenesis model. *Angiogenesis Protocols*, pages 167–177.

[134] Pike, D. B., Cai, S., Pomraning, K. R., Firpo, M. A., Fisher, R. J., Shu, X. Z., Prestwich, G. D., and Peattie, R. A. (2006). Heparin-regulated release of growth factors in vitro and angiogenic response in vivo to implanted hyaluronan hydrogels containing vegf and bfgf. *Biomaterials*, 27(30):5242–5251.

[135] Rao, R. R., Peterson, A. W., Ceccarelli, J., Putnam, A. J., and Stegemann, J. P. (2012). Matrix composition regulates three-dimensional network formation by endothelial cells and mesenchymal stem cells in collagen/fibrin materials. *Angiogenesis*, 15(2):253–264.

[136] Robert, A. (2003). Nanomedicine, volume iia: Biocompatibility.

[137] Sacchi, V., Mittermayr, R., Hartinger, J., Martino, M. M., Lorentz, K. M., Wolbank, S., Hofmann, A., Largo, R. A., Marschall, J. S., Groppa, E., et al. (2014). Long-lasting fibrin matrices ensure stable and functional angiogenesis by highly tunable, sustained delivery of recombinant vegf164. *Proceedings of the National Academy of Sciences*, 111(19):6952–6957.

[138] Sachlos, E., Reis, N., Ainsley, C., Derby, B., and Czernuszka, J. (2003). Novel collagen scaffolds with predefined internal morphology made by solid freeform fabrication. *Biomaterials*, 24(8):1487–1497.

[139] Saggiomo, V. and Velders, A. H. (2015). Simple 3d printed scaffold-removal method for the fabrication of intricate microfluidic devices. *Adv. Sci.*, 2:1500125.

[140] Sato, N., Sawasaki, Y., Senoo, A., Fuse, Y., Hirano, Y., and Goto, T. (1987). Development of capillary networks from rat microvascular fragments in vitro: the role of myofibroblastic cells. *Microvascular research*, 33(2):194–210.

[141] Schrieber, R. and Gareis, H. (2007). *Gelatine handbook: theory and industrial practice*. John Wiley & Sons.

[142] Seghezzi, G., Patel, S., Ren, C. J., Gualandris, A., Pintucci, G., Robbins, E. S., Shapiro, R. L., Galloway, A. C., Rifkin, D. B., and Mignatti, P. (1998). Fibroblast growth factor-2 (fgf-2) induces vascular endothelial growth factor (vegf) expression in the endothelial cells of forming capillaries: an autocrine mechanism contributing to angiogenesis. *The Journal of cell biology*, 141(7):1659–1673.

[143] Sevilla, C. A., Dalecki, D., and Hocking, D. C. (2010). Extracellular matrix fibronectin stimulates the self-assembly of microtissues on native collagen gels. *Tissue Engineering Part A*, 16(12):3805–3819.

[144] Sher, D. (2015). Bioprinted Tissues to Be Implanted Within 10 Years.

[145] Sherman, T. F. (1981). On connecting large vessels to small. the meaning of murray's law. *J. Gen. Physiol.*, 78(4):431–453.

[146] Shinde, U. P., Yeon, B., Jeong, B., et al. (2013). Recent progress of in situ formed gels for biomedical applications. *Progress in polymer science*, 38(3):672–701.

[147] Sierra, D. H. (1993). Fibrin sealant adhesive systems: a review of their chemistry, material properties and clinical applications. *Journal of Biomaterials Applications*, 7(4):309–352.

[148] Stock, U. A. and Vacanti, J. P. (2001). Tissue engineering: current state and prospects. *Annual review of medicine*, 52(1):443–451.

[149] Stratman, A. N., Malotte, K. M., Mahan, R. D., Davis, M. J., and Davis, G. E. (2009). Pericyte recruitment during vasculogenic tube assembly stimulates endothelial basement membrane matrix formation. *Blood*, 114(24):5091–5101.

[150] Stratman, A. N., Schwindt, A. E., Malotte, K. M., and Davis, G. E. (2010). Endothelial-derived pdgf-bb and hb-egf coordinately regulate pericyte recruitment during vasculogenic tube assembly and stabilization. *Blood*, 116(22):4720–4730.

[151] Sun, L., Hui, A.-M., Su, Q., Vortmeyer, A., Kotliarov, Y., Pastorino, S., Passaniti, A., Menon, J., Walling, J., Bailey, R., et al. (2006). Neuronal and glioma-derived stem cell factor induces angiogenesis within the brain. *Cancer cell*, 9(4):287–300.

[152] Takebe, T., Koike, N., Sekine, K., Fujiwara, R., Amiya, T., Zheng, Y.-W., and Taniguchi, H. (2014). Engineering of human hepatic tissue with functional vascular networks. *Organogenesis*, 10(2):260–267.

[153] Takebe, T., Sekine, K., Enomura, M., Koike, H., Kimura, M., Ogaeri, T., Zhang, R.-R., Ueno, Y., Zheng, Y.-W., Koike, N., et al. (2013). Vascularized and functional human liver from an ipsc-derived organ bud transplant. *Nature*, 499(7459):481–484.

[154] Tanaka, Y., Sung, K.-C., Tsutsumi, A., Ohba, S., Ueda, K., and Morrison, W. A. (2003). Tissue engineering skin flaps: which vascular carrier, arteriovenous shunt loop or arteriovenous bundle, has more potential for angiogenesis and tissue generation? *Plastic and reconstructive surgery*, 112(6):1636–1644.

[155] Therriault, D., White, S. R., and Lewis, J. A. (2003). Chaotic mixing in three-dimensional microvascular networks fabricated by direct-write assembly. *Nature materials*, 2(4):265–271.

[156] Thomson, K. S., Dupras, S. K., Murry, C. E., Scatena, M., and Regnier, M. (2014). Proangiogenic microtemplated fibrin scaffolds containing aprotinin promote improved wound healing responses. *Angiogenesis*, 17(1):195–205.

[157] Tille, J.-C. and Pepper, M. S. (2002). Mesenchymal cells potentiate vascular endothelial growth factor-induced angiogenesis in vitro. *Experimental cell research*, 280(2):179–191.

[158] Tsigkou, O., Pomerantseva, I., Spencer, J. A., Redondo, P. A., Hart, A. R., O'Doherty, E., Lin, Y., Friedrich, C. C., Daheron, L., Lin, C. P., et al. (2010). Engineered vascularized bone grafts. *Proceedings of the National Academy of Sciences*, 107(8):3311–3316.

[159] Tuan, T.-L., Song, A., Chang, S., Younai, S., and Nimni, M. E. (1996). In vitrofibroplasia: Matrix contraction, cell growth, and collagen production of fibroblasts cultured in fibrin gels. *Experimental cell research*, 223(1):127–134.

[160] Urbich, C., Aicher, A., Heeschen, C., Dernbach, E., Hofmann, W. K., Zeiher, A. M., and Dimmeler, S. (2005). Soluble factors released by endothelial progenitor cells promote migration of endothelial cells and cardiac resident progenitor cells. *Journal of molecular and cellular cardiology*, 39(5):733–742.

[161] Vailhé, B., Vittet, D., and Feige, J.-J. (2001). In vitro models of vasculogenesis and angiogenesis. *Laboratory investigation*, 81(4):439.

[162] van Cruijsen, H., Giaccone, G., and Hoekman, K. (2005). Epidermal growth factor receptor and angiogenesis: opportunities for combined anticancer strategies. *International journal of cancer*, 117(6):883–888.

[163] Vervoort, S. (2006). *Behaviour of hydrogels swollen in polymer solutions under mechanical action*. PhD thesis, École Nationale Supérieure des Mines de Paris.

[164] Voronov, E., Carmi, Y., and Apte, R. N. (2014). The role il-1 in tumor-mediated angiogenesis. *The regulation of angiogenesis by tissue cell-macrophage interactions*, page 52.

[165] Wang, X.-Y., Jin, Z.-H., Gan, B.-W., Lv, S.-W., Xie, M., and Huang, W.-H. (2014). Engineering interconnected 3d vascular networks in hydrogels using molded sodium alginate lattice as the sacrificial template. *Lab on a Chip*, 14(15):2709–2716.

[166] Wang, Z. Z., Au, P., Chen, T., Shao, Y., Daheron, L. M., Bai, H., Arzigian, M., Fukumura, D., Jain, R. K., and Scadden, D. T. (2007). Endothelial cells derived from human embryonic stem cells form durable blood vessels in vivo. *Nature biotechnology*, 25(3):317.

[167] Werb, Z. (1997). Ecm and cell surface proteolysis: regulating cellular ecology. *Cell*, 91(4):439–442.

[168] Wong, K. H., Truslow, J. G., Khankhel, A. H., Chan, K. L., and Tien, J. (2013). Artificial lymphatic drainage systems for vascularized microfluidic scaffolds. *Journal of Biomedical Materials Research Part A*, 101(8):2181–2190.

[169] Wu, S., Liu, X., Yeung, K. W., Liu, C., and Yang, X. (2014). Biomimetic porous scaffolds for bone tissue engineering. *Materials Science and Engineering: R: Reports*, 80:1–36.

[170] Wu, W., DeConinck, A., and Lewis, J. A. (2011). Omnidirectional printing of 3d microvascular networks. *Advanced materials*, 23(24).

[171] Wu, W., Hansen, C. J., Aragón, A. M., Geubelle, P. H., White, S. R., and Lewis, J. A. (2010). Direct-write assembly of biomimetic microvascular networks for efficient fluid transport. *Soft Matter*, 6(4):739–742.

[172] Wu, Y., Chen, L., Scott, P. G., and Tredget, E. E. (2007). Mesenchymal stem cells enhance wound healing through differentiation and angiogenesis. *Stem cells*, 25(10):2648–2659.

[173] Wyss Institute for Biologically Inspired Engineering at Harvard University (2017). Human organs-on-chips. https://wyss.harvard.edu/technology/human-organs-on-chips/.

[174] Ye, Q., Zünd, G., Benedikt, P., Jockenhoevel, S., Hoerstrup, S. P., Sakyama, S., Hubbell, J. A., and Turina, M. (2000). Fibrin gel as a three dimensional matrix in cardiovascular tissue engineering. *European Journal of Cardio-Thoracic Surgery*, 17(5):587–591.

[175] Zheng, Y., Chen, J., Craven, M., Choi, N. W., Totorica, S., Diaz-Santana, A., Kermani, P., Hempstead, B., Fischbach-Teschl, C., López, J. A., and Stroock, A. D. (2012). In vitro microvessels for the study of angiogenesis and thrombosis. *Proc. Natl. Acad. Sci. USA*, 109(24):9342–9347.

[176] Zisch, A. H., Schenk, U., Schense, J. C., Sakiyama-Elbert, S. E., and Hubbell, J. A. (2001). Covalently conjugated vegf–fibrin matrices for endothelialization. *Journal of Controlled Release*, 72(1):101–113.

Appendix A

Densified Collagen Structures

A.1 Introduction

A key component of a vascular system separate from the bulk tissue is connecting tubes. We investigated the use of densified collagen as a means of producing these tubes, which culminated in the production of a replacement bile duct.

A.2 Densified Collagen

Densified collagen is closer to its native form than standard collagen gels, in which collagen fibrils are aligned and organized into structures, providing mechanical strength. Further, standard hydrogels are hyper-hydrated (i.e. 99%) while native tissue structures have far less fluid. Densified collagen does not require chemical crosslinking to provide it with suitable strength for *in vivo* work (though this can be done). Finally, while densification does dramatically increase the matrix concentration, it is thought that since the fibers are well organized, cells can migrate around the structure more freely than a higher concentration collagen gel with randomly orientated fibrils.

To produce densified collagen, a normal collagen gel is first produced. Using relatively high concentrations of 5-10 mg/mL collagen, the gel plastically compresses to form a thin sheet as the water is withdrawn from the hydrogel. Experiments with other hydrogels (gelatin, alginate) suggest that they do not undergo this deformation. Further, once densified, immersion in water does not cause the structure to return to its original state but instead remains unchanged. Thus the collagen fibrils are actively remodelling themselves into a more stable configuration as water is removed, leaving a better organized construct.

The primary interest of using densified collagen was the formation of inlets and outlets for a tissue structure. Its use as a replacement for the bulk fibrin gel was likely to cause problems in producing capillary networks and would require a project in itself to optimize the gel thickness and concentration. As shown in Figure A.1(a), layers of densified collagen can be produced on planar surfaces of gels. Tubular structures can also be fabricated for use as inlets to the bulk gels, as shown in Figure A.1b,c.

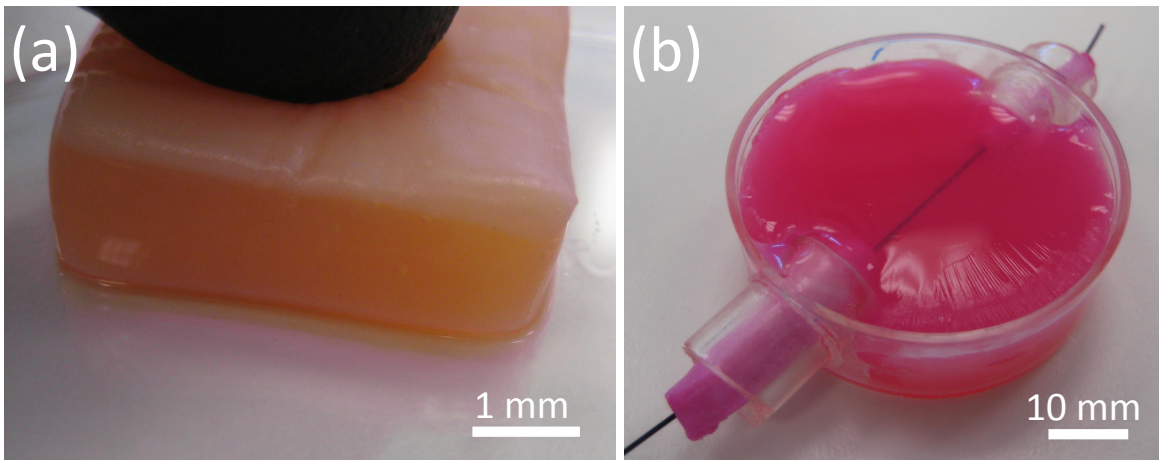

Fig. A.1 (a) Densified collagen gel is produced by loading the top surface of the gel whilst simultaneously withdrawing the water. The figure shows a region of densified collagen at the top with normal collagen gel underneath. (b) By rolling a sheet of partially-densified collagen into a tube and repeating the densification process, one is able to produce a large-scale tube structure. This tube can be placed at the inlets of collagen gel, which forms a weak bond with the tubes.

A.3 Replacement of a Common Murine Bile Duct

One of the primary aims of tissue engineering is an organ reconstruction or replacement using primary cells expanded *in vitro*. To this end, collaborators were able to mechanically isolate primary human cholangiocytes which formed into organoids. They subsequently approached us for a method for fabricating a bioengineered conduit into which these cells could be seeded and which then could be transplanted back into the animal.

Fabricating a collagen tube with a lumen diameter on the order of 250 μm with a wall thickness of 50-100 μm, provided a challenge. Several approaches were investigated, most notably rolling a thin sheet into a tube and suturing along its length. However, such approaches invariably led to leaking around the sutures and a lumen unable to support itself under its own weight. Thus we required a new method for the fabrication of a solid tube.

A.3.1 Method

Densified collagen tubes were prepared using a novel approach, shown in Figure A.2. A 3D printed chamber was fabricated from PLA, consisting of a funnel piece and a base plate 250 μm thick metallic wire was mounted into the base plate and fed through the centre of the funnel. Absorbent paper towels were compacted between the two 3D printed parts, which were then screwed together. 5 mg/mL collagen gel solution, loaded with cells, was poured into the funnel and gelled at 37°C for 30 min. After that time, the screws were loosened and, by placing the 3D printed chambers at 37°C for 2-4 h, water was drawn out of the collagen gel. A cell-loaded densified collagen tube was thus formed with a 250 μm lumen and a wall thickness of 30-100 μm, determined by the duration of the drying phase. Upon removal from the chamber, the tube was trimmed for excess collagen and cut to the required length.

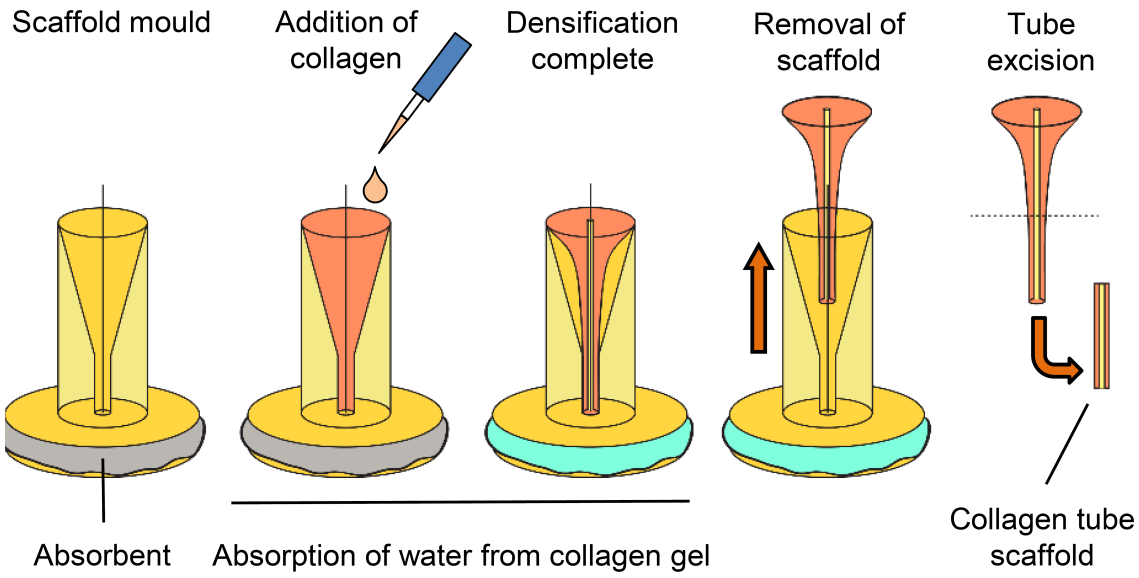

Fig. A.2 Fabrication process for replacement bioengineered conduit.

A.3.2 Results

As shown in Figure A.3, we were able to fabricate a tube by this process with a lumen of 250 μm and a wall thickness of 35 μm. The central channel was self-supporting and could be cannulated with suture wire and metal stents.

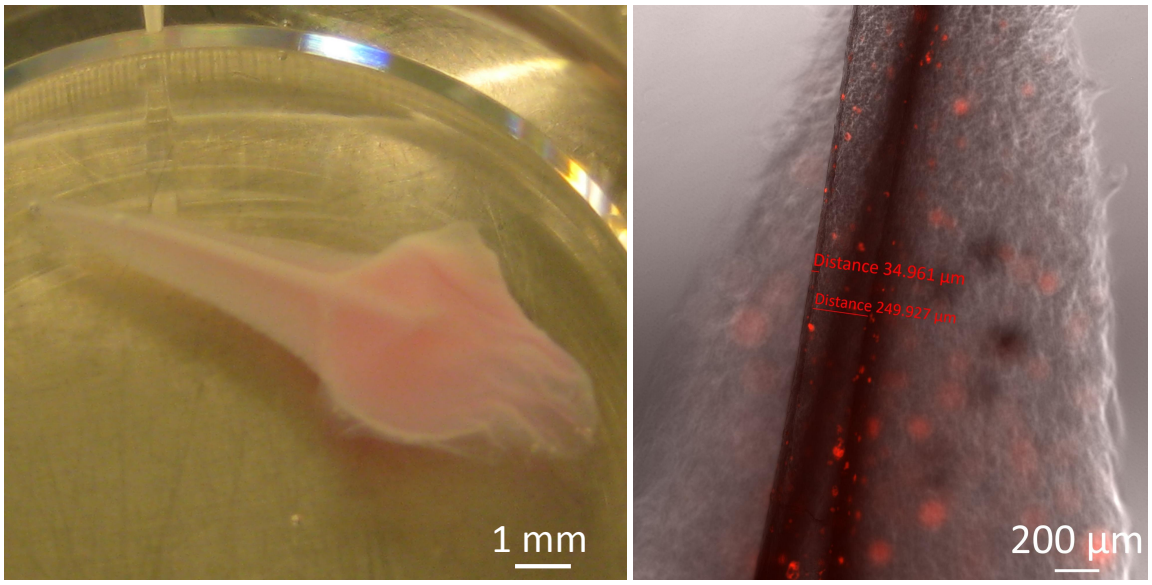

Fig. A.3 (a) Collagen tubes, seeded with primary human cholangiocytes, were generated via the above process. Shown here is a tube, after removal from the 3D printed support and prior to excision for implantation. (b) Tubes were fabricated with a lumen diameter of 250 μm and a wall thickness of 35 μm.

Extensive biological characterization of the replacement bile ducts was performed. However, we were not involved in this part of the project and it is outside the scope of this chapter on the tube fabrication method. The ability to produce fine collagen tubes over a range of dimensions is useful for our research as a potential means of producing bioengineered inlets for our devices.